Myeloid TRIB1 alters tumour microenvironment and breast tumour growth

By:

Taewoo Kim

A thesis submitted in partial fulfilment of the requirements for the degree of
Doctor of Philosophy

The University of Sheffield
Faculty of Medicine, Dentistry & Health
Department of Infection, Immunity & Cardiovascular Disease (IICD)

June 2020

Acknowledgements

I would like to express my sincere gratitude and thanks to my supervisors Professor Endre Kiss-Toth and Dr Munitta Muthana for their continuous effort and time, support and advice with their invaluable encouragement that allowed me to become a successful researcher and complete PhD. Thanks to Endre for the opportunities to be involved with other novice scientists around Europe working in similar fields and travel countries as a researcher.

I would like to thank staffs in IICD and BSU, notably Mrs Fiona Wright for the support in processing slides, Mr Steven Haynes and Ms Claire Bradshaw for their work in genotyping mice strains, and Mr Barry G Bird for the thoughtful care and attention in looking after the mice. I would also like to thank Dr Penelope Ottwell from Oncology department for providing cancer cell lines to develop mice models.

I also like to thank all my colleagues and friends in the lab and office, the members of Kiss-Toth group and Muthana group past and present who make the place full of excitement and laughter with conversations either personal or work-related and assistance in the lab. Particularly, Ahmed Bukari, Chiara Niespolo and Laura Martinez Campesino who were great help to acclimate to the environment at the start of PhD, Dr Jessica Johnston, Haider Al-Janabi, Mohammed Ridha Moamin, Kajus Baidžajevas, Yang Li, and Dr Ming Yang for their helped to develop lab skills and start the project. I would also like to thank Master student Fraser Hart who analysed the development of secondary tumours in the lung and liver tissues.

Last but not least, I would like to express my special thanks to my parents for their everlasting love, support, and encouragement. I would also like to thank my mentor, Father Paul Cho and his family Mrs Charitas Cho, Hayoung Cho, and Haeun Cho, who always treated me as their family member and prayed for me. My second home where I can rest and feel safe in a foreign country. This thesis would not have been completed without continuous supports from my parents and mentor's family. Thank you for everything, and I dedicate this thesis to all of you.

Table of Contents

List of Figures

List of Tables

List of Abbreviations

AKT	Protein kinase B
AML	Acute myeloid leukaemia
AMPK	AMP-activated protein kinase
ANGPT2	Angiopoietin 2
AP1	Activator protein 1
APOB	Apolipoprotein B
Arg1	Arginase 1
ATM	Ataxia telangiectasia mutated
ATR	Ataxia telangiectasia and Rad3-related protein
bFGF	Basic fibroblast growth factor
BMDM	Bone marrow-derived macrophage
BRCA	Breast Cancer gene
C/EBPα	CCAAT/enhancer-binding protein α
CA9	Carbonic anhydrase IX
CCL	C-C motif chemokine ligand
CCR	Chemokine receptor
CDK2	Cyclin-dependent kinase 2
cDNA	Complementary DNA
CDX	Cell line xenograft model
CHI3L1	Chitinase-3-like protein 1
CSF1	Colony-stimulating factor 1
CXCL	Chemokine (C-X-C motif) ligand
DAMP	Damage-associated molecular pattern
DBS	Double-stranded breaks
DCIS	Ductal carcinoa *in situ*
DMEM	Dulbecco’s Modified Eagle's Medium
DMSO	Dimethyl Sulfoxide
DNA	Deoxyribonucleic acid
ECM	Extracellular matrix
EDTA	Ethylenediaminetetraacetic acid
EGF	Epidermal growth factor
EGFR	Epidermal growth factor receptor
EGFR	Epidermal growth factor receptor
EMMPRIN	Extracellular matrix metalloproteinase inducer
ER	Estrogen receptor

ERK	extracellular signal-regulated kinase
ERK	Extracellular regulated MAP kinase
FACS	Fluorescence-activated cell sorting
FACS	Fluorescence-activated cell sorting
FBS	Foetal Bovine Serum
FFPE	Formalin-fixed paraffin-embedded
FIZZ1	Resistin-like molecule alpha 1
FOXP3	Forkhead box P3
GEMM	Genetically engineered mouse model
GM-CSF	Granulocyte-macrophage colony-stimulating factor
H&E	Haematoxylin & Eosin
HCC	Hepatocellular carcinoma
HER2	Human epidermal growth factor receptor 2
HGF	Hepatocyte growth factor
HLA-DR	Major histocompatibility complex, class II, DR
HR	Hormone receptor
HSC	Hematopoietic stem cell
IDC	Invasive ductal carcinoma
IDO	Indoleamine 2,3-dioxygenase
IFN	Interferon
IFNGR	Interferon-gamma receptor
IL	Interleukin
ILC	Invasive lobular carcinoma
IMDM	Iscove's Modified Dulbecco's Media
iNOS/NOS2	Inducible nitric oxide synthase
IRES	Internal ribosomal entry site
JAK	Janus kinase
JNK	c-JUN N-terminal kinase
LPS	Lipopolysaccharide
MAPK	Mitogen-activated protein kinase
MCP	Monocyte chemoattractant protein
M-CSF	Macrophage colony-stimulating factor
MDM	Monocyte-derived macrophage
MDP	Monocyte-macrophage dendritic cell progenitor
MDSC	Myeloid-derived suppressor cell

MHC	Major histocompatibility complex
MMP	Matrix metalloproteinase
MPK1	Mitogen-activated protein kinase 1
MRC1/MR	Mannose receptor C-type 1
mTOR	Mammalian target of rapamycin
NK cell	Natural killer cell
NO	Nitric oxide
PAMP	Pathogen-associated molecular pattern
PARP	Poly-ADP ribose polymerase
PBMC	Peripheral blood mononuclear cell
PBS	Phosphate Buffered Saline
PBSE	PBS–EDTA
pCR	Pathogenic complete response
PCR	Polymerase chain reaction
PD1	Programmed cell death protein 1
PDGF	Platelet-derived growth factor
PD-L1	Programmed death-ligand 1
PDX	Patient-derived xenograft
PEST	Proline, glutamic acid, serine, and threonine
PI3K	Phosphoinositide 3-kinase
PIK3CA	α-catalytic subunit of PI3K
PKC	Protein kinase C
PR	Progesterone receptor
PRR	Pattern recognition receptor
PSBP	Prostate steroid-binding protein
PTEN	Phosphatase and tensin homolog
PV TAM	Perivascular tumour-associated macrophage
PVDF	Polyvinylidene difluoride
PVM	Perivascular macrophage
RT-qPCR	Real-time polymerase chain reaction
RBC	Red blood cell
REDD1	Regulated in development and DNA damage response 1
RIPA buffer	Radioimmunoprecipitation assay buffer
RNA	Ribonucleic acid
RPMI	Roswell Park Memorial Institute Medium
SCARB1	Scavenger receptor class B type 1
SDS	Sodium dodecyl sulphate

STAT	Signal transducer and activator of transcription
SUSD2	Sushi domain containing 2
TAM	Tumour-associated macrophage
TBST	Tris-buffered saline-Tween
TCR	T cell receptor
TDM	Tumour dissociation medium
TGFβ	Transforming growth factor-beta
T_H	T helper cell
TIC	Tumour-initiating cell
TIE2	TEK receptor tyrosine kinase
TLR	Toll-like receptor
TMEM	Tumour microenvironment of metastasis
TNBC	Triple-negative breast cancer
TNF	Tumour necrosis factor
TNM	Tumour, Node, Metastasis
TP53	Tumour protein p53
Tregs	Regulatory T cells
TRIB	Tribbles homolog
TSC	trisodium citrate
VCAM-1	Vascular cell adhesion molecule 1
VEGF	Vascular endothelial growth factor
VLDL	Very-low density lipoprotein
YAP	YES-associated protein
YM1	Chitinase-like 3

Abstract

Tumour-associated macrophages (TAMs) recruited and re-educated by cancer cells account for up to 50% of the solid tumour mass and enhance tumour development mainly through their phenotypic alterations. TRIB1 is one of the myeloid cell regulatory genes emphasised for the regulation in macrophage physiology and reported to be oncogenic in acute myeloid leukaemia (AML). However, the role of myeloid TRIB1 in tumour development has not been studied. Here, we knockdown *TRIB1* in primary human monocyte-derived macrophages (MDMs) *in vitro*, and developed *in vivo* breast cancer models with myeloid *Trib1* overexpressing ($Trib1^{mTg}$) and knockout ($Trib1^{mKO}$) mice strains to investigate the myeloid *TRIB1*-dependent regulation of breast tumour growth.

Our data showed that *TRIB1* regulates human MDM phenotypes, markedly *TRIB1* knockdown significantly increased the oncogenic cytokine expression in TAMs developed from human MDMs. However, interestingly, our *in vivo* mouse model revealed both alterations of myeloid *Trib1* expression accelerated murine mammary tumour growth, but with the earlier stage enhancement in the $Trib1^{mKO}$ animals. Post-mortem analysis demonstrated a significant reduction of macrophages in the tumours from both strains, but the reduction in $Trib1^{mTg}$ tumours was in hypoxic TAMs whilst the reduction of perivascular TAM numbers was observed in $Trib1^{mKO}$ tumours. Furthermore, myeloid *Trib1* overexpression significantly inhibited polarisation of TAMs towards a pro-inflammatory phenotype and reduced T cell infiltration, especially CD8+ cytotoxic T cells. $Trib1^{mTg}$ animals also had accelerated development of secondary tumours in the lung.

Current results denote that the regulation of myeloid *Trib1* expression has distinct oncogenic mechanisms in breast cancer growth. *Trib1*-deficiency disrupts the homing of myeloid cells into the tumour and enhances oncogenic cytokine expression in TAMs to accelerate breast

tumour growth, whilst overexpression enhances growth of the mature tumour by the reduction of pro-inflammatory TAMs and recruitment of T-cells, suggesting potential importance of myeloid *Trib1* expression in the development of breast cancer therapies.

Chapter 1. Introduction

1.1 Breast cancer

Breast cancer is a group of malignant cells with abnormal growth observed in mammary glands and for many years, had highest incidence of all cancers in women worldwide (Feng et al., 2018). However, upon development of personalised medicine and novel treatments, significant improvement of cancer survival has been observed in most countries. In breast cancer, mortality rates started to fall from 1990 in most of western Europe, United States and Australia due to the early detection of disease with widespread mammographic screening and precise diagnosis which increased the number of early diagnoses and treatment (Veronesi et al., 2005). However, breast cancer is still the most common and leading cause of cancer death in females worldwide. In 2012, 1,676,600 cases of breast cancer were diagnosed in women with 521,900 cases of deaths world-wide, followed by colon cancer (614,300 cases of diagnosis with 320,300 cases of deaths) and lung cancer (583,100 cases of diagnosis with 491,200 cases of deaths), which accounts for 25% of all cancer cases and 15% of all cancer deaths among females (Torre et al., 2015). In 2015, the incidence of breast cancer increased to 2,378,000 cases in females worldwide, but the mortality rate declined to 523,000 cases which imply that early detection and enhanced diagnosis of breast cancer reduced the disease burden (Fitzmaurice et al., 2017). Statistical analysis of breast cancer incidence, however, revealed that the mortality rate declined in high-income countries with a historically higher rate of breast cancer death, but continued to increase in low-rate countries, such as in Latin America, Caribbean, and parts of Asia due to the changes of risk factors and lack of early detection and treatments (Azamjah et al., 2019, Fitzmaurice et al., 2017). Risk factors include genetic mutations either inherited from parents or resulted from ageing or other lifestyle-

related factors, and non-genetic factors, such as pregnancy-related hormone changes, anthropometric indices, dietary factors, especially with excessive alcohol consumption, lack of physical activity, and history of radiation or hormone replacement therapy treatments at the early age (Veronesi et al., 2005, Feng et al., 2018).

1.1.1 Origin of breast cancer

The development of breast cancer is initiated from the formation of a tumour niche by cancer-initiating cells or breast cancer stem cells derived from mutated mammary stem cells, progenitor cells, and differentiated cells (**Figure 1.1A**) (Feng et al., 2018, Sin and Lim, 2017). The historical nomenclature of luminal and basal-like breast cancers was derived from similar transcriptomic signatures between breast tumours and the corresponding normal mammary luminal and basal epithelium which originated from the oncogenic events of different types of mammary cells (Zhou et al., 2019). For instance, mutation of PIK3CA (α-catalytic subunit of PI3K) is observed in 30% of breast cancers, both luminal and basal-like tumours but mutation of PIK3CA in luminal cells generated both luminal and basal-like breast tumours. However, basal cells only induced luminal tumours and a mutation of PIK3CA and BRCA1 in luminal cells, and BRCA1 and p53 in basal cells generated basal tumours (**Figure 1.1B**)(Yang et al., 2017, Zhang et al., 2017a, Zhou et al., 2019).

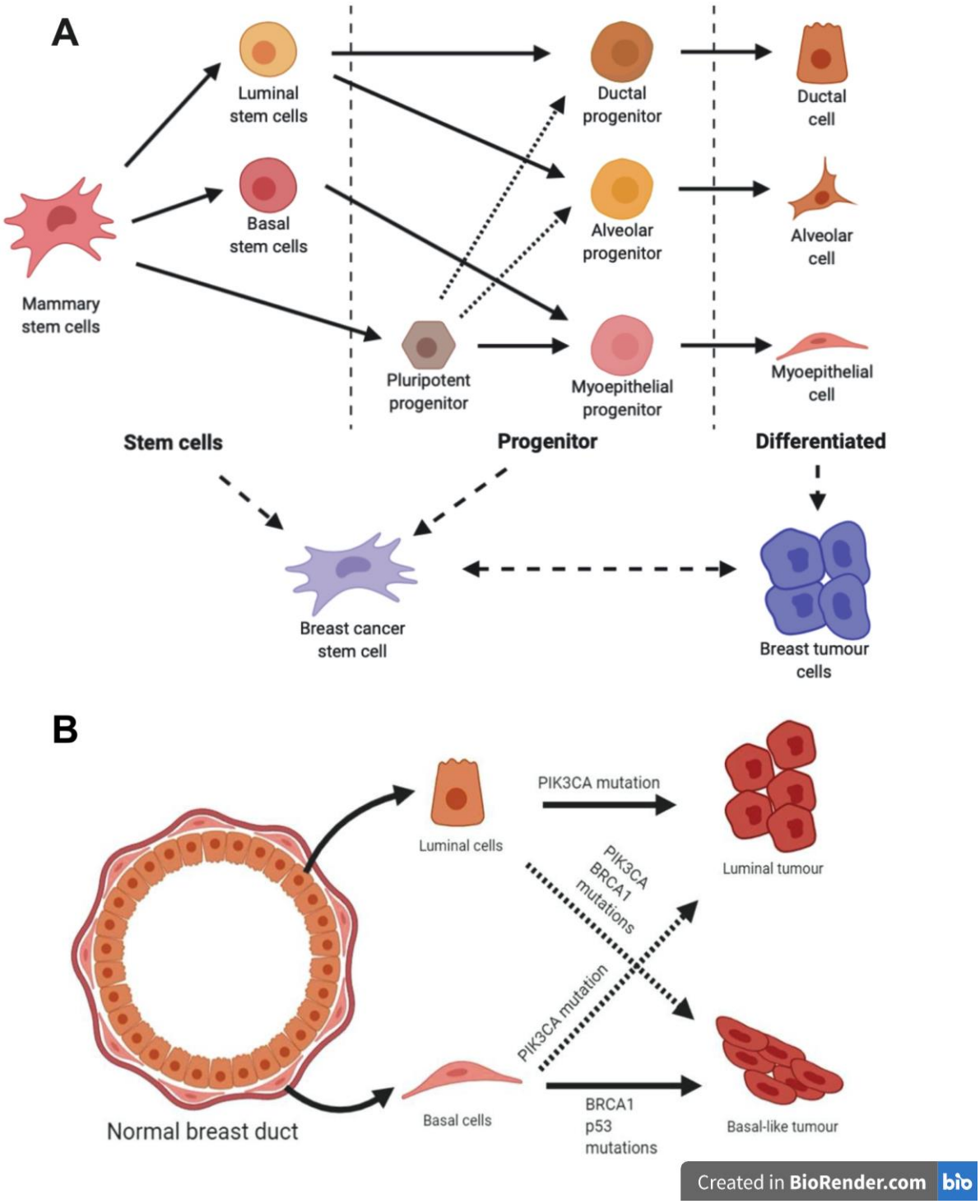

Figure 1.1. Hierarchy of mammary cells and the development of breast tumour cells. [adapted from (Feng et al., 2018, Zhou et al., 2019)]. (A) Schematic diagram of the breast cancer stem cell and breast tumour cell hierarchy from mammary cells. (B) Schematic diagram of the breast tumour cell origin depending on the gene mutations.

1.1.1.1 Classification of breast cancer

The classification of breast cancer varies from simple histological differences to molecular changes. Histological grading differentiates tumour and healthy tissues via the abnormality of tissues observed under a microscope (grade 1-4), and the Tumour (T) Lymph node invasion (N) Metastasis (M) system classifies breast cancer with the numbers 0-4. These describe the size and location of tumours, number of lymph nodes invasion, and the number of metastases (**Table 1.1 & Table 1.2**) (Taherian-Fard et al., 2015). However, heterogeneity in breast cancer further developed the concept of molecular classification in 2000, which divided breast cancer into luminal A, luminal B, HER2 enriched, basal and normal-like subgroups depending on the oestrogen receptor (ER), progesterone receptor (PR), and human epidermal growth factor receptor 2 (HER2) expression in the tissues (**Table 1.3**) (Eliyatkin et al., 2015). The molecular classification correlates with the clinical classifications, especially with ER and HER2 status, proliferation markers, and histological grades but recent studies suggested the further development of molecular classification since the categorization of breast cancer depends on the expression of hormone receptors (ER and PR) in 1% of tumour cells and observation of HER2 overexpression or amplification in 10% of tumour cells, and also due to the heterogeneity of cancer (Eliyatkin et al., 2015, Jackson et al., 2020).

Table 1.1. TNM system and anatomic stage groups of breast cancer. [adopted and modified from (Taherian-Fard et al., 2015, Feng et al., 2018)]

Classifications		Definition
TNM system	Tumour (T) 0	No evidence of tumour
	T1	Invasive tumour size ≤20mm and carcinoma *in situ*
	T2	Invasive tumour size 20-50mm
	T3	Invasive tumour size >50mm
	T4	Tumour has grown into the chest wall and skin
	Lymph node invasion (N) 0	No cancer cell in the lymph nodes
	N1	Cancer spread to three nodes
	N2	Cancer spread to four to nine nodes
	N3	Cancer spread to ≥10 nodes
	Metastasis (M) 0	No metastasis
	M1	There is evidence of metastasis to another body part
Anatomic stage system	Stage 0	Ductal carcinoma *in situ*
	Stage 1A	Primary invasive tumour size with a size of ≤20mm. No nodal involvement
	Stage 1B	Nodal micro-metastases (>0.2mm, <2.0mm) with or without ≤20mm primary tumour
	Stage 2A	Movable ipsilateral Level I, II lymph node metastases with ≤20mm primary tumour; or >20mm, ≤50mm tumour with no nodal involvement
	Stage 2B	Movable ipsilateral Level I, II lymph node metastases with >20mm, ≤50mm tumour; or >50mm tumour with no nodal involvement
	Stage 3A	Movable ipsilateral Level I, II lymph node metastases with >50mm tumour; or any size of the primary tumour with fixed ipsilateral Level I, II or internal lymph node metastases
	Stage 3B	Primary tumour with chest wall and/or skin invasion
	Stage 3C	Any size of the primary tumour with supraclavicular or ipsilateral Level III lymph node metastases; or with ipsilateral Level I, II and internal lymph node metastases.
	Stage 4	Any case with distant organ metastasis

Table 1.2. Types of breast cancer. [modified from (Feng et al., 2018)]

Cancer	Descriptions
Ductal carcinoma *in situ* (DCIS)	Non-invasive or pre-invasive breast cancer developed inside normal ducts
Invasive or infiltrating breast cancer	Cancer invades and spread outside of the normal breast lobules and ducts
Invasive ductal carcinoma (IDC)	The most common type of breast cancers which accounts for 80% of all cases. IDC includes tubular carcinoma, medullary carcinoma, mucinous carcinoma, papillary carcinoma, and cribriform carcinoma of the breasts.
Invasive lobular carcinoma (ILC)	The second most common type of breast cancer that accounts for 10-15% of all invasive breast cancers. ILC developed as single cells arranged individually, single file, or in sheets in the lobules and invades the tissue of the breast.

Table 1.3. Molecular subtypes of breast cancer [Adopted from (Eliyatkin et al., 2015)]

Cancer	Gene expression pattern	Clinical and biological properties
Luminal A	Expression of luminal (low molecular weight) cytokeratins, high expression of hormone receptors and related genes	50% of invasive breast cancer, ER/PR positive, HER2/neu negative
Luminal B	Expression of luminal (low molecular weight) cytokeratins, moderate-low expression of hormone receptors and related genes	20% of invasive breast cancer, ER/PR positive, HER2/neu expression variable, higher proliferation than Luminal A, higher histologic grade than Luminal A
Her2/neu	High expression of HER2/neu, low expression of ER and related genes	15% of invasive breast cancer, ER/PR negative, HER2/neu positive, high proliferation, diffuse TP53 mutation, high histologic grade and nodal positivity
Basal-like	High expression of basal epithelial genes and basal cytokeratins, low expression of ER and related genes, low expression of HER2/neu	~15% of invasive breast cancer, most ER/PR/HER2/neu negative (triple-negative), high proliferation, diffuse TP53 mutation, BRCA1 dysfunction (germline, sporadic)

1.1.2 Gene mutations in breast cancer

Breast cancer susceptibility gene 1 (BRCA1) was the first dominant gene, associated with hereditary breast cancer. Approximately 10-20% of breast cancer patients have the first-degree relative with breast cancer, and up to 20% of women with a family history have a mutation in the BRCA1 or BRCA2 (Feng et al., 2018). BRCA1 is also a substrate of central DNA damage response kinase ATM (ataxia telangiectasia mutated) and ATR (ataxia telangiectasia and Rad3-related protein) which regulate DNA damage response (Vega, 2013, Tarsounas and Sung, 2020). The C-terminal of BRCA1 binds to a GAL 4 DNA binding domain to regulate transcription activation; binds to phospho-peptides involved in the DNA repair and cell cycle checkpoint; and fuse with RAD51 to detect and recombine the double-stranded breaks (DBS) (Sheikh et al., 2015). BRCA2 is also involved in homologous recombination and recruits RAD51 to the site of DNA damage or localises to DBS together with BRCA1 and interacts with PALB2 to undertake DNA repair at the S phase checkpoint (Vega, 2013, Sheikh et al., 2015).

The mutations of BRCA1 and BRCA2 are classified as high-penetrance genes which, together with others, cause 82% of lifetime breast cancer risk. Other high-penetrance genes include PTEN (85% lifetime risk), TP53 (25% risk by the age of 74), CDH1 (39% risk of lobular breast cancer), and STK11 (32% risk by the age of 60) (Shiovitz and Korde, 2015). PTEN is known to downregulate the PI3K/AKT pathway by dephosphorylation of PIP3, inhibiting the growth and survival signals to suppress tumour growth and about half of breast tumours show loss of PTEN activities (Kechagioglou et al., 2014, Carbognin et al., 2019). The frequency of PTEN loss is up to 30-40% in sporadic breast carcinomas, and the expression of PTEN is negatively correlated with the aggressiveness of breast cancer (tumour size, lymph node metastasis, and TNM stage), and poor differentiation. PTEN loss is also

significantly correlated with ER and PR expression (Zhang et al., 2013, Li et al., 2017). In addition, mutually exclusive but the dysregulation of the PI3K/AKT pathway is also caused by PIK3CA mutations which consist of up to 30% of breast cancer patients (Feng et al., 2018).

Tumour suppressor gene TP53 encodes p53 which binds to DNA in response to DNA damage and drives p21 and CDK2 interaction that blocks cell cycle in case of uncontrolled cell division and ultimately tumour formation or activates transcription of proteins involved in DNA repair (Huszno and Grzybowska, 2018). The somatic mutation of TP53 accounts for 40% of breast cancer cases but the germline TP53 mutation also increases the risk of early onset of severe breast cancer together with Li-Fraumeni Syndrome (Sheikh et al., 2015, Huszno and Grzybowska, 2018). CDH1 encodes another tumour suppressor gene E-cadherin, which is involved in the formation of cellular architecture, maintenance of tissue integrity and function of epithelial tissues and the mutation of CDH1 and dysfunction of E-cadherin decreased the adhesion activity which results in the increased cellular motility primarily associated with cancer metastasis (Sheikh et al., 2015).

1.1.2.1 Aberrant signalling pathways in breast cancer

Mutations of genes observed in breast cancer alter different signalling pathways involved in tumour development, including MAPK, AKT, and WNT pathways (**Table 1.4**). Mitogen-activated protein kinase (MAPK) signalling is one of the pathways altered in cancer. MAPKs are serine-threonine kinases and form a three-member cascade: MAPK, MAP2K, and MAP3K, where MAP3K activates MAP2K and MAP2K activate MAPK by phosphorylation of S/T and Y/T residues (Lawrence et al., 2008, Soares-Silva et al., 2016). MAPKs include p38, c-JUN N-terminal kinase (JNK), and extracellular signal-regulated kinase (ERK) which

are activated by cellular stress or pro-inflammatory cytokines, IL-1β (Kim and Choi, 2010, Guo et al., 2020). MAPK/ERK pathway is mostly targeted for the cell proliferation by EGFR, KRAS and BRAF mutations because ERK in the cytoplasm affects cell movement and trafficking, metabolism and cell adhesion. After MAPK/ERK activation, ERK translocates to the nucleus and phosphorylates and activates transcription factors such as CPS II, which facilitates cell cycle progression (Burotto et al., 2014). Additionally, activation of the EGFR-ERK pathway promotes intestinal hypertrophy, colonic polyps and cancer growth. The ERK/MAPK is reported to proliferate and inhibit apoptosis in different cancers by regulating the activity of downstram cell cytcle regulatory proteins, apoptosis-related proteins and other effector molecules such as G1/S specific cyclin D1, SPARCRC-like protein1, and AP1 complex, which balances cell proliferation and apoptosis (Fang and Richardson, 2005, Guo et al., 2020).

AKT kinases (protein kinase B) are downstream of tyrosine kinases and phosphatidylinositol 3-kinase (PI3K) and also play a role in oncogenesis. AKT regulates a number of cellular processes, including glucose metabolism and genome stability. The AKT pathway consists of tumorigenesis-related proteins, including subunits of PI3K, BCL3, eIF4E and PKT (acting as oncoproteins) and PTEN, LKb1, TSC2/TSC1, NF1 and VHL (which are tumour suppressors that are often mutated in cancer) (Altomare and Testa, 2005, Testa and Tsichlis, 2005, Urban et al., 2016). The alteration of AKT 1 and AKT2 reported to influence initial tumour, and metastasis development, where co-expression of ErbB2/AKT1 facilitates tumour formation and reduces metastasis, whereas ErbB2/AKT2 co-expression accelerates metastases compared to ErbB2/AKT1 or ErbB2 expression alone (Clark and Toker, 2014, Toker and Marmiroli, 2014). The mutations of ErbB2 also also enhances the proliferation of breast cancer cells and ErbB2/AKT pathway promoted chemoresistance to lapatinib (Yang et al.,

2020). In the tumour, cell survival is improved by the inhibition of apoptosis. According to Toulany and Rodemann (Toulany and Rodemann, 2013), AKT inactivates ‘pro-apoptotic proteins such as BAD, BAX and caspase-9’ and stimulates the expression of anti-apoptotic proteins including ‘FLIP, surviving, cIAP1/cIAP2, A1/Bfl-1, and XIAPs’.

Table 1.4. Aberrant signalling in Tumorigenesis due to Genetic Alterations. [Adopted from (Cell Signaling Technology; (Dreesen and Brivanlou, 2007, McCleary-Wheeler et al., 2012)].

Functions	AKT Pathway	GPCR Pathway	Ras Signalling	TGF-β Signalling	WNT/β-Catenin signalling	Hedgehog Signalling	Notch Signalling
Apoptosis evasion	AKT Bax FoxO PI3K Bcl2 PTEN		Fos/Jun RTKs			Gli Hedgehog Smo Ptch Su(fu)	Notch
Promote tumour growth	LKB1 TSC1/TSC2	Ga GPCR	B-Raf Fos/Jun Ras RTKs NF1/2	MYC	β-catenin RAR WNT1 APC WNT5A	Gli Hedgehog Smo Ptch Su(fu)	
Reduce anti-growth sensitivity				Smad2/3 Smad4 TGFβR			
Invasion & Metastasis			RTKs Integrin		α-catenin		
Angiogenesis			RTKs				

The WNT/β-catenin pathway is one of the key cascades associated with cancer. It is commonly divided into the β-catenin-dependant canonical, and β-catenin-independent non-canonical WNT pathways. WNT also plays a role in embryonic development and homeostasis, which facilitates the formation of cancer stem cells and cancer (Kazi et al., 2016). In cancer, the WNT pathway is upregulated by inhibiting the *APC* gene, which forms a destruction complex with the scaffold protein Axin and kinases (GSK3β and casein kinase) and degrades β-catenin by phosphorylation before localisation to the nucleus or activates the *β-catenin* gene (Zhan et al., 2017, Tung et al., 2017). MAPK signalling is also associated with proliferation and cell survival in colorectal cancer by the activation of WNT and p38delta MAPK (Horst et al., 2012, Stramucci et al., 2019).

1.1.3 Breast cancer treatments

1.1.3.1 Early breast cancer treatments

In early breast cancer without metastasis, patients with tumours undergo surgical removal of cancer together with systemic therapies either before the surgery (neoadjuvant) to reduce the tumour burden in large tumours or to improve the clinical outcome, or after surgery (adjuvant), in case of increased risk of recurrence (Harbeck et al., 2019). The development of surgical treatment focused on breast conservation enabled breast-conserving surgery via systemic neoadjuvant therapy and enhanced oncoplastic techniques but the increased rate of prophylactic mastectomies. This removes healthy breasts for prevention with the equivalent relapse-free and overall survival to the conservation surgery with radiotherapy, reduced the success of the development focussed on conservation (Harbeck et al., 2019, Waks and Winer, 2019).

Radiotherapy was emphasised for breast cancer treatment for many years where postoperative radiotherapy enhances the disease-free and overall survival of patients with early or advanced breast cancer, and also reduced the locoregional recurrence of breast cancer up to 75% together with local control and reduced up to 35% followed by lumpectomy (Pfeffer, 2018, Waks and Winer, 2019, Harbeck et al., 2019). Radiotherapy induces DNA damage of cells via direct ionization, or production of free-radicals by ionization or excitation of water leading to the cell death, especially in cancer as the cancer cells have slow DNA repair and produce more DNA breaks compared to normal cells (Baskar et al., 2014). Systemic therapies are essential for enhanced disease-free survival of patients, and the drugs given as systemic therapy are classified as hormone, chemo-, and molecular target therapies, neoadjuvant and adjuvant (Shien and Iwata, 2020). Neoadjuvant chemotherapy and hormone therapy are used, especially with HER2+ or ER+ breast cancer patients, to improve breast-conserving rates of patients without distant metastasis, but, a meta-analysis confirmed similar disease-free and overall survival with the use of same drugs either as adjuvant or neoadjuvant systemic therapies (Van De Wiel et al., 2017, Shien and Iwata, 2020). Triple-negative breast cancer (TNBC) has a significantly lower response to therapies compared to other subtypes, and chemotherapy is preferable as neoadjuvant with the pathogenic complete response (pCR) of about 40% (Pandy et al., 2019, Van De Wiel et al., 2017, Waks and Winer, 2019). The standard TNBC chemotherapy typically consists of taxane and anthracycline where taxane promotes cell-cycle arrest and apoptosis by binding to β-tubulin and stabilize microtubule complexes and promotes microtubule polymerization, and anthracycline interacts with DNA and topoisomerase II to impair DNA replication and repair which thereby promoting apoptosis (Moreno-Aspitia and Perez, 2009). The general mutation of BRCA gene in TNBCs which results in the susceptibility of cells to DNA damage compounds such as platinum

drugs and the biological hallmark of deficient DNA damage repair in some TNBCs emphasised the role of platinum chemotherapy, where neoadjuvant chemotherapy with carboplatin increased the pCR which depends on the varying treated agents together with platinum therapy and TNBC subtypes (Pandy et al., 2019, Waks and Winer, 2019). However, the increased toxicity with platinum treatment and unclear mechanism of the treatment requires further development of this approach in TNBCs (Pandy et al., 2019). pCR at surgery is essential in neoadjuvant chemotherapy of TNBC where patients who achieved pCR improved prognosis compared to those who did not and in the case of non-pCR, additional adjuvant treatment of capecitabine produces anti-metabolite fluorouracil and improves disease-free survival and overall survival (Waks and Winer, 2019, Harbeck et al., 2019, Xu et al., 2019).

In HER2+ breast cancer, which consists of 20% of all cancer cases, neoadjuvant chemotherapy with anti-HER2 therapy became the standard of care in tumours with ≥tumour (T) 2 and ≥lymph node invasion (N) 0, where the standard neoadjuvant treatment includes the anthyracycline-taxane sequence (or docetaxel and carboplatin) with dual HER2 blockade (anti-HER2 antibodies trastuzumab and pertuzumab) to improve pCR rates and disease-free survival (Harbeck et al., 2019). Depending on the pCR status at surgery, postoperative anti-HER2 therapy can be switched to T-DM1 (HER2 blockade with a cytotoxic agent trastuzumab-emtansine) in non-pCR to improve the outcome (Harbeck et al., 2019, Shien and Iwata, 2020). In small HER2+ tumours without lymph node invasion (pT1, pN0), adjuvant paclitaxel (taxane) with trastuzumab treatment is considered efficient (Shien and Iwata, 2020).

In all luminal (hormone receptor-positive) breast cancer, adjuvant hormone therapy or endocrine therapy is the primary systemic therapy for patients where the standard treatment

contains oral antiestrogen medication for 5-10 years after surgery, and the sensitivity directly correlates with the degree of hormone receptor positivity (Waks and Winer, 2019, Harbeck and Gnant, 2017). Tamoxifen is an estrogen antagonist that competitively disrupts the binding of estrogen to the receptor and effective in both pre- and postmenopausal women, whilst aromatase inhibitors suppress estrogen biosynthesis to convert androgen to estrogen by inhibition of aromatase and effective only in postmenopausal women (Morales et al., 2005). Compared to the non-systemic therapy, 5 years of tamoxifen treatment to hormone receptor (HR) positive patients was shown to reduce breast cancer recurrence rate by 50% and the inhibition was more efficient in a postmenopausal woman with 5 years of aromatase inhibitor where a 10-year breast cancer recurrence risk of tamoxifen and aromatase inhibitors were 22.7% and 19.1% respectively (Harbeck et al., 2019, Waks and Winer, 2019). A meta-analysis also demonstrated reduced mortality by 15% in HR+ patients with aromatase inhibitors compared to tamoxifen but the longer administration of aromatase inhibitors correlated to the increased bone-related adverse events such as fracture, pain and osteoporosis (Shien and Iwata, 2020). Different strategies have been explored to extend adjuvant endocrine therapy from 5-10 years, and most of the data suggest best outcomes on patients with the highest risk of relapse with 5 years of tamoxifen and up to 3 years of an aromatase inhibitor treatment to patients (Pondé et al., 2019). Premenopausal patients are at highest risk of relapse after adjuvant chemotherapy, ovarian suppression with a gonadotropin-releasing hormone analogue enhanced the disease-free survival of both tamoxifen and aromatase inhibitors compared to endocrine therapy alone (Pondé et al., 2019, Waks and Winer, 2019). In addition to endocrine therapy, chemotherapy is also recommended to luminal HER2-negative breast cancer depending on the individual risk of recurrence when the estimated risk

is >10% over 10 years and for high clinical risk patients with N3, anthracycline-taxane regimen is preferred (Harbeck et al., 2019).

1.1.3.2 Advanced metastasis breast cancer treatments

Advanced breast cancer consists of inoperable, locally advanced breast cancer without distant tumours and metastatic breast cancer which commonly spread to the bone (67%), liver (40.8%), and lung (36.9%) (Harbeck et al., 2019). Metastatic breast cancer is classified incurable disease that caused almost all patient deaths with a median overall survival of 2-3 years, thereby, the therapeutic goal of metastatic breast cancer is to maintain quality of life and relieve symptoms (Harbeck and Gnant, 2017, Harbeck et al., 2019). Radiation therapy has a critical impact on the metastases to bone, brain and soft tissues with sufficient reduction of tumour volumes, and the use of radiotherapy is emphasised in the field of immunotherapy as the most of metastatic breast cancer types are immune cold tumours, resistant to immunotherapy (Harbeck et al., 2019).

For all luminal-like metastatic breast cancers (HR+), endocrine-based therapy is prescribed until the patients build endocrine resistance or observe severe organ dysfunction (Harbeck et al., 2019). Similar to early breast cancer, endocrine therapy (tamoxifen, an aromatase inhibitor, or fulvestrant) alone or co-treatment of ovarian suppressor to pre-menopausal patients can be used as first-line therapy, CDC inhibitors or mTOR inhibitors are typically incorporated to delay and overcome the development of endocrine resistance (Waks and Winer, 2019, Pondé et al., 2019).

In HER2+ metastatic breast cancers, standard first-line therapy consists of dual blockade of HER2 (trastuzumab and pertuzumab) with chemotherapy, where the HER2 blockade significantly increased the time to disease progression, objective response rate, the median

duration of response as well as enhanced overall survival (Burcombe, 2017). The antibody-drug conjugate Trastuzumab emtansine is frequently used as second-line therapy as the antibody ensures maximal cytotoxicity in the HER2+ tumour cells which result in the improved quality of life and reduced adverse events compared to other second-line therapy (Burcombe, 2017, Harbeck and Gnant, 2017). For TNBCs, however, cytotoxic chemotherapy is the only option for the patients without germline BRCA1/2 mutations, and with PD-L1 expressing TNBCs, combination therapy with immunotherapy can be administered as first-line therapy where the nab-paclitaxel with atezolizumab (anti-PD-L1 antibody) demonstrated an objective response rate of 67% followed by 25% in second-line and 29% in the third or further lines (Sugie, 2018, Waks and Winer, 2019). Platinum-based therapy is also one of the preferred options, and for germline BRCA11/2-associated TNBCs, PARP inhibitors, which interrupts identification of DNA damage and blocks DNA repair, demonstrated improved progression-free survival and quality of life compared to monochemotherapy (McCann and Hurvitz, 2018, Harbeck et al., 2019).

However, despite the decades of cancer therapy development, about 90% of failure rate was reported in solid tumour treatment, particularly with chemotherapy and immunotherapy (Maeda and Khatami, 2018). The genetic mutations caused by molecular agents or targeted drugs with additional increase of drug-induced immune suppression and the influence of growth pathways such as PI3K/AKT/mTOR increased cancer relapse in chemotherapy, and immunotherapy which applies adaptive and innate immune cells such as cytotoxic T cells, NK cells, and dendritic cells to target surface molecules still requires a fundamental understanding of immune and non-immune cell composition, the interaction of host immune and target tumour cells and their responses (Maeda and Khatami, 2018). Therefore, understanding cancer biology is a critical aspect to improve breast cancer treatment.

1.1.4 Experimental mouse models of breast cancer studies

None of the 'models' to study human disease is perfect regardless of the degree of sophistication (Manning et al., 2016). However, *in vivo* modelling provides advanced knowledge to the breast cancer field, thereby an increasing number of animal models are available to study breast cancer, in particular, mouse models due to the small size, inexpensive housing, convenient handling, rapid breeding with relatively long life span, availability of complete mouse genome sequence, genetic characterization, and ease of mouse genome manipulation (Sakamoto et al., 2015, Manning et al., 2016).

Cell line xenografts (CDX) are the simplest and most frequently used model systems in cancer. Immortalized human cancer cell lines are transplanted into an immunocompromised mouse host (orthotopic transplant into the mammary fat pad to investigate primary tumour and metastasis, or inject cancer cells into mouse tail veins to monitor experimental metastasis) (Park et al., 2018) (**Table 1.5**). CDX is as a useful bridge between *in vitro* and *in vivo* studies to investigate target genes of interest or evaluate preclinical drugs for breast cancer due to the numbers of well-established and annotated human breast cancer cell lines from all molecular subtypes, similar stromal characteristics from human tumours, and ease of tumour growth and interrogation (Manning et al., 2016). However, developing human breast cancer in immunodeficient mice arouse vital limitations which ignore the effect of the immune system in cancer development and therapeutic responses, cross-species of tumour cells and stroma, and lack of heterogeneity compared to the clinical breast cancer (Manning et al., 2016, Holen et al., 2017).

Table 1.5. Brief overview of breast cancer CDX, PDX, and syngeneic mouse models. [Modified from (Park et al., 2018)]

Model	Mice strain	Cell line
CDX	BALB/c	BT20
	Nude	BT474
	NOD/SCID	MCF7
	C57BL	MDA-MB-231
		MDA-MB-435
		SUM1315
		SUM149
		T47D
		Hs578T
		ZR-75-1
		SK-BR-3
PDX	BALB/c	
	Nude	
	NOD/SCID	
	NSG	
	C57BL	
Syngeneic model	BALB/c	4T1
	C57BL	EMT6
		JC

In order to address the shortcoming of CDX, patient-derived xenografts (PDX), transplanting primary human cancer cells or surgically implanting tumour pieces into host mice were developed to improve clinical relevance (Holen et al., 2017). PDX approach was able to obtain genetic diversity and heterogeneity of cancer and available in various cancer subtypes, but the emphasis of PDX was to maintain many genetic and phenotypic integrities of the primary human tumour, especially the response to therapy (Manning et al., 2016). Among subtypes, it was particularly challenging to model ER+ luminal breast cancer due to the correlation of xenotransplantation success and the aggressiveness of breast cancer, which is unravelled by transplanting ER+ cells directly into the mouse ductal epithelium, hence avoiding TFGβ pathway activation and preserve the luminal phenotype (Holen et al., 2017). Although PDX models improved the investigation of mechanisms, building clinically relevant treatment resistance, PDXs have limitations that are identical to CDXs in many

aspects as follows: (1) forbids specific endogenous mutations in tumour cells; (2) immunodeficient host prevents development and evaluation of immunotherapy or any therapies with direct or indirect involvement of immune system; (3) species-related incompatibility; and (4) limited use to cohort-based preclinical studies (Sakamoto et al., 2015, Holen et al., 2017).

Instead of immunocompromised mice, syngeneic mouse models transplant mouse mammary tumours or tumour cell lines into the syngeneic immunocompetent host. This incorporates the impact of the immune system in tumour development and allows these cell types to be studied following therapies which provide a distinct advantage when studying cancer biology (Manning et al., 2016). For instance, implantation of TNBC cells (4T1) into the immunocompetent host with the mammary intraductal method provides a sequential progression of breast cancer development and invasion to metastasis via lymphatic or hematogenous dissemination within four weeks which allow details investigation of the underlying mechanisms of TNBC growth and therapies (Ghosh et al., 2018). The high invasiveness of murine cancer cells improve the investigation of anti-tumour and anti-metastatic roles of multiple drugs, but at the same time, the rapid growth rate of many cell lines limits the use in longer-term studies and the limited number of established, well-annotated cell lines are available for syngeneic models (Manning et al., 2016, Park et al., 2018).

In contrast to the CDX, PDX, and syngeneic models described above, genetically engineered mouse models (GEMMs) generate spontaneous breast tumour initiation modulation in mice via regulation of oncogenic transgenes in the mammary epithelium (Fantozzi and Christofori, 2006, Holen et al., 2017). Modification of mouse oncogenes are driven by promoters expressed in mammary cells (**Table 1.6**), and the transgene can be regulated by for instance

the Tet-On/Tet-Off system which can switch on or off the gene of interest in a time-specific manner (Fantozzi and Christofori, 2006). The conditional GEMM further emulate spatial and temporal activation or deletion of genes in human disease by *Cre/loxP* system, which generates recombination of DNA between *loxP* sites with tissue-specific promoter-driven *Cre* recombinase (Holen et al., 2017). GEMMs, therefore, can produce natural murine tumour microenvironment within the tissue of origin with an intact immune system that allows studying both early and late stages of tumour progression (Manning et al., 2016, Holen et al., 2017). However, genetics does not necessarily represent human tumours with uncontrolled transgene expressions or redundant expression/activity in non-mammary tissues, as well as extensive breeding programmes (especially in conditional GEMMs) limit the use of GEMMs (Holen et al., 2017, Manning et al., 2016).

C57BL/6 mouse strain is the inbred strain derived from the C57BL mouse, and in our study, we have used C57BL/6N originally developed at the Jackson Institute at the National Institutes of Health in 1950 (Kang et al., 2019). The basic immunological properties of C57BL/6 mouse are well described as the strain was established for anti-cancer and immunological studies and an international effort of Knockout Mouse Project allowed C57BL/6N mouse to harbour mutations embryonic stem cells which give benefit in reverse genetic studies (eg. Knockouts and transgenics) (Bryant, 2011). In our study, we have used C57BL/6N mouse developed myeloid-specific TRIB1 knockout and transgenic strains which were used in breast cancer models.

Table 1.6. Mammary gland-specific promoters. [adopted from (Fantozzi and Christofori, 2006)]

Promoter	Origin	Expression	Activation
MMTV-LTR	Mouse mammary tumour virus	Breast epithelial cells, several other tissues	Steroid hormones
WAP	Whey acidic protein	Secretory mammary epithelium	Lactogenic hormones
C3(1)	Rat prostate steroid-binding protein (PSBP)	Epithelial cells of the prostate and mammary gland	Estrogen (ductal and alveolar mammary epithelium)
B-LG	Bovine β-lactoglobulin	Mammary gland	Pregnancy and lactation
MT	Metallothionein	Most mammary cells	Zn^{2+}

1.2 Tumour microenvironment

Upon tumour development, the malignant cells recruit healthy, non-transformed cells to create a tumour microenvironment. The microenvironment consists of different stromal and immune cells, which possess anti-cancer properties by promoting immunosuppression and inhibiting tumorigenesis. However, once they have been re-educated to a tumour-associated neighbour by stimuli from the cancer cells, these cells start to express a wide range of cytokines, chemokines, growth factors, and proteinases which promote tumour development (Chen et al., 2015). Regulatory T cells (Tregs) induce immune suppressive function in the tumour microenvironment by the expression of IL-10 and TGF-β and evade tumour cells via cytotoxic T-lymphocyte antigen 4, and the deficiency of IL-10 disrupts neuopilin-1 in Tregs which activates Th1 and Th17 immunity (Balkwill et al., 2012, Wang et al., 2016a). B lymphocytes and myeloid-derived suppressor cells (MDSCs), which encompass ‘immature dendritic cells, neutrophils, monocytes, and early myeloid progenitors’, also exert immunosuppressive features, where the frequency of MDSCs generally increase in the spleen and blood of mouse tumour models, and in human, enhanced immunosuppressive $CD15^{+}$

MDSCs frequency was observed in spleen of cancer patients (Jordan et al., 2017). MDSCs also promote tumour neovascularization and disrupt normal immunosurveillance (Quail and Joyce, 2013, Chen et al., 2015). Tumour-associated neutrophils have both pro- and anti-cancer features. When these cells are oncogenic, they facilitate tumour growth, invasion, angiogenesis, metastasis and prognosis in different cancer types (Powell and Huttenlocher, 2016). Cancer-associated fibroblasts also facilitate cell cycle progression and tumour growth by secreting different growth factors, including fibroblast growth factor and insulin-like growth factor 1, and CXCL12 production. These cells promote immunosuppression by inducing epithelial-mesenchymal transition in malignant cells (Balkwill et al., 2012, Quail and Joyce, 2013, Liu et al., 2019a). Additionally, tumour microenvironment also consists of natural killer cells, tumour-associated macrophages (TAMs), adipocytes, vascular endothelial cells, dendritic cells, pericytes and lymphatic endothelial cells which secrete different cytokines, cell factors and proteins that form a network across the microenvironment to facilitate tumorigenesis and generate difficulties in identifying target markers for cancer therapy (Wang et al., 2017b). However, TAMs, which can comprise up to 50% of the tumour microenvironment, is one of the most important cell types in the promotion of tumour initiation and development, and the presence of these cells is associated with poor prognosis, angiogenesis and immunosuppression (Guo et al., 2016).

1.2.1 Tumour-associated macrophages

1.2.1.1 Origin of macrophages and tumour-associated macrophages

Macrophages are professional phagocytes of hematopoietic origin, which promote host defence by innate and adaptive immunity. They are first observed in the extraembryonic yolk sac during early gestation. At this stage, the yolk sac only produces white blood cells, but

upon development, hematopoietic stem cells (HSCs) emerge from the aorta-gonad-mesonephros and produce other immune cells (Epelman et al., 2014). The HSCs then migrate to the foetal liver at embryonic day 10.5 in mice, and the complete lineage of immune cells are produced from the perinatal period where 'bone marrow HSCs become the primary site of haematopoiesis' (Epelman et al., 2014).

Macrophages are produced from the yolk sac and become tissue-resident macrophages when they migrate to different tissues; however, macrophages can also differentiate from monocyte-macrophage dendritic cell progenitors (MDPs) (

Table 1.7). Monocytes are precursors of the mononuclear phagocytic system that includes macrophages and produced by the common monocyte progenitors and HSCs in the bone marrow (Hettinger et al., 2013, Guilliams et al., 2018). Monocytes are classified into 'classical' and 'non-classical' cells, where the murine classical ($Ly6c^{hi}$) monocytes distinguished by the larger size express $CCR2^{hi}/CX_3CR1^{lo}$ and secrete inflammatory cytokines (Boyette et al., 2017). These cells are able to differentiate to inflammatory macrophages when migrated to inflamed tissue. The non-classical or resident ($Ly6c^{lo}$) monocytes, in contrast, are characterised by CX_3CR1^{hi} and $CCR2^{lo}$ expression and patrol the lumen of the blood vessel to clear damaged endothelial cells. Non-classical monocytes express a low level of pro-inflammatory cytokines to bacteria-derived stimuli in comparison to classical monocytes which potentially affect the timing of recruitment for cells into inflammatory sites where Arnold et al., (2007) reported a subsequent increase of $Ly6c^{lo}$ CX_3CR1^{hi} monocytes in the injured site followed by $Ly6c^{hi}$ monocytes (Arnold et al., 2007, Thomas et al., 2015). Olingy et al., (2017) also reported recruitment of non-classical monocytes into the skin injury site, which mostly differentiated to anti-inflammatory $CD206^{+}$ macrophages to promote wound healing (Olingy et al., 2017).

Table 1.7. Types of tissue-resident macrophages and their origin [Modified from (Davies et al., 2013, Udalova et al., 2016, Ginhoux and Guilliams, 2016)].

Tissue	Cell types	Origin
Spleen	Marginal zone macrophages	Monocyte-derived macrophages
Adipose tissue	Adipose-associated macrophages	Unclear
Blood	Ly6C^{lo}monocytes	Monocyte-derived macrophages
Bone	Osteoclasts	Expected to be monocyte-derived macrophages
	Bone marrow macrophages	Yolk sac-derived or fetal monocyte-derived macrophages
Central nervous system	Microglia	Yolk sac-derived
	Perivascular macrophages	Monocyte-derived
	Meningeal macrophages	Monocyte-derived
	Choroid plexus macrophages	Monocyte-derived
Gastrointestinal tract	Intestinal macrophages	Monocyte-derived macrophages
Liver	Kupffer cells (sessile)	Mostly yolk sac-derived
	Motile liver macrophages	Monocyte-derived
Lung	Alveolar macrophages	Fetal monocyte-derived macrophages
	Interstitial macrophages	Mixed monocyte-derived and yolk sac-derived
Serosal tissues		
a. **Peritoneal cavity**	Large peritoneal macrophages	Yolk sac-derived or fetal monocyte-derived macrophages
	Small peritoneal macrophages	Monocyte-derived
b. Pleural cavity	Pleural macrophages	Monocyte-derived
Skin	Dermal macrophages	Mixed but mainly monocyte-derived macrophages
	Langerhans cells	Mostly fetal monocyte-derived macrophages
Spleen	Marginal zone macrophages	Monocyte-derived macrophages
	Metallophilic macrophages	Monocyte-derived macrophages
	Red pulp macrophages	Both Monocyte-derived and yolk sac-derived macrophages but predominantly yolk sac derived macrophages
	White pulp (tingible body) macrophages	

1.2.1.1.1 Markers for identifying TAMs

MDP, generated from HSCs, produces both monocyte-derived macrophages and dendritic cells. However, they can be distinguished by the expression of F4/80 (human homolog EMR1), CD11b and Fc receptors in both human and mouse macrophages (Galli et al., 2011, Waddell et al., 2018). In mouse macrophages, F4/80 is an essential factor to initiate immunological tolerance and CD8+ Tregs activation by interaction with NK cells (Lin et al., 2005, van den Berg and Kraal, 2005, Waddell et al., 2018). CD11b is a surface integrin receptor which recognises viral-produced dsRNA, a viral pathogen-associated molecular pattern (PAMP), and regulates innate immune responses of macrophages (Zhou et al., 2013). CD11b also affects the recruitment of macrophages to inflammatory sites (Kirby et al., 2006, Schmid et al., 2018). Fc receptors in macrophages mediate endocytosis and facilitate phagocyte activation and influence macrophage polarisation, producing several pro-inflammatory cytokines and chemokines in Fcγ receptor-activated monocytes and macrophages (Mellman et al., 1988, Guilliams et al., 2014).

1.2.1.1.2 Development of tumour-associated macrophages

TAMs are macrophages found in the tumour microenvironment and known to express both pro- and anti-tumour features. TAMs are generated by the recruitment of tissue-resident macrophages, circulating monocytes or macrophages to cancer cells. The number of TAMs correlates with the tumour volume, which results from the external recruitment of circulating $Ly6C^{+}CCR2^{+}$ pro-inflammatory monocytes and macrophages because of their high proliferative capacity (Franklin et al., 2014). Secretion of monocyte chemoattractant protein-1 (MCP-1/CCL2) is one of the mechanisms cancer cells use to recruit monocytes and macrophages, and in breast cancer, MCP-1 is increased by the promotion of SUSD2 (Hultgren et al., 2017). Although polarisation of TAMs often misunderstood to emerge by

virtue of their location itself, they require signals from the microenvironment such as colony-stimulating factor 1 (CSF1) from cancer cells. Cancer cells also secrete chemokines (CCL2, CCL3, and CCL14), which stimulate macrophage proliferation and polarisation, and IL-4 and IL-10, which inhibit pro-inflammatory cytokines and induce polarisation to anti-inflammatory phenotypes (Yang and Zhang, 2017, Rhee, 2016). Additionally, IL-4/IL-13, IL-10, immunoglobulin derived from T_H2, Treg, and B cells in the tumour microenvironment as well as VEGF and hypoxia in cancer cells and migration inhibitory factor from macrophages (which is known to induce anti-inflammatory polarisation and cell motility) are known to stimulate TAM polarisation in the tumour (Yang and Zhang, 2017, Colegio et al., 2014, Solinas et al., 2010).

1.2.1.2 Macrophage phenotypes

Traditionally, macrophages were classified into pro- and anti-inflammatory M1/classical and M2/adaptive macrophages, respectively, by the cytokines expressed in a cell (T helper cells type 1 (T_H1) and T helper cells type 2 (T_H2)) (Mills et al., 2000, Orecchioni et al., 2019). However, the oversimplified concept of the M1/M2 paradigm was not able to capture the heterogeneity and plasticity of macrophages (**Table 1.8**).

'M1' macrophages are generally stimulated by the combination of IFN-γ and bacterial lipopolysaccharide (LPS) *in vitro*, where IFN-γ is recognised by the receptors IFNGR-1 and IFNGR-2 and controls the expression of 'cytokine receptors (CSF2RB, IL15RA, IL2RA, and iL6R), cell activation markers (CD36, CD28, CD69, and CD97) and cell adhesion molecules'. LPS activates toll-like receptor 4 (TLR4) and induces pro-inflammatory cytokines (IL-1β, TNF, IL-6, IL-12 and IL-18) and chemokines (CCL2, CXCL10, CXCL11) (Martinez and Gordon, 2014). TNF and granulocyte-macrophage colony-stimulating factor

(GM-CSF) can also polarise macrophages into pro-inflammatory macrophages ($M^{GM\text{-}CF}$). It has been identified that both human and mouse 'M1' macrophages, especially $M^{IFN\gamma+LPS}$, also activate inducible nitric oxide synthase (NOS2 or iNOS) to generate nitric oxide, and secrete other pro-inflammatory cytokines such as IL-1, IL-23 and CD86 (Duque and Descoteaux, 2014, Martinez et al., 2006, Italiani and Boraschi, 2014, Lv et al., 2017).

The stimulation of macrophages with IL-4 was the first observed M2 stimulus used in the traditional M1/M2 paradigm. IL-4 stimulates M2a macrophages by binding to IL4RA1, paired with standard gamma chain or IL13RA1 and activates JAK1, JAK3, and consequently, STAT6 to induce macrophage fusion and reduced phagocytosis (Gordon and Martinez, 2010, Zhang et al., 2017b). Both human and mouse $M^{IL\text{-}4}$ macrophages secrete CD163, transglutaminase 2, mannose receptor (CD206) and MHC II but arginase-1, FIZZ1, and YM1 are only produced in mouse macrophages (Roszer, 2015a, Martinez and Gordon, 2014).

The M2b macrophage is a type II-activated macrophage, which is stimulated by TLRs and immune complexes. Although these cells share similar features with pro-inflammatory 'M1' macrophages (such as TNF, CD86, IL-1 and IL-6), the significant increase in IL-10, which is a hallmark of the M2b macrophages, activates a T_H2 response and the expression of Cd163, CCL1, and LIGHT which act as the inhibitory factors in the polarisation of tissue-resident macrophages to an 'M1' phenotype (Ohama et al., 2015, Gensel and Zhang, 2015). Similar to M2b macrophages, M2c macrophages stimulated by IL-10 are the regulatory macrophages initiated at a later stage of the adaptive immune response and limit inflammation. IL-10 binds to the receptors IL10R1 and IL10R2, which activate the transcription factor STAT3 and inhibit the secretion of pro-inflammatory cytokines (Martinez and Gordon, 2014, Cevey et al., 2019). The M2c macrophages induce CXCL13, CXCL4, TLR1 and TLR8 expressions but also share some features with M2a macrophages such as the release of TNG-β, CD206,

IL-10, and CD163 (CD163 is significantly expressed among other polarisation states) (Martinez and Gordon, 2014, Iqbal and Kumar, 2015).

In contrast to other 'M2' macrophage subsets (M2a, M2b and M2c), M2d macrophages have only been identified in mice. The polarisation to M2d macrophages can be stimulated by IL-6 or the agonists of both TLRs and adenosine A2 receptor either from M0 or M1 macrophages (Chistiakov et al., 2015, Wang et al., 2010). The activated adenosine signals suppress inflammatory cytokine expression in macrophages, including TLR-dependent TNF, IL-12, and IFN-γ release and induce VEGF, IL-10 and iNOS which function in angiogenesis and facilitates tumour growth (Ferrante et al., 2013, Roszer, 2015a, Sanmarco et al., 2017).

In addition to the M1/M2 subsets, there are different sets of nomenclatures to classify and characterise macrophages. For instance, macrophages could be delineated by the stimulating factors used *in vitro* to differentiate bone marrow and $CD14^+$ monocytes to macrophages and the stimuli used to polarise macrophages to different subsets (**Table 1.8**). The characterisation of these cells based on markers of macrophage activation could also generate better macrophage classification. For instance, 169^+ macrophages express CD169, CD206, and VCAM-1 and secrete CCL22 to facilitate the follicular accumulation of Tregs and promote immunological tolerance, whilst TCR^+ macrophages express TCR-αβ or TCR-γδ and CD3 and secretes CCL2 with high-phagocytosis capacity (Chavez-Galan et al., 2015, Murray et al., 2014, Asano et al., 2018). However, it is recommended to consider different parameters in the classification of macrophages, which includes mouse strain, the concentration of cytokines, culture conditions and macrophage yield, such as *in vivo*, the macrophage isolation procedures used and the conditions of the experiment, such as in the case of TAMs isolated from a tumour, are essential considerations (Murray et al., 2014).

Table 1.8. The spectrum of macrophages in *in vitro* experiments [Modified from (Murray et al., 2014, Roszer, 2015a)].

Nomenclatures		**Expressed Cytokines, and Chemokines**
M1/M2 Subsets	M1	CD80, CD86, MHC II, IL-1R, CD68, TNF, IL-1β, IL-6, IL-12, CCL10, CCL11, CCL5, CCL2
	M2a	CD163, CD206, CCL17, CCL22, CCL24 Mouse only: Arg-1, YM1/2, Fizz1
	M2b	CD86, MHC II, IL1, IL6, IL10, TNF, CCl1
	M2c	CD163, TLR1, TLR8, IL-10, TGF-β, CCL2
	M2d	VEGF, IL-10, IL-12, TNF, TGF-β
Differentiation from Monocyte		
a. Bone marrow monocytes	CSF-1 cultured macrophages	
	GM-CSF cultured macrophages	
b. $CD14^{+}$ monocytes	CSF-1 cultured macrophages	
Stimuli	$M^{IFN\text{-}\gamma + LPS}$	TNF, IL-6, IL-27, IL-12, iNOS Mouse: Arg-1, iNOS+++
	M^{LPS}	TNF, IL-8, IL-6, IL-1β, CXCL10 Mouse: Arg-1
	$M^{IFN\text{-}\gamma}$	$CCL18^{-ve}$
	$M^{IL\text{-}4}$	CCL17, MRC1, CD163 Mouse: Arg-1 +++
	M^{Ic}	IL-10, IL-6, CXCL13, CCL20
	$M^{IL\text{-}10}$	IL-10, CD163, TLR1, CCR2
	$M^{GC + TGF\text{-}\beta}$	TGFBR2 ++, Il-17RB
	M^{GC}	CD163, STAB1, TGFBR2 ++

1.2.1.3 Differences between macrophage polarisation states

Upon tissue injury or infection, pattern recognition receptors (PRRs) on immune cells recognise PAMPs or damage-associated molecular patterns (DAMPs) to initiate an immune response, and macrophages are one of the major cell types involved in the inflammatory response (Newton and Dixit, 2012, Hayashi et al., 2018). After recruitment and differentiation of circulating monocytes into an inflammatory site, including bacterial or parasitic infection, majority of macrophages polarise to the 'M1' phenotype with high expression of pro-inflammatory mediators (TNF, IL-6, IL-12, IL-1β, and nitric oxide) which attract neutrophils to the area, facilitating an inflammatory response, and promoting the removal of damaged tissue (Liu et al., 2014, Gensel and Zhang, 2015). The enhanced phagocytic abilities of 'M1' macrophages also allow the removal of apoptotic neutrophils, debris, and bacteria; whereas polarisation to 'M2' phenotype promotes host protection via wound healing (Liu et al., 2014).

'M2' macrophages generally dominate at the inflammatory sites in later stages of the immune response because of their role in wound healing and suppressing inflammation. Adaptive macrophages, such as M2a phenotype, up-regulate TGF-β upon their activation which promotes the expression of extracellular matrix (ECM) components including collagen type VI, fibronectin, by keratinocytes, and fibroblasts (Novak and Koh, 2013). Abundant neutrophils in the early wound sites disturb wound repair by degrading ECM components and inducing oxidative stress; thereby macrophages remove apoptotic neutrophils to facilitate wound healing (Koh and DiPietro, 2011, Wang, 2018). The regulatory macrophage phenotype, 'M2b', is also involved in wound healing where the increase in IL-10 secretion is vital for cell proliferation. Additionally, 'M2' macrophages also have a high potential to

regulate angiogenesis by fibroblast growth factor-placenta growth factor signalling, involving the ‘M2a’ and ‘M2c’ phenotypes (Jetten et al., 2014).

1.2.1.4 Tumour-associated macrophages in tumorigenesis

Several reports demonstrated that TAMs express both pro-inflammatory cytokines such as TNF and anti-inflammatory cytokines such as IL-10, IL-6 and CCL2 (**Figure 1.2A**) (Karnevi et al., 2014, Estko et al., 2015). However, based on the pro- and anti-inflammatory M1/M2 polarisation subset paradigm, TAMs are generally observed as ‘M1’ macrophages upon entering to the tumour site and polarise to ‘M2’ phenotypes due to their anti-cancer features (Yuan et al., 2015). ‘M1’ macrophages suppress tumorigenesis and angiogenesis and enhance drug sensitivity by the expression of cytokines and nitric oxide (NO) production. The produced NO has a controversial role in cancer biology, but when anti-tumorigenic, NO demonstrates cytostatic and/or cytotoxic effect by activating aconitase and ribonucleotide reductase or by mediating apoptosis by releasing mitochondrial cytochrome C into the cytosol (Choudhari et al., 2013). The pro-inflammatory cytokines secreted by macrophages, including IL-12, suppress tumours by initiating immune responses mediated by NK cells, T_H1 cells and cytotoxic T lymphocytes (Quatromoni and Eruslanov, 2012).

However, TAMs also secrete pro-inflammatory markers to facilitate cancer development. For instance, IL-6 secretion by TAMs is reported to activate STAT3 for the transduction of tumour-promoting signals, facilitating the proliferation and survival of cancer cells (Grivennikov et al., 2009, Wang et al., 2016b). According to Nie et al., (2017), expression of IL-23 in breast tumour promoted MMP-9 and CD31, an angiogenesis marker in the tumour, and increased expression of IL-10, TGF-β, and VEGF, thereby enhanced tumour growth and metastasis (Nie et al., 2017). Additionally, IL-1 also promotes angiogenesis in cancer;

knockout of IL-1 has been shown to inhibit angiogenesis, VEGF expression leading to reduced tumour size and in melanoma and mammary adenocarcinoma (Voronov et al., 2014, Gong et al., 2018).

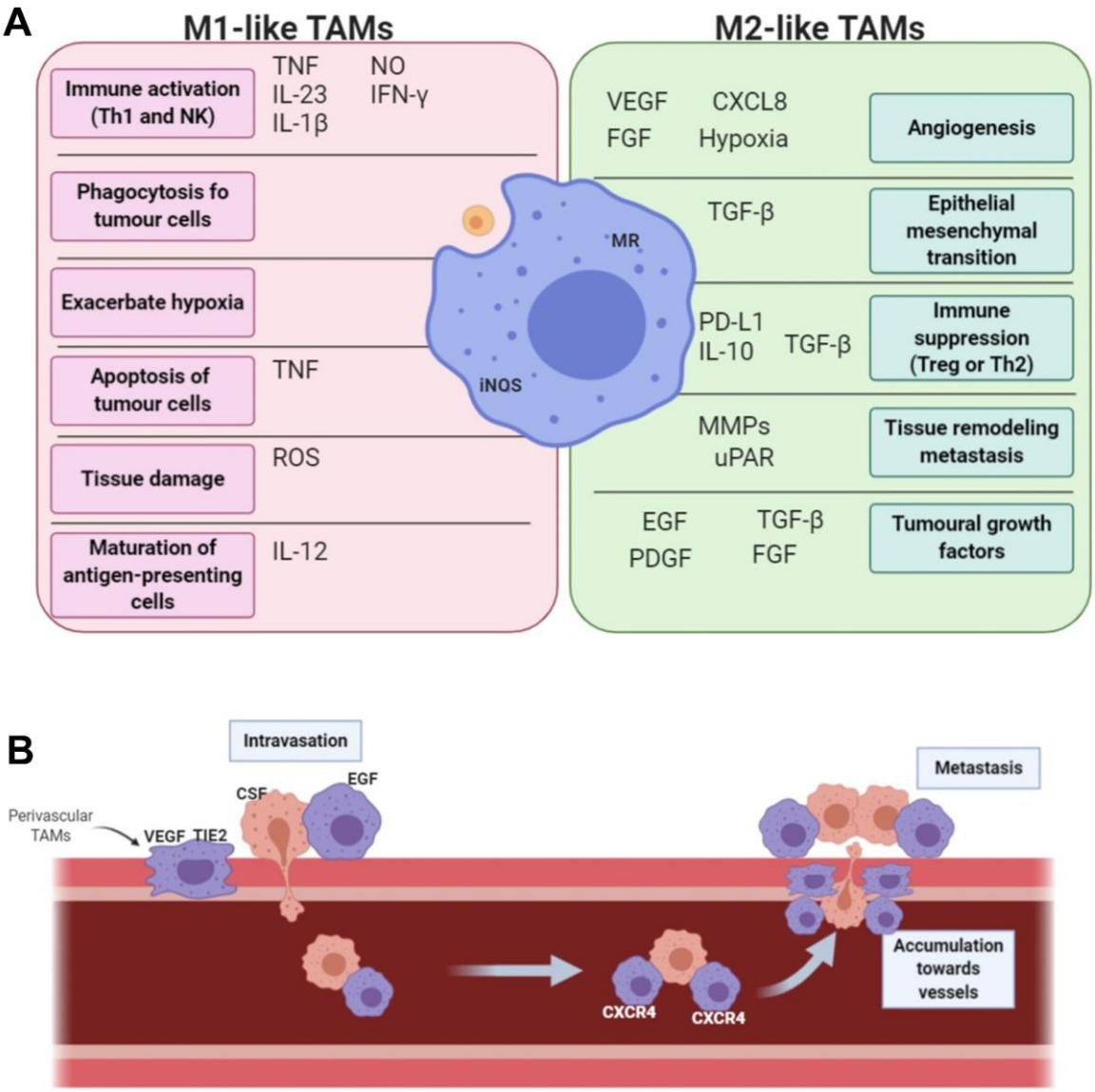

Figure 1.2. Oncogenic and anti-tumour functions of TAMs and schematic diagram of cancer metastasis [(A) adopted from (Anfray et al., 2019)]. (A) Features of TAM functions depending on the phenotypic changes. (B) The functional role of TAMs and perivascular TAMs in the promotion of metastasis.

TAMs are generally known to express ‘M2’ phenotype where according to Ma et al., (2010), staining lung cancer with CD68 (a pan-macrophage marker), HLA-DR (stains M1 macrophages) and CD163 (stains M2 macrophages) demonstrated that about 70% of macrophages expressed $CD68^{+}/CD163^{+}$ (Ma et al., 2010). Recruited and activated TAMs, with the majority demonstrating an anti-inflammatory phenotype, play a crucial role in tumour initiation, growth, angiogenesis, metastasis and immunosuppression (Caux et al., 2016). Inflammation is one mechanism to initiate cancer and macrophages produce a mutagenic microenvironment by generating free radicals or altering microbiome to allow bacterial infection (Noy and Pollard, 2014). TAMs produce growth factors (EGF, PDGF, HGF, and bFGF) to stimulate the proliferation and survival of a tumour (Caux et al., 2016, Mantovani et al., 2017). For instance, EGF signalling promoted formation and self-renewal of colon cancer stem cells and cancer stem cells also enhanced survival via activation of EGFR followed by downstream interactions: Ras-ERK cascade and PI3K/AKT pathway (Feng et al., 2012). HGF plays a critical role in cancer invasion where Caco-2 cells derived from human colon carcinoma enhanced endogenous HGF-dependent production of proteases such as MMPs to promote cancer invasion, and this process was closely related to PI3K and PKC expression, and a prognostic marker in patients with colerctal cancer (Noriega-Guerra and Freitas, 2018, Huang et al., 2017).

Tumour metastasis is a complex process, requiring ‘invasion of healthy tissue, intravasation, migration and survival in circulation, extravasation, angio- and lymph-angiogenesis, matrix remodelling, pre-metastatic niche formation, dormancy escape, proliferation and macro-metastases formation’ (Sousa and Maatta, 2016). Recruited cells in a tumour, including TAMs and Tregs (which are also stimulated by CCL22 produced by TAM), regulate toll-like receptor signalling and cytokine production to increase MMP-2 and MMP-9 and reduce cytotoxic

effects which promote immunosuppressive function and enhance the survival of a tumour during metastasis (Singh et al., 2017, Ke et al., 2016). TAMs also produce pro-angiogenic factors to initiate angiogenic switch, to allow tumour cells to enter the vasculature where the cell can rapidly become invasive, metastatic and characterised as malignant (Noy and Pollard, 2014, Riabov et al., 2014). VEGF is one of the major pro-angiogenic cytokines associated with hypoxia, where hypoxia-inducible factor 1α increases VEGF-A expression in TAMs and allows the enzymatic cleavage of ECM by matrix metalloproteinases (Riabov et al., 2014). The secretion of IL-1, NO, and EMMPRIN by TAMs also mediate carcinogenesis and angiogenesis via induction of MMP-9 and VEGF (Rahat and Hemmerlein, 2013, Amit-Cohen et al., 2013, Voronov et al., 2014). Hypoxia also facilitates TAM-mediated angiogenesis by regulating development and DNA damage response 1 (REDD1), where REDD1 suppresses mTOR activity and glycolysis in TAMs which allows sufficient glucose to the endothelial cells (Mantovani and Locati, 2016). Moreover, TAMs secrete other pro-angiogenic factors including TNF, bFGF, thymidine phosphorylase, urokinase-type plasminogen activator, adrenomedullin, semaphorin 4D, and CCL18 to stimulate angiogenesis and facilitate tumorigenesis (Riabov et al., 2014, Lin et al., 2015).

TAMs in tumour microenvironment also promote immune-suppression and immune evasion to enhance tumour development. According to Guo et al., (2017), at the initial stage of cancer, tumour-initiating cells (TICs) in liver recruited macrophages via activation of Hippo pathway effector Yes-associated protein (YAP) and inhibition of the macrophage recruitment to TICs abolished tumorigenesis via eliminating TICs via immune clearance (Guo et al., 2017). CCR2 expression in TAM is one of the most important immunosuppressive mediators where Yao et al., (2017), showed that disrupting CCR2 in TAMs significantly reduced liver cancer development via blocking TAM-mediated immunosuppression (Yao et al., 2017). In

renal cancer, TAM highly expressed 15-lipoxygenase-2 to promote lipoxygenase activity, which reduces the production of CCR2 and immunosuppressive cytokine IL-10 when inhibited and induces FOXP3 and CTLA-4 to promote immune evasion (Daurkin et al., 2011). Additionally, TAMs express programmed cell death protein ligand 1 (PD-L1) and based on Prima et al., (2017), the COX2/mPGES1/PGE_2 pathway is involved in PD-L1 expression in myeloid cells, and PD-$L1^+$ bone marrow-derived myeloid cells promote apoptosis of activated T cells *in vitro* to promote immunosuppression in cancer (Prima et al., 2017).

TAMs also mediate resistance to cancer chemotherapy by producing survival and anti-apoptotic factors. In breast cancer, resistance to the chemotherapy was shown to be induced primarily via expression of IL-10 with an increase of IL-10 expression observed in TAMs when treated with paclitaxel *in vitro* and the resistance to the therapy was induced by IL-10 mediated STAT3 activation and anti-apoptosis gene Bcl-2 expression (Yang et al., 2015). De Beule *et al*. (2017) also reported the importance of STAT3 activation in drug resistance. The presence of anti-inflammatory macrophages enhanced survival of bone marrow cancer, and multiple myeloma cells were observed in the treatment of bortezomib (proteasome inhibitor) and melphalan (alkylating agent) *in vitro*, whilst inhibition of STAT3 activation abrogated TAM-mediated cell survival (De Beule et al., 2017). Resistance to doxorubicin and etoposide has also been suggested to be caused by the activation of STAT3, IL-6 and other factors derived from macrophages which allow cells to proliferate (Ruffell and Coussens, 2015). The presence of TAMs is also linked to the prognosis of cancer. If the dominant population of TAMs demonstrated ‘M2’ phenotypes, the poor prognosis was observed in cancer patients (Hughes et al., 2015a). However, treatment of TAMs with IFN-γ drives M2-like

immunosuppressive macrophages to become M1-like cells which have anti-cancer features and emphasise the potential of these cells are a therapeutic target (Kim and Bae, 2016).

1.2.1.4.1 Perivascular Tumour-associated macrophages

Macrophages have distinct functions depending on their location and phenotypes, and some macrophages that are close contact with blood vessels (within 250μm radius of blood vessels), called perivascular macrophages (PVM), facilitate tumour development (Lapenna et al., 2018, Hughes et al., 2015b). Perivascular TAMs (PV TAM) are characterised by high expression of TIE2, and compared to other TAMs from the same tumour, PV TAMs express a higher level of MRC1 and tumour-promoting genes including MMP9, VEGF, CXCL12, TLR4, NRP1, and PDGF (Claire et al., 2016, Lapenna et al., 2018). PVMs are known to bridge between endothelial tip cells, enhancing vascular anastomosis in mouse embryos and high expression of VEGF and are especially involved in the branching of angiogenic vessels (Lapenna et al., 2018). The angiogenic role of PV TAMs in the tumour was reported in several tumour types including mammary cancers in mice where the elimination of PV TAMs using a conditional suicide strategy impaired the vascularization and tumour growth whilst co-injection of PV TAMs, TAMs, and mammary tumour cells significantly increased vascularized tumours (Claire et al., 2016). In addition, angiopoietin 2 (ANGPT2), highly expressed in the tumour endothelial cells, upregulates proangiogenic factors in PV TAMs and also works as a chemoattractant to accumulate PVMs and macrophages around blood vessels in mouse tumours (Lapenna et al., 2018).

PV TAMs are also involved in the intravasation of cancer cells, both in primary mammary tumours and distant metastases. The VEGF expressing PV TAMs are critical for the formation of paracrine loops (CSF1 from cancer cells, EGF from TAMs, and HGF from

endothelial cells) enabling tumour cell escape from the primary tumours and VEGF expressing PV TAMs are vital for the micro-anatomical site of tumour escape, tumour microenvironment of metastasis (TMEM), where the cancer cell intravasation at the TMEM sites depends on the VEGF-derived vascular endothelial cadherin reduction in and around TMEM to disrupt vascular junction stability (Arwert et al., 2018, Claire et al., 2016). In case of circulating cancer cells, motile TAMs upregulate CXCR4, promoted by TGFβ from cancer cells and the expression of CXCL12 by perivascular fibroblasts leading to accumulated TAMs towards the blood vessels together with motile cancer cells, which then differentiates TAMs into PV TAMs promoting vascular leakiness and intravasation (**Figure 1.2B**) (Arwert et al., 2018). PV TAM also promotes resistance to chemotherapy, where the anti-inflammatory TAMs accumulate in the perivascular areas depending on the CXCR4 expression to promote tumour revascularization and regrowth after chemotherapy and the expression of VEGF by PV TAMs involves in the promotion of tumour relapse after therapy (Hughes et al., 2015b).

1.2.1.4.2 Tumour-associated macrophages and hypoxia

In solid tumours, disorganised vascularisation of blind-ended vessels and leaky endothelial lining promote hypoxic conditions in tumours including breast cancer, and the crosstalk between hypoxic tumours and TAMs are crucial in the development and aggressiveness of the tumour (Obeid et al., 2013). Hypoxia induces chemokines (such as CCL2, CCL5, CSF1, VEGF, SEMA3A, EMAP-II, SDF1α, eotaxin, and oncostatin M) that accumulate macrophages and TAMs and trap in the hypoxic area via upregulated MPK1 which dephosphorylate chemoattractant receptors and inhibit pathways triggered by migration stimulating factors, which are associated with the aggressive tumour behaviour in breast cancer (Lin et al., 2019, Obeid et al., 2013). The entrapped TAMs exert pro-tumoural

functions where upregulation of growth factors such as EGF in breast cancer produce CSF1 to enhance survival of macrophages and stimulate tumour cell growth, and hypoxic TAMs express angiogenic molecules (VEGF, FGF2, CXCL8, IL-8, VEGFR1, angiopoietin) to facilitate tumour vascularisation (Henze and Mazzone, 2016). HIF1α is expressed in hypoxia and upregulates VEGF expression to enhance pro-angiogenic functions in TAMs and hypoxia also increases TIE2 and angiopoietin2 expression that promotes autocrine loop in vascular endothelial cells to initiate angiogenesis (Chen et al., 2019b). Hypoxic TAMs also play a vital role in immune evasion were TAMs under hypoxic conditions secrete more immunosuppressive factors such as prostaglandin E2, IL-10, and PD-L1 which promotes dysfunction of T-cells, inhibit T-cell proliferation and function by IDO expression and attract Tregs via secretion of CCL17 and CCL22 (Obeid et al., 2013, Henze and Mazzone, 2016).

1.3 Tribbles homologues

Tribbles homologues (TRIB) are pseudokinase proteins. Human TRIBs is named after that highly conserved *Drosophila* homologue, *tribbles,* which is involved in the regulation of 'proteasomal degradation of CDC25 dual-specificity phosphatases and Slbo levels, and affect the cell cycle and oogenesis by initiating S-phase and mitosis' (Murphy et al., 2015, Eyers et al., 2017, Richmond and Keeshan, 2020). Human TRIBs are also involved in development but have more distinct features affecting different signalling, developmental, and metabolic processes (Murphy et al., 2015).

TRIB proteins consist of three domains: N-terminal PEST (proline, glutamic acid, serine, and threonine) region, a pseudokinase domain which includes an N-lobe and a canonical C-lobe, and a C-terminal, COP1-binding peptide region. The N-lob in the pseudokinase domain recruits most catalytic machinery whilst preserving the putative substrate-binding site in C-

lobe (Eyers et al., 2017). The C-terminal tail affects the protein-protein interactions by two motifs which regulate E3 ubiquitin ligases and interact with MAPK signalling, including via MEK1 and MEK4 (Eyers et al., 2017). In humans, there are three Tribbles homologs (TRIB1, TRIB2, and TRIB3) which share similar amino acid homologs up to 71% (between TRIB1 and TRIB2)(Cunard, 2013).

TRIB1 is one of the Tribbles homologs expressed in several tissues, including the pancreas, bone marrow, and adipose tissue. TRIB1 regulates MAPK signalling as well as liver metabolism and lipid levels and is involved in macrophage differentiation (Richmond and Keeshan, 2019). In the liver, secretion of very-low-density lipoprotein (VLDL) via lipids, which is strictly regulated by apolipoprotein B (APOB), is vital in providing fatty acids to the peripheral tissues; TRIB1 was identified to regulate the secretion of VLDL and APOB via MAPK activity (Soubeyrand et al., 2016). The alteration of CCAAT/enhancer-binding protein α (C/EBPα) and C/EBPβ transcription levels via TRIB1 are also involved in hepatic lipid biosynthesis (Iwamoto et al., 2015).

Among TRIB family, TRIB2 was first identified as a mouse oncogene where the overexpression of TRIB2 developed a potent transplantable AML (Eyers et al., 2017). The oncogenicity of TRIB2 was also reported in different cancers where TRIB2 was overexpressed in colorectal cancer, which inhibits p21 (transcription factor involved in cell cycle inhibition), and interacts with AP4 regulate AP4/p21 signalling to inhibit cellular senescence and accelerate the proliferation of cancer cells (Hou et al., 2018). In liver cancer, TRIB2 was discovered as a downstream target of Wnt/TCF essential for the protection of liver cancer cells, HepG2, from apoptosis, and involved in the overexpressed Yes-associated protein (YAP) which were observed in more than 50% of tumours via disruption of C/EBPα (Wang et al., 2013). TRIB2 is also reported to promote malignant phenotype of melanoma

cells via suppressing FOXO, and TRIB2 expression induces the chemotherapy resistance in cancer cells via increased AKT expression by COP1 domain (Zanella et al., 2010, Hill et al., 2017).

Similarly, the oncogenic role of TRIB3 was also reported in cancer cells *in vitro*. The knockdown of TRIB3 in HepG2 and colorectal carcinoma cell line (HCT-8) inhibited cell invasion, and TRIB3 also maintains the epithelial-mesenchymal transition (EMT) status in HepG2 cells important for the conversion of early-stage tumours into invasive malignancies by enhancing α-SMA expression whilst inhibiting E-cadherin (Hua et al., 2011). The overexpression of TRIB3 in human gastric cancer was also reported to promote poor prognosis and tumour angiogenesis in gastric cancers, in relation to positively correlated VEGF expression (Dong et al., 2016). In breast cancer, TRIB3 was known to reduce the disease-free survival (DFS), metastasis-free survival and overall survival of patients as well as DFS of patients postoperative radiotherapy, and though TRIB3 is not a tumour hypoxia marker, ATF4 dependent TRIB3 expression induces hypoxia and hypoxia sensitivity in breast cancer cells (Wennemers et al., 2011b). TRIB3 also suppress FOXO1 degradation by TRIB3-AKT interaction which promotes the transcriptional expression of SOX2 to enhance cancer cell stemness of solid tumours (Yu et al., 2019).

1.3.1 Role of TRIB1 in tumours

The amplified TRIB1 gene has been observed in different types of cancer. In acute myeloid leukaemia (AML), trisomy 8 is typically observed, which often carries MYC and promotes proliferation. TRIB1 is located on chromosome 8, near to the MYC gene and is co-amplified. In addition, expression of C/EBPα, which is also regulated by TRIB1, is essential for AML development (Keeshan et al., 2016). Furthermore, TRIB1 promotes prostate cancer by

regulating endoplasmic reticulum chaperone GRP78 and facilitates cell survival (Dugast et al., 2013, Mashima et al., 2014). TRIB1 acts as a critical regulator of cell cycle progression and is involved in cancer development and survival via interaction with the MEK/ERK pathway, where the inhibition of MEK1/MEK2 resulted in the cell cycle arrest at G1; and the cell cycle machinery, CCND1, is regulated by TRIB1 through NFκB and AP1 interaction (Gendelman et al., 2017). Increased TRIB1 levels and phosphorylation of FAK, Src and ERK proteins activate MMP-2, hence facilitating migration and adherence of cancer cells (Wang et al., 2017c, Wu et al., 2016). The interaction of TRIB1 with NFκB influences downstream products involved in metastasis formation (CSF2 and CXCL1) and tumour inflammation (IL-8). Additionally, the NFκB pathway is involved in resistance to chemotherapy and the upregulation and interaction of TRIB1 with HDAC induced resistance in non-small cell lung cancer to cisplatin treatment (Wang et al., 2017a).

1.3.1 TRIB1 in macrophages

Among other TRIBs, TRIB1 is most highly expressed in the myeloid lineage (Richmond and Keeshan, 2019). TRIB1 expression in macrophages promotes the polarisation to alternatively activated M2-like macrophages, where depletion of TRIB1 results in the reduction of anti-inflammatory macrophages in various tissues (Satoh et al., 2013). In myocardial infarction (MI), TRIB1 also promoted ‘M2’ polarisation where TRIB1 knockdown mice promoted depletion of ‘M2’ macrophages after MI and reduced tissue repair (Shiraishi et al., 2016). Although there are no reports on molecular details, the potential mechanism of TRIB1-dependent macrophage polarisation involves MAPK signalling, primarily via MEK1/2, where the MEK1/2 inhibitors have been shown to enhance STAT6 phosphorylation and significantly increased M2a-like bone marrow-derived and alveolar macrophages (Long et

al., 2017). The depletion of C/EBPα also altered the macrophage polarisation states and one of the E3 ubiquitin ligases, natural killer lytic-associated molecule, was identified to ubiquitinate and activate C/EBPβ affecting the macrophage polarisation (Lee et al., 2014, Ye et al., 2012, Li et al., 2018).

Moreover, TRIB1 affects other functions of macrophages, including macrophage development and migration. For instance, TRIB1 knockdown in RAW264.7 cells produced monocyte-like morphology and the depletion of ERK1/ERK2, which is the downstream signal of MEK1/MEK2, hence reduced the number of M-CSF induced macrophages due to the lack of ERK-dependent genes regulated by M-CSF (Liu et al., 2013, Richardson et al., 2015). TRIB1 potentially regulates macrophage migration by the ERK1/2 pathway and C/EBPβ inhibition via MCP-1 (CCL2), which is a crucial chemokine in the recruitment and migration of monocytes and macrophages (Liu et al., 2013, Arndt et al., 2018).

1.4 Hypothesis and aims

The development and regulation of TAMs are essential oncogenic factors to promote tumour initiation, angiogenesis, immune suppression and evasion, and metastasis as well as the survival of cancer cells in the blood vessel. There is a growing interest of TRIB1 function in tumour development and macrophages, suggesting a potential role for TRIB1 in cancer itself and for TRIB1-dependent regulation of macrophages. However, despite the potential importance of TRIB1 in macrophage function and tumour growth, the impact of TAM expressed TRIB1 in tumorigenesis has not been explored. Therefore, our overarching **hypothesis** highlights that *TRIB1* expression in myeloid cells modulates macrophage function and phenotype, thus modulating TAM recruitment by cancer cells and by doing so

promotes tumour development. In order to test our hypothesis, we developed syngeneic breast cancer models in myeloid-specific *Trib1* overexpressing and knockout mice.

The project aims to:

- Investigate the expression of TRIB1 expression in human and murine breast cancer (Chapter 3)
- Validate the *TRIB1* dependent phenotypic and functional changes in macrophages and TAMs (Chapter 3)
- Determine the impact of myeloid *Trib1* in murine mammary tumour growth (Chapter 4~5)
- Investigate the mechanisms of myeloid *Trib1*-dependent regulation of tumorigenesis (Chapter 4~5)

Chapter 2. Materials and Methods

2.1 Research Ethics:

All human blood samples were collected under the University of Sheffield Research Ethics Committee (ref. SMBRER310). The human breast breast tissue samples were under the NHS National Research Ethics Service Sheffield Research Ethics Committee REC reference number 09/H1308/138, and the human breast tumour tissues were provided by the Breast Cancer Now Tissue Bank. The mouse strains were housed in the University of Sheffield Biological Service Unit and bred under the University of Sheffield code of ethics, and Home Office regulations project licence number P5395C858/3. The experiments with mice strains were performed according to the University of Sheffield code of ethics and Home Office regulations project licence number 70/8670, personal licence number I2AB6392A.

2.2 In vitro methods:

2.2.1 Cell Maintenance

2.2.1.1 Cancer cell culture

Human MDA-MB-231 cell (human adenocarcinoma) was cultured in RPMI-1640 medium (Gibco) with additional supplements: 10% (v/v) low endotoxin heat-inactivated foetal bovine serum (Biowest), 1% L-glutamine (Lonza). Mouse Eo771 cell (medullary breast adenocarcinoma) was cultured in DMEM (Gibco) with additional supplements: 10% (v/v) low endotoxin heat-inactivated foetal bovine serum (Biowest), 1% L-glutamine (Lonza). Cells were monitored and sub-cultured every 48 hours at 1:5 – 1:10 dilution and maintained at 37°C at 5% CO_2.

2.2.1.2 Primary cell culture

Human MDMs were cultured in complete growth medium: 500 ml RPMI-1640 (Gibco), 10% (v/v) low endotoxin heat-inactivated foetal bovine serum (Biowest), 1% (v/v) streptomycin/penicillin (Gibco), 1% L-glutamine (Lonza). Mouse bone marrow-derived macrophages (BMDMs) were cultured in both complete DMEM growth medium: 500 ml DMEM (Gibco), 10% (v/v) low endotoxin heat-inactivated foetal bovine serum (Biowest), 1% (v/v) L-glutamine (Lonza), 1% (v/v) streptomycine/penicillin (Gibco); and L929 cell-conditioned medium: 500 ml DMEM (Gibco), 10% (v/v) low endotoxin heat-inactivated foetal bovine serum (Biowest), 10% (v/v) L929 cell-conditioned medium, 1% (v/v) L-glutamine (Lonza), 1% (v/v) streptomycine/penicillin (Gibco).

2.2.2 Preparation of Tumour-conditioned medium

When MDA-MB-231 and Eo771 cells become 70-80% confluent in a T75 flask, cells were washed twice in PBS, and fresh medium was added to the flask and incubated at 37°C at 5% CO_2 for 48 hours. The medium was then recruited and centrifuged at 600 x g for 5 minutes to remove any cells and debris and supernatants were kept in -20°C freezer.

2.2.3 Isolation of human blood monocytes

The study was approved by the University of Sheffield Research Ethics Committee (ref. SMBRER310). Human blood was provided from health consented adults and gently mixed with 3.8% trisodium citrate dehydrate ($Na_3C_6H_5O_7 * H_2O$, Sigma) in 9:1 dilution.

In sterile 50 ml tubes, 15 ml of Ficoll-Paque PLUS (GE Healthcare) were added and 30 ml of citrated blood were gently layered on Ficoll-Paque PLUS. It was then centrifuged at 900 x g for 20 minutes at RT with acceleration and brake at 1 to avoid any post-mix after separation.

Most of the top plasma layer was removed, and the peripheral blood mononuclear cells (PBMCs) were recruited in PBS–2mM ethylenediaminetetraacetic acid (EDTA, Thermo Fischer) solution (PBSE). The sample was then centrifuged at 1500 rpm (radius = 161mm) or 406 x g for 5 minutes at RT.

$$RCF = 1.12 \times r \times \left(\frac{rpm}{1000}\right)^2$$

Erythrocytes were lysed in pre-warmed 10 ml of RBC lysis buffer (155 mM NH_4Cl, 10mM $KHCO_3$, 0.1M EDTA in H_2O) at RT for 5 minutes. 40 ml of PBSE were then added to the cells and centrifuged at 1500 rpm or 406 x g for 5 minutes. The PBMCs were resuspended in PBSE and counted using a haemocytometer (Hawksley).

The PBMCs were centrifuged and resuspended in 90 µl 4°C MACS buffer (0.5% [w/v] bovine serum albumin [BSA, Sigma] – PBSE) and 10 µl $CD14^+$ microbeads (Miltenyi Biotec) per 10^7 PBMCs and incubated for 15 minutes at 4°C. 2 ml of MACS buffer were then added and centrifuged at 1200 rpm (radius = 161mm) or 260 x g for 5 minutes. An LS column (Miltenyi Biotec) was placed in a MidiMACS™ Separator (Miltenyi Biotec) and rinsed with 3 ml of 4°C MACS buffer. The PBMCs resuspended in 500 µl of 4°C MACS buffer were then applied to the column and washed three times with 3 ml of 4°C MACS buffer. The column was removed from MidiMACS™ Separator and $CD14^+$ cells were flushed out in 4 ml of MACS buffer to 15 ml falcon tube with 1 ml MACS buffer. Cells were counted with a haemocytometer and pelleted by centrifugation at 1200 rpm or 260 x g for 5 minutes.

2.2.4 Human monocyte-derived macrophage differentiation

Isolated monocytes were resuspended in complete growth medium with 100 ng/ml recombinant human (rh) macrophage-colony stimulating factor (M-CSF) (Peprotech) to

facilitate differentiation of monocytes to macrophages. The monocytes were seeded into 6-well plate ($5 \times 10^5 – 10 \times 10^6$ cells per well) or 12-well plate ($2.5 \times 10^5 – 5 \times 10^5$ cells per well) and incubated for seven days at 37°C at 5% CO_2

2.2.5 TRIB1 siRNA transfection

Viromer Green (Lipocalyx) was used to transfect siRNA to primary human MDMs. TRIB1 siRNA (ON-TARGET *plus* siRNA, Dharmacon) or Non-Targeting Control siRNA (ON-TARGET *plus* siRNA, Dharmacon) were used in the study. siRNA mix and Viromer mix was prepared in the separate tubes, and 180µl of viromer mix was added to the 20µl of siRNA mix. The siRNA/Viromer mix was then incubated at room temperature for 15 minutes and added to 2 ml of fresh complete growth medium and incubated at 37°C at 5% CO_2 for 24 hours (**Table 2.1**). Transfection of siRNA with Viromer Green on macrophages was confirmed with siGLO transfection (**Supplementary figure 1**).

Table 2.1. Preparation of siRNA and Viromer mix

Tubes	Reagent	Total volume
Tube 1	siRNA (2.8µM) + Buffer Green	20µl
Tube 2	Viromer (2µl) + Buffer Green (178µl)	180µl

2.2.6 Human monocyte-derived macrophage polarisation

Human MDMs were gently washed with PBS and incubated for 24 hours at 37°C at 5% CO_2 in fresh complete growth medium with polarisation stimuli: 20 ng/ml IFN-γ (Peprotech) and 100 ng/ml *E. coli* lipopolysaccharide (Serotype R515 TLR*grade*™, Enzo Life Sciences) for M1; 20 ng/ml IL-4 (Peprotech) for M2a; 20 ng/ml IL-10 (Peprotech) for M2c; and 50% tumour-conditioned medium for tumour-associated macrophages.

2.2.7 Murine bone marrow isolation

The femur and tibias were collected from mice, and the tissues were gently removed from the bones. The end of the bones was cut with scissors or scalpel blade. The bone marrow was flushed with medium (RPMI, without phenol red, without L-glutamine) using a 2.5 ml syringe fitted with a 25G needle. Any clump of cells was dispersed with a pipette and passed through 70μm cell strainer (Fisher Scientific). The cell suspension was centrifuged at 500 x g for 5 minutes, and the pellet was cultured or frozen at -80 °C for further experiments.

2.2.8 Murine bone marrow-derived macrophage differentiation

Murine bone marrows were thawed and incubated in T75 flask with L929 cell-conditioned DMEM medium. After 24 hours, the medium was transferred to new T75 flask for the floating cells to attach in the flask and the fresh medium (L929 cell-conditioned medium) was added to the old flask and cultured for 5days at 37°C. Cells were then gently washed with PBS and collected with the fresh L929 cell-conditioned medium. Cells were counted and seeded into the appropriate plates for 24 hours at 37°C at 5% CO_2.

2.2.9 Murine bone marrow-derived macrophage polarisation

The differentiated BMDMs were gently washed with PBS and incubated for 24 hours at 37°C in fresh complete growth medium with polarisation stimuli: 20 ng/ml IFN-γ (Peprotech) and 100 ng/ml *E. coli* lipopolysaccharide (Serotype R515 TLR*grade*™, Enzo Life Sciences) for M1; and 20 ng/ml IL-4 (Peprotech) for M2a; 20 ng/ml IL-10 (Peprotech) for M2c.

2.2.10 RNA extraction

Total RNA was isolated using the miRNeasy Mini Kit (Qiagen). Cells were recruited prior to RNA isolation, but isolation was also performed from plates. Cells were gently washed twice in PBS and incubated at room temperature (15 - 25°C) for 5 minutes in 700µl of QIAzol lysis reagent to homogenate the cells. 140µl of chloroform was added to the cells, shaken vigorously for 15 seconds and incubated at room temperature for 2-3 minutes. Cells were then centrifuged at 12,000 x g at 4°C for 15 minutes. The upper aqueous phase was collected to the new collection tube, and 1.5 volumes of 100% ethanol were added. The sample was then transferred to the RNeasy Mini column in a 2ml collection tube and centrifuged at ≥8000 x g for 15 seconds at room temperature. Buffer RWT (350µl) was added and centrifuged at ≥8000 x g for 15 seconds, followed by incubation of the column with the 80µl of DNase I incubation mix (10µl DNase I stock solution and 70µl Buffer RDD) for 15 minutes at room temperature. The column was washed with Buffer RWT (350µl) and centrifuged at ≥8000 x g for 15 seconds. 700µl of Buffer RWT was added and centrifuged for 15 seconds at ≥8000 x g, and Buffer RPE (500µl) was added to the column followed by centrifugation for 15 seconds at ≥8000 x g. Buffer RPE (500µl) was added to the column and centrifuged for 2 minutes at ≥8000 x g. The column was transferred to a new 1.5 ml collection tube and RNeasy-free water (30-50µl) was added to the column and centrifuged at ≥8000 x g for 1 minute. The isolated RNAs were kept in -80°C until it used.

2.2.11 cDNA synthesis

cDNA was produced from total RNA using the iScript cDNA synthesis kit (Bio-Rad) according to the manufacturer's instruction. The extracted RNA was quantified using the Nanodrop Spectrophotometer ND1000. The appropriate amount of RNA was mixed with 1µl

of iScript reverse transcriptase and 4µl of 5x iScript Reaction mix, which will end up 25ul. The RNA/iScript mix was then incubated in a thermal cycler using the protocol provided by the manufacturer (**Table 2.2**). The cDNA was kept in -20°C or diluted for RT-qPCR analysis.

Table 2.2. cDNA synthesis reaction parameters

Reaction	**Temperature**	**Time**
Priming	25°C	5 minutes
Reverse transcription	46°C	20 minutes
RT inactivation	95°C	1 minute
Optional step	4°C	Hold

2.2.12 Real-time quantitative PCR

Quantitative RT-PCR was performed using primers designed with NCBI BLAST to target human macrophage polarisation markers (**Table 2.3**) and PrecisionPLUS SYBR-Green master mix (Primerdesign). 364-well plate was used in the experiment to assess the expression of genes in the samples. SYBR green master mix with forward and reverse primers (**Table 2.4**) were added to each well of the 364 well RT-qPCR plates at a total volume of 5.6µl. Followed by the addition of 5µl of cDNA (0.4 ng/ul) and the plate was centrifuged for 2 minutes at 2000rpm. The RT-qPCR plate was then assessed on a Bio-Rad I-Cycler PCR machine with the protocol provided by the manufacturer.

Table 2.3. Real-time quantitative PCR reaction parameters

Reaction		**Temperature**	**time**
Hotstart		95°C	2 minutes
Cycling x40	Denaturation	95°C	15 seconds
	Anneal (Data Collection)	60°C	1 minutes
Melt curve		60°C	
		95°C	

Table 2.4. The SYBR RT-qPCR primer sequences

Gene	Species	Forward primer 5' – 3'	Reverse primer 5' – 3'
IL-1β	Human	GCTCGCCAGTGAAATGATGG	GAAGCCCTTGCTGTAGTGGT
IL-8	Human	TGCCAAGGAGTGCTAAAG	CTCCACAACCCTCTGCAC
IL-10	Human	GCCTTTAATAAGCTCCAAGAG	ATCTTCATTGTCATGTAGGC
IL-15	Human	ACAGAAGCCAACTGGGTGAA	GCTGTTACTTTGCAACTGGGG
SCARB1	Human	GAATCCCCATGAACTGCTCTGT	TCCCAGTTTGTCCAATGCCTG
MRC1	Human	AGATGGGTGGGTTATTTACAAAGA	ATATTTCCATAGAAACTTCTTTTCACTT
PD-L1	Human	AGGGCATTCCAGAAAGATGAGG	GGTCCTTGGGAACCGTGAC
VEGF	Human	ATGCGGATCAAACCTCACCA	GCTCTATCTTTCTTTGGTCTGC
SPARC	Human	TGATGGTGCAGAGGAAACCG	TGTTCTCATCCAGCTCGCAC
TRIB1	Human	CTCCACGGAGGAGAGAACCC	GACAAAGCATCATCTTCCCCC
GAPDH	Human	ATTGCCCTCAACGACCACTTT	CCCTGTTGCTGTAGCCAAATTC
IL-15	Mouse	GACACCACTTTATACACTGACAGTG	TCACATTCCTTGCAGCCAGA
B-actin	Mouse	GGGACCTGACAGACTACCTCATG	GTCACGCACGATTTCCCTCTCAGC

2.2.13 Cell lysis and protein extraction

Cell lysis was performed to extract the proteins from primary and established cells. Cells were washed with PBS and collected into a 1.5ml Eppendorf tube. 50µl to 200µl of lysis buffer (RIPA buffer with 1% protease and phosphatase inhibitor) were added into the tube and pipette to rupture the cell wall and incubated at -80°C for 30 minutes to allow further lysis. Cells were further lysed by sonication for 15 seconds and then lysed cells were centrifuged at 15,000 x g for 10 minutes at 4°C. The supernatant was collected and stored at -80°C for further experiment.

2.2.14 Quantification of proteins

Proteins extracted from cells were quantified using Pierce^{TM} BCA Protein Assay Kit (Thermo Scientific). It measures the reduction of Cu^{2+} to Cu^{1+} by the protein in an alkaline condition through the production of purple-coloured reaction, which can be detected at 562nm in a

spectrophotometer. Bovine serum albumin (BSA) standard provided by the manufacturer was diluted to appropriate concentrations according to the table. The standard (10µl) was then added in the 96-well plate as triplicate. The 10µl of samples were added to the plate as duplicate, and 200µl of working reagent (1:50 ratio of reagent B and reagent A) was added to each well. The plate was then incubated at 37°C for 30 minutes. The plate was then cooled on ice and measured on a spectrophotometer. The protein concentration was quantified according to the standard curve.

2.2.15 Western blot

The cell lysate with equal protein concentrations (10 to 20 µg) was mixed with 5x laemmli buffer. The mixtures were incubated at 100°C for 10 minutes and immediately transferred in the ice. The samples were loaded to each well of either 10 or 15 well NuPAGE™ 4-12% Bis-Tris Gel (Invitrogen) placed in the Invitrogen tank containing 1x NuPAGE MOPS SDS running buffer (Novex). 5 µl of prestained protein ladder (10-250 kDa, Thermo Scientific™) was loaded into on column, and the gel was run at 100v for 75 minutes until the blue dye ran off the bottom of the gel. The gel was transferred to a PVDF (Polyvinylidene difluoride) membrane (Millipore) using NuPAGE transfer buffer (Novex) with methanol and antioxidant (Invitrogen) run at 35v for 60 minutes. The membrane was blocked with 5% milk-TBST at RT for 1 hour and incubated overnight with primary antibodies (**Table 2.5**) diluted in 5% milk-TBST at 4°C on the roller. The membrane was then washed with 0.1 v/v TBST for 5 minutes in the roller 3 times and incubated with secondary-HRP antibodies (**Table 2.5**) diluted in 5% milk-TBST at RT for 1 hour. The membrane was then washed with TBST three times for 5 minutes, incubated with pre-mixed ECL, and imaged with Bio-Rad imager.

Table 2.5. Antibodies used for analysing *TRIB1* levels in breast cancer subtypes using western blot

Antibodies	Company (Cat No.)	Dilution
TRIB1	Millipore (09-126)	1:1000
Polyclonal Goat anti-Rabbit Immunoglobulin/HRP	Dako (P0448)	1:2500
HSP90	Abcam (ab53497)	1:5000
Polyclonal Rabbit anti-Rat Immunoglobulin/HRP	Dako (P0450)	1:5000

2.2.16 *TRIB1* Immunocytochemistry

Cells were seeded in the 8-well chamber slides with cover (Lab-Tek) for 24 hours to 8 days depending on the experiments and gently washed twice with PBS to remove growth medium. Cells were fixed with 4% formalin or PFA at RT for 30 minutes and washed three times with PBS. After that, cells were permeabilised with 0.1% Triton X-100 for 15 minutes and washed with PBS three times to remove detergent. The samples were incubated with 2% BSA-PBS for 45 minutes and incubated with primary antibodies (**Table 2.6**) at RT for 1 hour or at 4% for overnight. The samples were then washed with PBS three times and incubated with secondary antibodies (**Table 2.6**) at RT for 1 hour and washed with PBS 5 times. The chamber was then removed from the slide and mounted with Antifade mounting medium with DAPI (Life Technology) and kept in the dark for overnight at RT and imaged immediately or stored at 4°C until needed.

Table 2.6. Antibodies for assessing *TRIB1* expression in human macrophages via immunocytochemistry

Antibodies	Company (Cat no)	Fluorochrome	Dilution
TRIB1	Millipore (09-126)		1:11
Goat anti-Rabbit IgG (H&L)	ImmunoReagents (GtxRb-003-D550NHSX)	DyLight 550	1:100

2.2.17 Immunofluorescence staining of frozen tissues

The frozen tissue sections were put at RT and flooded with ice-cold acetone for 10 minutes to fix the tissue. The slides were allowed to air dry and re-hydrated in PBS-T for 3 minutes. The non-specific binding of the secondary antibody was blocked with protein block serum-free at RT for 30 minutes and incubated with primary antibodies (**Table 2.7**) for 1 hour at RT. The samples were washed in PBS-T for 5 minutes twice, and secondary antibodies (**Table 2.7**) were added to the slide for 1 hour at RT. Slides were washed in PBS-T for 5 minutes three times and mounted with Antifade mounting medium with DAPI (Life Technology) and kept in the dark for overnight at RT and imaged immediately or stored at 4°C until needed. The images were captured by Leica AF6000 microscope using or Nikon A1 confocal microscope. Fluorescence staining of TRIB1 was optimized as noted in **Appendix 2**.

Table 2.7. Antibodies used to analyse the immune cells in the tumour microenvironment

Antibodies	Company (Cat no)	Fluorochrome	Dilution
F4/80	Bio-rad (MCA497A488)	Alexa Fluor 488	1:25
CD31	Biolegend (102516)	Alexa Fluor 674	1:100
NOS2	Abcam (ab15323)		1:50
MR	Abcam (ab64693)		1:100
Goat anti-Rabbit IgG (H&L)	ImmunoReagents (GtxRb-003-D550NHSX)	DyLight 550	1:50
CD3	Tonbo Bioscience (145-2C11)	APC	1:50
CD4	Biolegend (100423)	Alexa Fluor 488	1:100
CD8	Biolegend (100707)	PE	1:100
CA9	Abcam (ab184006)		1:50
TRIB1	Millipore (09-126)		1:50

2.2.18 Immunofluorescence staining of PEFF tissues

Immunofluorescence was performed in paraffin wax embedded human breast tissues. The slides were dewaxed with xylene for 5 minutes twice and rehydrated with degrading alcohol gradients (99%, 99%, 95%, and 70% ethanol) for 2 minutes each and the slides were washed in running tap water for 1 minute to remove xylene and ethanol. The endogenous peroxide activity is blocked with incubation of slides with 3% hydrogen peroxide (H_2O_2) in methanol for 20 minutes and washed in running tap water for 1 minute. The antigens were retrieved with 0.01M trisodium citrate (TSC) pH6 for 10 minutes in the microwave. The slides were cooled down in running tap water for 2 minutes, and the non-specific binding of the secondary antibody was blocked with protein block serum-free at RT for 30 minutes. The primary antibodies (**Table 2.8**) diluted in PBST were incubated for 1 hour at RT and washed with PBST for 5 minutes on a magnetic stirrer twice. The sections were incubated with secondary antibodies (**Table 2.8**) diluted in PBST for 1 hour at RT and washed in PBST for 5 minutes on a magnetic stirrer. The slides were mounted with Antifade mounting medium with DAPI (Life Technology) and kept in the dark for overnight at RT and imaged immediately or stored at 4°C until needed. The images were captured using Nikon A1 confocal microscope (**Appendix 4**).

Table 2.8. Antibodies used to analyse the *TRIB1* expressing TAMs in the human breast tumour tissues

Antibodies	Company (Cat no)	Fluorochrome	Dilution
TRIB1	Millipore (09-126)		1:50
CD68	Abcam (ab125157)		1:100
Goat anti-Rabbit IgG (H&L)	ImmunoReagents (GtxRb-003-D550NHSX)	DyLight 550	1:50
Donkey Anti-Mouse IgG NorthernLights™ NL493	R&D Systems (NL009)	NL493	1:100

2.2.19 Haematoxylin and Eosin staining

The frozen tissue sections were put at RT for 30 minutes to air dry and fixed with methanol for 10 minutes. The slide was then gently washed with PBS and further washed with PBS for 3 minutes twice. For the FFPE samples, the sections were de-waxed with xylene for 5 minutes twice and re-hydrated by incubating with 100% ethanol for 3 minutes twice followed by 95% and 70% ethanol for 3 minutes, and rinsed with tap water for 1 minute. The sections were stained with Carazzi's haematoxylin for 1 minute and rinsed in water until water runs clear and dipped in the Scotts water for 15 seconds. Samples were then stained with eosin for 30 seconds, and the slides were dipped in water, followed by 70%, 95%, and 100% ethanol three times each. The sections were incubated again with 100% ethanol for 30 seconds and incubated in the mounting xylene for 5 minutes. The slides were then fixed with DPX mountant and kept at RT to dry.

2.2.20 Dissociation of Eo771 tumour

The tumour tissue collected from mice was shredded with scissors, and the tumour chunks were placed in 5 ml of tumour-dissociation medium (Serum-free IMDM medium, 0.2mg/ml of collagenase IV, 2mg/ml dispase, 1.25ug/ml DNase 1) in a 15ml bijou tube, and rotated at 37°C for 30 minutes. After, 5ml of 10% FBS-TDM was added into the tube and passed through a 70µm filter (Fisher Scientific) and placed directly on ice. The samples were then transferred into 1.5ml Eppendorf tube and centrifuged at 4500 rpm for 5 minutes. The cell pellet was washed three times with 500µl PBS and stained for flow cytometry analysis.

2.2.21 Flow cytometry

Cells were re-suspended in PBS and centrifuged at 500 x g for 5 minutes. The samples were then re-suspended in 100µl LIVE/DEAD Fixable Blue Dead Cell Stain kit (Invitrogen) and incubated for 15 minutes at RT in the dark. After that, 200µl of PBS was added to the tube and centrifuged at 500 x g for 5 minutes. The cell pellet was re-suspended with PBS to aliquot if required and centrifuged at 500 x g for 5 minutes. Cells were stained with antibodies (**Table 2.9**) diluted in FACS buffer (5% FBS in PBS) for 15 minutes at 4°C protected from light, and 100µl FACS buffer was added into the tubes and centrifuged at 500 x g for 5 minutes. Cells were then washed with 150µl FACS buffer and centrifuged at 500 x g for 5 minutes twice. The pellet was re-suspended in 200µl FACS buffer and analysed with LSRII flow cytometer (Biolegend).

2.2.21.1 Compensation of antibodies

The antibodies used for flow cytometry analysis were compensated using ABC^{TM} Total Antibody Compensation Bead Kit (Invitrogen). A drop of ABC^{TM} Total compensation bead was added to 1.5ml Eppendorf tube and mixed with 1µl of antibodies (**Table 2.9**). The compensation bead and antibody mix were then incubated in the dark for 15 minutes, and the drop of negative bead was added to the tube. The 200µl of FACS buffer was then added to the tube, and the compensation was performed with the LSRII flow cytometer (Biolegend).

Table 2.9. Antibodies used to analyse the tumour microenvironment via flow cytometry

Antibodies	Company (Cat No.)	Fluorochrome	Dilution
F4/80	Bio-rad (MCA497A488)	Alexa Fluor 488	1:25
CD206	Biolegend (141705)	PE	1:100
CD274	Biolegend (124313)	PE/Cy7	1:200

Ly-6C	Biolegend (128024)	Alexa Fluor 700	1:100
NK1.1	Biolegend (108723)	APC-Cy7	1:100
Ly-6G	Biolegend (127612)	Pacific Blue	1:100
CD3	Tonbo Bioscience (145-2C11)	APC	1:100
CD4	Biolegend (116011)	PerCP/Cy5.5	1:100
CD8	Biolegend (100713)	APC-Cy7	1:100
CD279	Biolegend (135205)	PE	1:100

2.3 In vivo studies:

2.3.1 Mouse strains with altered *Trib1* expression in myeloid cells

Characterisation of these mouse strains has been published in (Johnston et al., 2019a).

2.3.1.1 *Trib1*- overexpressing mouse: *ROSA26. Trib1Tg x Lyz2Cre*

The myeloid-specific transgenic mouse strain was generated by inserting STOP-*Trib1*-EGFP cassette into the *Rosa26* locus of C57BL/6N mice. The cassette includes splicing acceptor (SA) site followed by neomycin resistance gene (Neo) and SV40 transcriptional terminator (STOP) flanked between two Cre recognition sites (loxP) which allow specific deletion of Neo-STOP cassette in myeloid cells when crossed with mice expressing Cre recombinase transgene under control of the Lyz2 promoter (*Lyz2Cre*; (B6.129P2-Lyz2tm1(cre)Ifo/J; jax.org) and enables the transcription of the *Trib11* transgene encoding *Trib1* and EGFP proteins tagged with FLAG (**Figure 2.1A**).

2.3.1.2 Trib1 knockout mouse: Trib1 fl/fl x Lyz2Cre

The targeting cassette, which consists of SA, internal ribosomal entry site (IRES) and LacZ expression cassette (LacZ-pA) followed by loxP site and Neo expression cassette was flanked by FRT sites and inserted into the first intron of *Trib1* which generate null allele of mRNA by

encoding the first exon of Trib1 and LacZ. The second exon of *Trib1* was also flanked by two loxP sites. This mouse strains were then crossed with strains expressing the FRT recombinase in germline cells to excise the targeting cassette, which resulted in the production of wild-type *Trib1* mRNA (**Figure 2.1B**).

The myeloid-specific *Trib1* floxed mice were generated by crossing female mice with homozygous floxed Trib1 allele and male mice with Cre recombinase transgene under control of the Lyz2 promoter (*Lyz2Cre*; (B6.129P2-Lyz2tm1(cre)Ifo/J; jax.org) which delete the second exon of Trib1 and generate null allele via producing truncated Trib1 protein (120aa) without central kinase-like domain and the C-terminal region (**Figure 2.1B**).

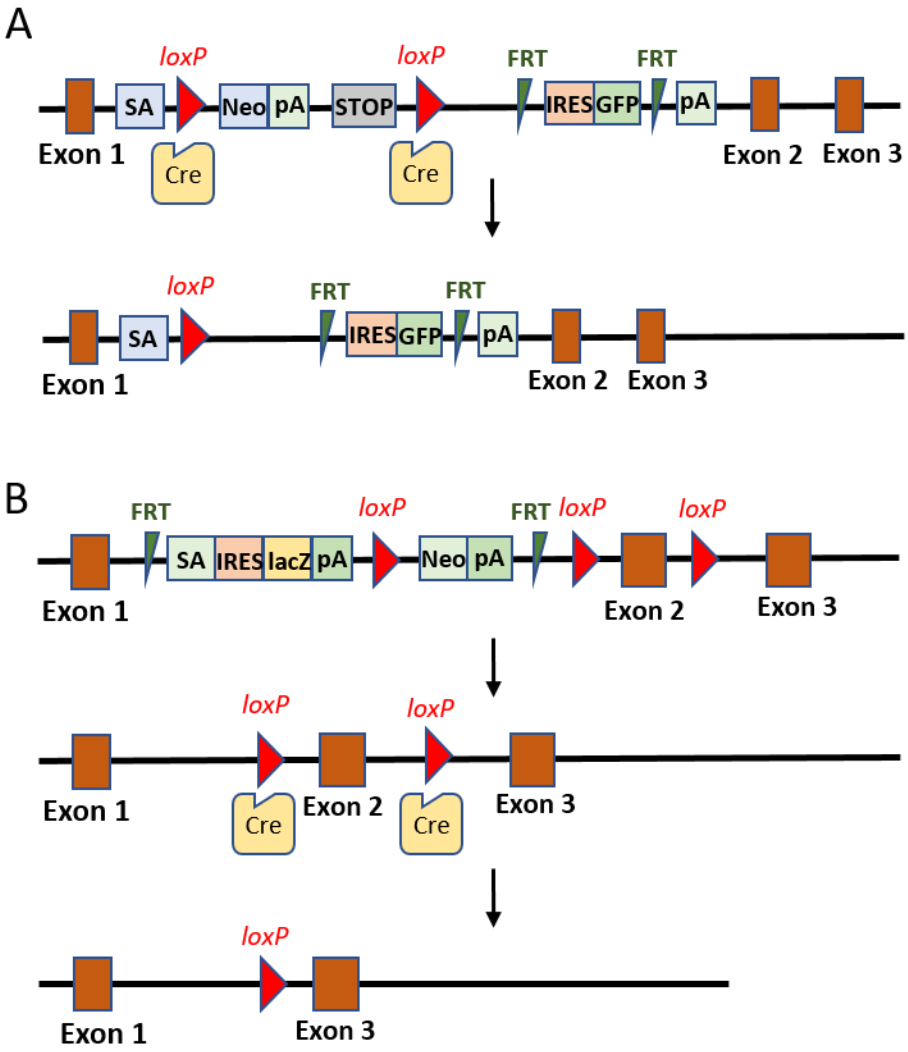

Figure 2.1. Schematic of *ROSA26.Trib1Tg x Lyz2Cre* and *Trib1 fl/fl x Lyz2Cre* generation. [Modified from Johnston (2019)]. (A) STOP-*Trib1*-EGFP cassette in *ROSA26.Trib1Tg x Lyz2Cre* strains consist of splicing acceptor site (SA) and neomycin resistance gene (Neo) with SV40 transcription terminator (STOP) flanked by Cre recognition (*loxP*) sites which will be removed when *Cre* is expressed in the cell. The removal of Neo-STOP region generates the bi-cistronic expression of the cassette, which enables transcription and encoding of *Trib1* and EGFP proteins. (B) To generate *Trib1 fl/fl x Lyz2Cre* strains, targeting cassette and two *loxP* sites flanking exon 2 were inserted in the first intron of *Trib1*. The inserted cassette promotes null allele of *Trib1* by encoding the first exon of *Trib1* and *Lacz*. The targeting cassette flanked by FRT sites were then removed by FLP-FRT recombination, which generates transcription of *Trib1* via endogenous promotor and results in wild-type *Trib1* mRNA expression. The *Trib1* is then floxed by *Cre*-mediated recombination and removing exon 2 region of *Trib1* which produce null allele.

2.3.2 Genotyping

2.3.2.1 DNA extraction from mouse ear clips

DNA was extracted from mouse ear clips by digesting the tissue in lysis buffer [50µM Tris-HCl (pH 8.5), 1µM EDTA (pH 8.0), 0.5% (v/v) Tween-20], proteinase K (300µg/ml)] for overnight at 56°C. The samples were then vortexed briefly and incubated at 100°C for 12 minutes. Sterile H_2O was added to the sample, and vortexed and isolated DNAs were kept in 4°C.

2.3.2.2 *Trib1* Tg & *Trib1* floxed & *Lyz2Cre* PCR

DNAs extracted from mouse ear clips were used to analyse mouse strains via PCR. *Lyz2Cre* PCR was performed according to the manufacturer's instruction (*Lyz2Cre*; (B6.129P2-Lyz2tm1(cre)Ifo/J; jax.org). *Trib1* transgene and floxed PCR were performed with 2x BioMix™ Red (BIOLINE) and primers designed to target *Trib1* regions (**Table 2.10**). The samples were then analysed via agarose gel electrophoresis.

Table 2.10. The sequence of *ROSA26.Trib1Tg* and *Trib1 FL/FL* genotyping PCR primers

Genotype	Label	Sequence
ROSA26.Trib1Tg	FW	GTGATCTGCAACTCCAGTCTTTCTAG
	WT REV	CGCGACACTGTAATTTCATACTGTAG
	TRANS REV	CCTTCTTGACGAGTTCTTCTGAGG
Trib1 fl/fl	dTRIB1cKO F2	ACCTTGATCTGCAGTCCTAGG
	dTRIB1cKO WT R	AGCTGGTTTCAGGGGAAGAC
	dTRIB1cKO FL R	AAGTTCACATTTGAACTGATGGC

2.3.3 Murine mammary tumour development

ROSA26.Trib1Tg x *Lyz2Cre* and *Trib1 fl/fl* x *Lyz2Cre* animals were housed in the University of Sheffield Biological Service Unit and cared according to the University of Sheffield code of ethics and Home Office regulations. Personal licence number I2AB6392A.

The mice were allowed to acclimatise for 1 week in the experimental unit and injected with 3 x 10^5 Eo771 cells at 8-9 weeks old using the following protocol. The animals were anaesthetised with inhalant isoflurane (IsoFlo) the and the abdominal area was shaved with hair removal cream to expose nipples. 3 x 10^5 Eo771 cells in 20µl cell suspension (33% Matrigel; 66% PSB; and 1% trypan blue or phenol red) were injected into the nipple using the insulin syringe. Mice were monitored and weighed every 2 days, and the tumour volume was measured using callipers and recorded.

$$Tumour\ volume\ (mm^3) = \frac{W^2 \times L}{2}$$

Once the tumour reached 15mm in diameter (~1500mm^3), mice were culled by cervical dislocation and the organs and tumours were collected for the post-mortem analysis.

2.4 Bioinformatics analyses:

2.4.1 Analysis of microarray

Cardiogenic Consortium transcriptomic data set (Schunkert et al., 2011, Heinig et al., 2010, Rotival et al., 2011) was analysed in collaboration with Professor Alison Goodall and Dr Stephen Hamby at the University of Leicester. The analysis was performed as described in (Johnston et al., 2019a). In brief, top and bottom quartiles of *TRIB1* expressing monocytes (N = 758) and macrophages (N = 596) were compared and obtained the *TRIB1* co-regulated, differentially expressed genes using FDR adjusted p-values of <0.01, cut-off log-2 fold

changes of >0.071 (upregulated) and >-0.071 (down-regulated) (Johnston et al., 2019a). The gene list was further analysed with QuSage to identify the pathways enriched in the TRIB1 co-expressed gene sets.

2.4.2 Statistical analysis of experimental data

All statistical analyses and graphs were generated using GraphPad Prism 8 software (La Jolla, California, USA). The tumour growth was analysed using two-way ANOVA, and post-mortem analysis of tumour microenvironment, lung and liver metastasis, and quantitative RT-PCR results from BMDMs were analysed with an unpaired test. Quantitative RT-PCR results from human MDMs were analysed by paired test, and all graphs are shown as mean ±SEM.

Chapter 3. *TRIB1* alters TAM phenotype

3.1 Introduction

The regulation of macrophage phenotype is crucial for their response to different diseases through secretion of different cytokines and chemokines (Shapouri-Moghaddam et al., 2018) and a number of papers have already reported TRIB1-dependent modulation of macrophage polarisation (Satoh et al., 2013, Arndt et al., 2018, Liu et al., 2019b, Chen et al., 2020). For example, Satoh *et al.* (2013) reported a reduction of anti-inflammatory macrophages expressing *Mrc1*, *Arg1*, and *Fizz1* in spleens from *Trib1* deficient mice (Satoh et al., 2013). This was also observed previously in our laboratory where livers from myeloid-specific *Trib1* knockout ($Trib1^{mKO}$) mice demonstrated a significant increase of pro-inflammatory macrophages in $Trib1^{mKO}$ livers; and a significant reduction of pro-inflammatory macrophages and increase of anti-inflammatory macrophages in the livers from myeloid-specific *Trib1* overexpressing ($Trib1^{mTg}$) animals (Johnston, 2017). In addition, analysis of microarray transcriptomic datasets from Cardiogenics Consortium comparing *TRIB1* high and low human monocytes and macrophages revealed that *TRIB1* high macrophages showed selectively upregulated anti-inflammatory markers compared to *TRIB1* low macrophages. However, the same difference was not observed between *TRIB1* high and low monocytes (**Figure 3.1**) (Johnston, 2017), demonstrating the specific regulation of macrophage polarisation through *TRIB1* expression.

In oncogenesis, a potential oncogenic role of TRIB1 was reported in different cancer types. Regulation of macrophage phenotype via TRIB1 emphasised the role of TRIB1 in acute myeloid leukaemia (AML), where the overexpression of *TRIB1* was observed in AML

patients and TRIB1 enhances AML development (Keeshan et al., 2016, Velasco, 2016). The upregulation of TRIB1 was also reported in prostate cancer and colorectal cancer, where high-throughput analysis of colorectal cancer and *in silico* analysis of prostate cancer tissues revealed amplification and overexpression of *TRIB1* in these cancers (Camps et al., 2009, Moya et al., 2018), and TRIB1 is reported to promote prostate cancer by enhancing cancer cell survival (Mashima et al., 2014). However, the oncogenic role of TRIB1 in breast cancer has not been studied yet, especially in relation to stromal cell populations, including TAMs.

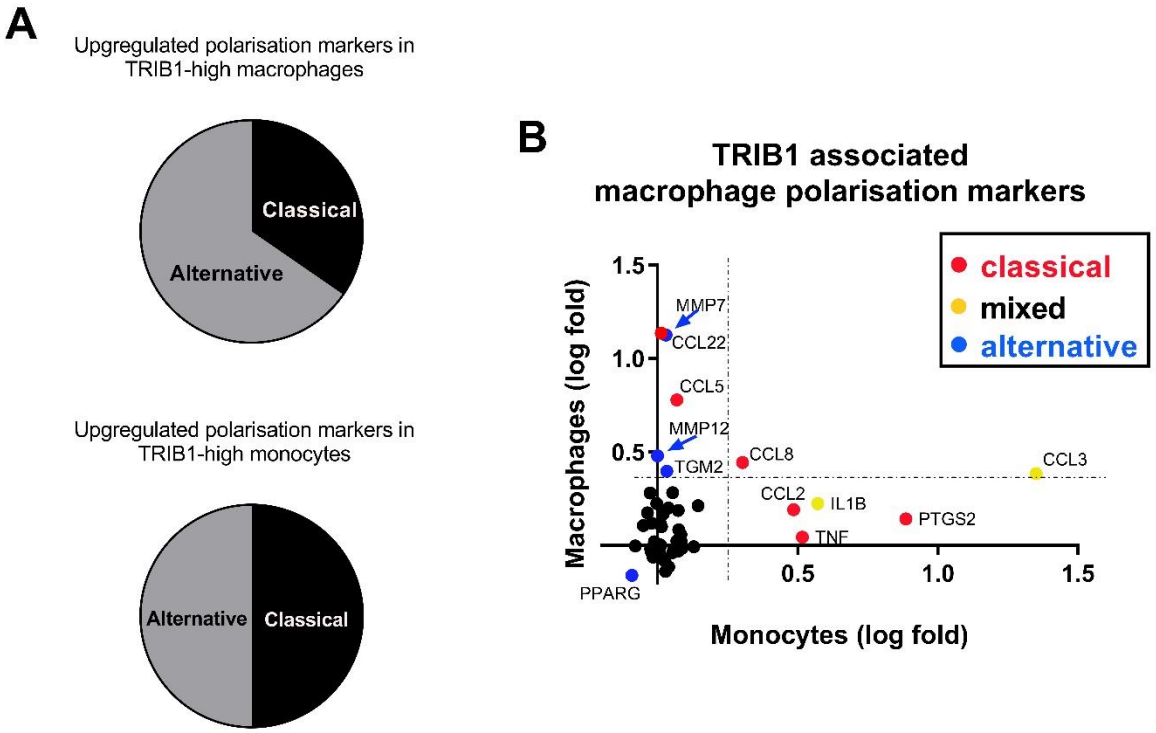

Figure 3.1. *TRIB1* expression is associated with overexpression of alternatively activated macrophages [Adapted from the thesis of Jessica M. Johnston, 2017]. (A) The analysis of microarrays comparing *TRIB1* high and low human monocytes and macrophages revealed polarisation markers of pro-inflammatory or classical, and ani-inflammatory or alternative phenotypes in *TRIB1* high monocytes and macrophages compared to *TRIB1* low monocytes and macrophages. (B) Expression of genes associated with *TRIB1* in monocytes and macrophages.

Therefore, this chapter will delineate the regulatory role of TRIB1 specifically in macrophages and provide the background of potential oncogenicity of TRIB1 in breast cancer through regulation of TAM functions.

3.2 Hypothesis and aims

Work in this chapter tests the hypothesis that myeloid-TRIB1 is oncogenic in breast cancer development and that it acts via the regulation of oncogenic roles of TAMs. *In silico* analysis of datasets and *in vitro* analysis of human MDMs were used to investigate the expression of *TRIB1* in breast cancer and *TRIB1*-dependent regulation of TAM functions.

1. Bioinformatics of TRIB1 in breast cancer and myeloid cells
2. *In vitro* analysis of TRIB1 in the regulation of macrophages and TAMs

3.3 Results

3.3.1 *TRIB1* regulate monocytes and macrophages with distinct regulatory functions

To analyse the regulatory function of *TRIB1* in macrophages, the microarray of monocytes (n=758) and macrophages (n=596) from human participants from Cardiogenics Consortium transcriptomic data set (Heinig et al., 2010, Schunkert et al., 2011, Rotival et al., 2011) were aligned according to *TRIB1* levels. The list of genes differentially expressed between the top and bottom quartile of the dataset were taken forward for analysis for the functional role of *TRIB1* in monocytes and macrophages. As discussed in the introduction, previous work in our lab observed the *TRIB1*-dependent regulation of polarization markers in macrophages, where macrophage *TRIB1* elevated the expression of anti-inflammatory markers but not in monocytes. The distinct role of *TRIB1* between monocytes and macrophages were also confirmed by further analysis of the list of genes altered depending on *TRIB1* expression with functionally related Gene Ontology terms. It demonstrated that the top 10 functional roles modified depending on *TRIB1* in macrophages were not altered in monocytes (**Figure 3.2**).

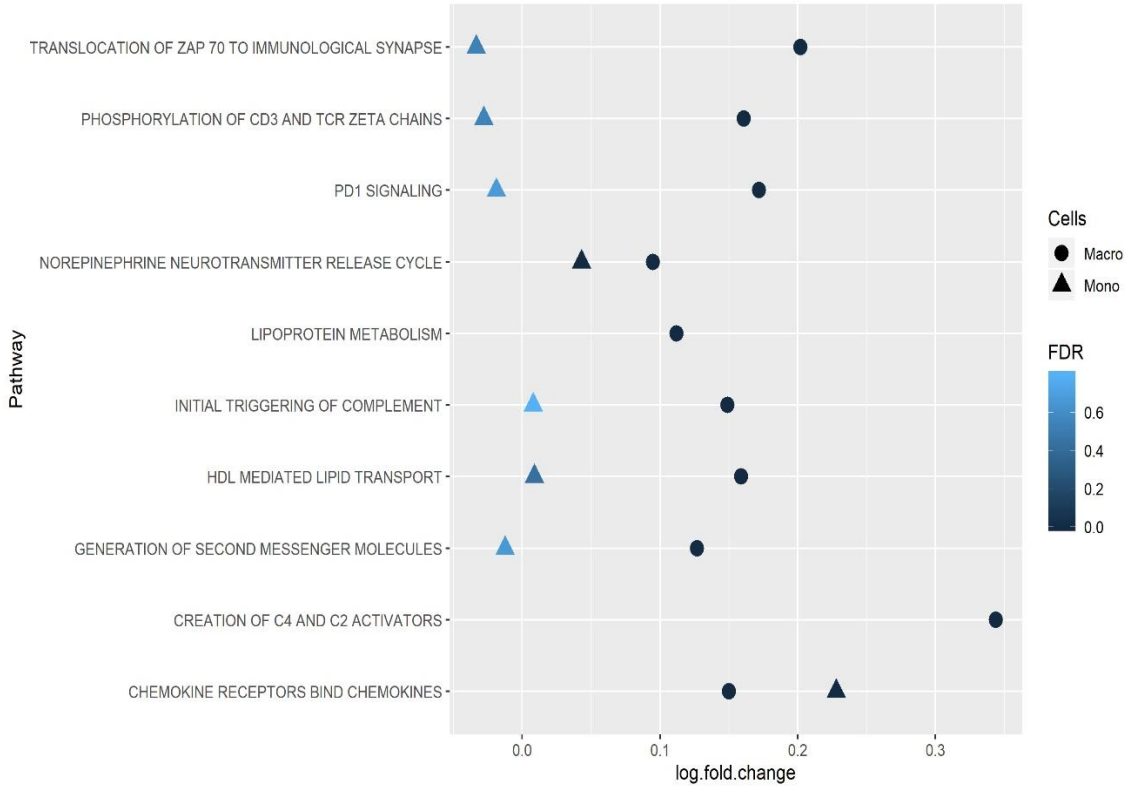

Figure 3.2. Top 10 functional roles modified based on *TRIB1* expression in macrophages were not altered in monocytes. The microarray of human monocytes (n=758) and macrophages (n=596) from Cardiogenic Consortium transcriptomic data set were aligned according to *TRIB1* expression levels and compared *TRIB1* high and low monocytes and macrophages by analysing the top and bottom quartile of the data set. The identification of pathways enriched in TRIB1 co-expressed gene sets was performed with QuSAGE (Johnston, 2017), and compared the enrichment of top 10 upregulated functional roles in *TRIB1* high macrophages (Circle) to *TRIB1* high monocytes (Triangle). FDR is represented as degrading colour of each point.

3.3.2 Myeloid TRIB1 modulates macrophage polarisation

The correlation of macrophage phenotype and *TRIB1* expression in human MDMs were investigated using transfection of *TRIB1* siRNA and analysed the changes of polarisation markers. The schematic workflow can be seen in **Figure 3.3A**. Up to 70% of the knockdown of *TRIB1* after siRNA transfection was confirmed using RT-qPCR, as shown in **Figure 3.3B**. *IL-1β* and *IL-8* are two pro-inflammatory markers used in the study. *IL-1β* is one of the alarm cytokines secreted by macrophages to initiate inflammation on activation of TLRs and also induces other pro-inflammatory genes that encode inducible nitric oxide synthase, *IL-6* and

other cytokines or chemokines (Tschopp et al., 2003). *IL-8* is another pro-inflammatory cytokine secreted by macrophages when exposed to inflammatory stimuli and is a chemoattractant for other immune cells (Duque and Descoteaux, 2014). *MRC1* or *CD206* and *SCARB1* are polarisation markers known to be highly expressed in anti-inflammatory macrophages (Roszer, 2015b). The knockdown of *TRIB1* in human MDMs demonstrated the significant increase of pro-inflammatory cytokines *IL-1β* (**Figure 3.3C**) and *IL-8* (**Figure 3.3D**) but the expression of anti-inflammatory markers *MRC1* (**Figure 3.3E**) and *SCARB1* (**Figure 3.3F**) were not altered which implies *TRIB1* expression in macrophages negatively correlates with pro-inflammatory macrophage polarisation. Other cytokines were not altered between control and TRIB1 KD macrophages (**Supplementary figure 5**).

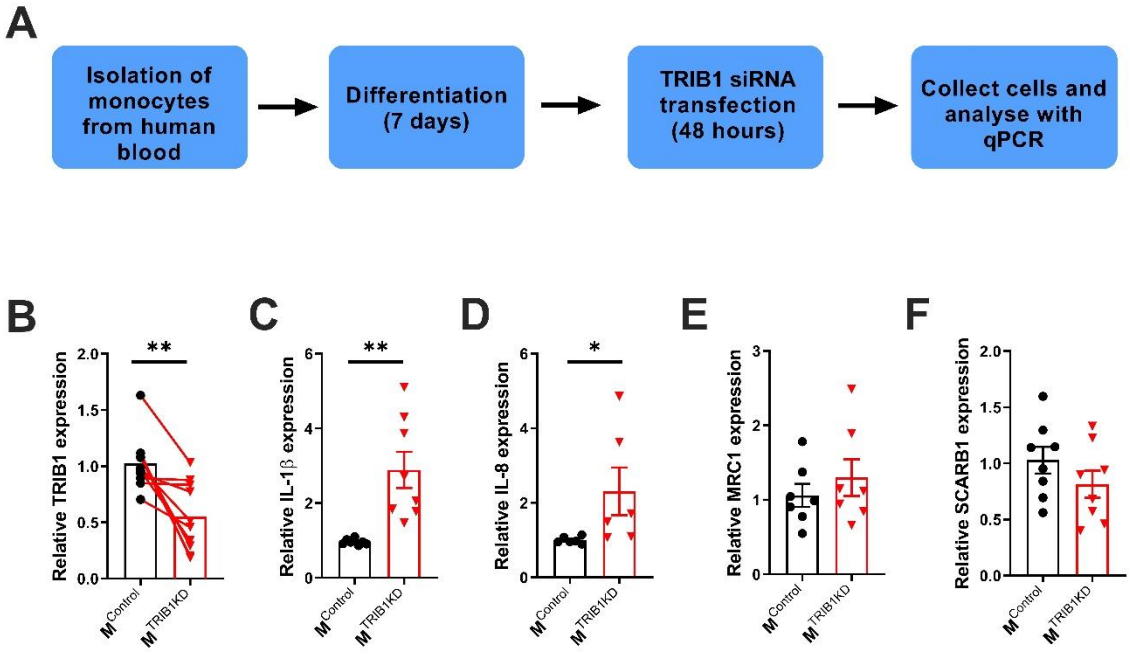

Figure 3.3. *TRIB1* knockdown in human MDMs drives macrophage polarisation towards pro-inflammatory macrophages. (A) Human MDMs were generated from monocytes isolated from human blood. The isolated monocytes were differentiated to macrophages for 7 days and transfected with *TRIB1* siRNA to knockdown *TRIB1* expression. Cells were then analysed with RT-qPCR. (B) *TRIB1* RNA levels (relative to *GAPDH*) in macrophages 48 hours after control or *TRIB1* siRNA transfection. RNA levels of *IL-1β* (C) *IL-8* (D) *MRC1* (E) and *SCARB1* (F) 48 hours after control or *TRIB1* siRNA transfection. Results of paired T-test are presented as * $p<0.05$, ** $p<0.01$, and data represent mean±SEM of n=6-9donor/group.

3.3.3 *TRIB1* expression is altered in breast cancer tissues and is overexpressed in TNBC cells

The analysis of *TRIB1* expression in breast cancer tissues was first performed with data mining of published human datasets from cBioportal (Cerami et al., 2012, Gao et al., 2013). The *in silico* analysis of datasets demonstrated amplification and mutation of the TRIB1 gene in different cancer types and breast cancer is listed as third-highest cancer with alteration frequency compared to other cancers. Among 1084 cases of breast cancer, 13.28% of cases demonstrated the alteration of TRIB1 gene (12.55% (136 cases) of amplification, 0.55% (6 cases) of mutation, and 0.18% (2 cases) of multiple alterations) (**Figure 3.4A**). RNA Seq from three datasets processed and normalized using RSEM also demonstrated *TRIB1* expression of about 11 fold (log2) in breast cancer patients (**Figure 3.4B**), and further analysis of patient survival with *TRIB1* mutation revealed a significant reduction in overall survival with alterations in TRIB1 gene (**Figure 3.4C**), which implies potential oncogenicity of TRIB1 in breast cancer development.

However, published human cancer datasets of gene expression microarray from GENT2 (Park et al., 2019) demonstrated a significant reduction of *TRIB1* expression in breast cancer tissues in the Affymetrix U133A platform (GPL96)(92 normal breast tissues and 4293 breast cancer tissues) (**Figure 3.5A**), whilst in Affymetrix U133Plus2 (GPL570)(475 normal breast tissues and 5574 breast cancer tissues) revealed similar *TRIB1* expression between normal and breast cancer tissues (**Figure 3.5B**). The analysis also demonstrated the significant overexpression of *TRIB1* expression in TNBC tissues compared to other subtypes (**Figure 3.5C**).

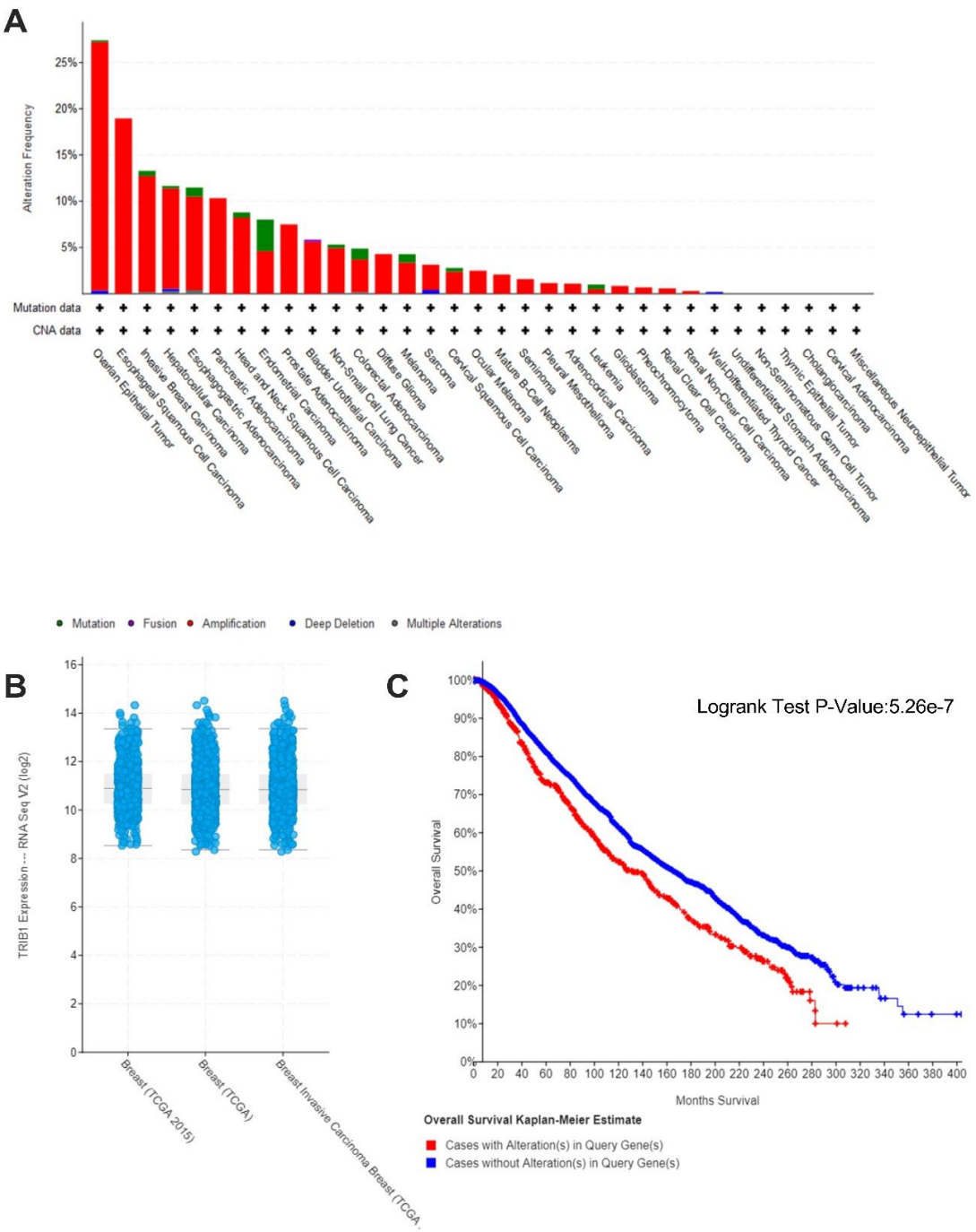

Figure 3.4. Mutation of TRIB1 gene is oncogenic in breast cancer. The *in silico* analysis of TRIB1 gene in breast cancer patients from published human datasets were performed using cBioportal website. (A) The alteration of the TRIB1 gene in 32 cancer types regarding amplification (red), mutation (green), deep deletion (blue), and multiple alterations (grey). Breast cancer is listed as the third-highest alteration frequency on TRIB1 with 13.28% from 1084 reported cases preceded by ovarian cancer with 27.4% from 584 cases and oesophagus cancer with 19.78% from 182 cases, and 12.55% of 1084 cases reported the amplification of TRIB1 in breast cancer tissues. (B) RNA seq of *TRIB1* mRNA level in the breast cancer tissues from three different datasets. The expression of *TRIB1* is plotted log2 scaled. (C) The overall patient survival of 816 cases of breast cancer patients with TRIB1 alteration (red) and 6731 cases of patients without alteration (blue) over 404 months. The Kaplan-Meier estimate of overall patient survival represents p=5.26e-7.

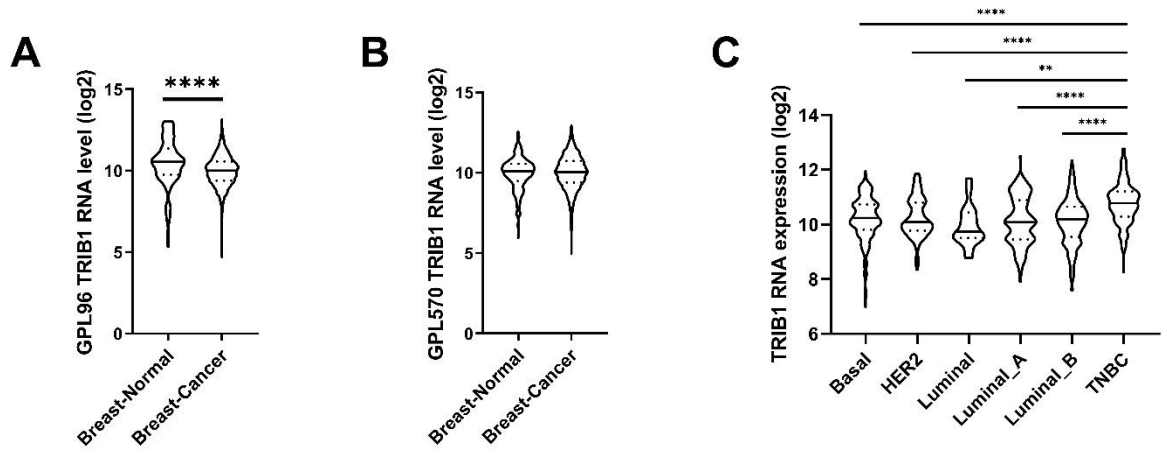

Figure 3.5. *TRIB1* RNA level is reduced in breast cancer tissues but highly expressed in TNBC tissues. The *in silico* analysis of *TRIB1* RNA levels in breast cancer and healthy tissues from published human datasets were performed using GENT2 website. (A) *TRIB1* RNA level from Affymetrix U133A platform (GPL96) including microarray of 92 healthy breast tissues and 4293 breast cancer tissues. (B) *TRIB1* RNA level from Affymetrix U133Plus2 platform (GPL570) including microarrays of 475 healthy breast tissues and 5574 breast cancer tissues. (C) The microarray of *TRIB1* in different breast cancer subtypes: Basal (363 samples), HER2 (230 samples), Luminal (17 samples), Luminal A (379 samples), Luminal B (244 samples), and TNBC (TNBC)(251 samples). Results of paired T-test and ANOVA are presented as **p<0.01 ****p<0.0001, and data represented in violin plot.

We also investigated the expression of TRIB1 protein in breast cancer cells *in vitro* using western blot with different breast cancer subtypes. The molecular analysis of breast cancers with gene expression profiling classified breast cancers into four broad subtypes, where luminal A represents ER positive and/or PR positive and HER2 negative breast cancers; luminal B represents ER-positive and/or PR/HER2 positive or negative breast cancers; HER2 enriched represents HER2 only positive breast cancers; and triple-negative or basal-like represents breast cancer with negative ER, PR, and HER2 (Fragomeni et al., 2018). The western blot of TRIB1 with SK-BR3 (HER2 enriched), BT474 (luminal B), MCF7 (luminal A), and MDA-MB-231 (triple-negative) breast cancer cell lines demonstrated the high expression of TRIB1 in breast cancer cells, but among four subtypes, MDA-MB-231 cells

displayed highest TRIB1 protein expression (**Figure 3.6A**). A representative image of the western blot is shown in **Figure 3.6B**.

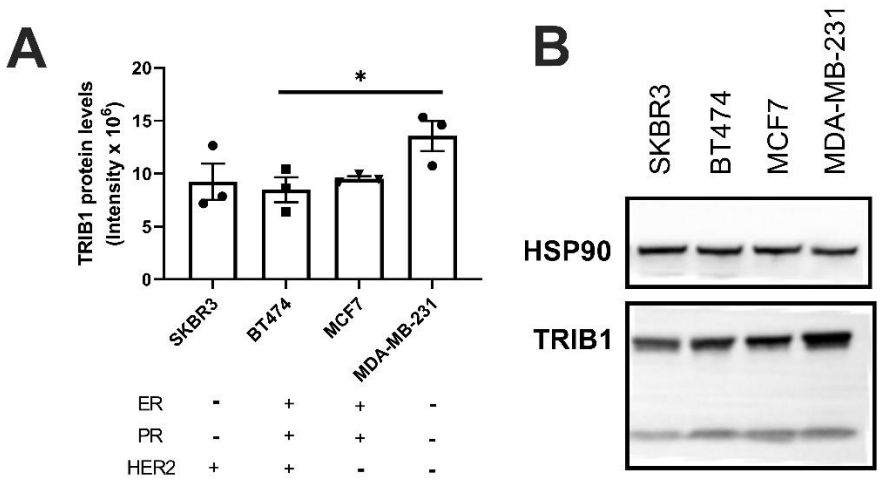

Figure 3.6. Breast cancer cell lines express high TRIB1 levels *in vitro*. Western blot was performed in four different breast cancer cell lines to investigate the expression of TRIB1 depending on the subtypes. (A) The fluorescence intensity of TRIB1 protein expressions (relative to housekeeper HSP90) in SKBR3 (HER2 enriched), BT474 (luminal A), MCF7 (luminal B), and MDA-MB-231 (triple-negative) cell lines. Result of ANOVA is presented as *$p<0.05$, and data represent mean±SEM of n=3samples/group. (B) The representative images of TRIB1 and housekeeper western blots with SKBR3, BT474, MCF7, and MDA-MB-231 cell lines.

3.3.4 TRIB1 is highly expressed by TAMs in the tumour microenvironment

Human MDMs isolated from blood were used to assess the expression of TRIB1 in TAMs *in vitro*. In this study, isolated MDMs were treated with the tumour-conditioned medium from human TNBC cell line MDA-MB-231 for 24 hours to develop TAMs and assessed both TRIB1 mRNA and protein levels using RT-qPCR and immunocytochemistry (**Figure 3.7A**). RT-qPCR analysis demonstrated the overexpression of *TRIB1* in TAMs, compared to unpolarised and pro-inflammatory LPS and INF-γ stimulated MDMs (**Figure 3.7B**). In contrast, immunocytochemistry of TRIB1 on TAMs and unpolarised MDMs revealed a significant reduction of TRIB1 protein signals in TAMs compared to unpolarised MDMs *in*

vitro (**Figure 3.7D)**. A representative image of TRIB1 immunocytochemistry is shown in **Figure 3.7C**. Prior to chapter 4 *in vivo* mouse model studies, primary murine breast tumours developed in the wild-type C57BL/3 mice through intra-nipple injection of murine TNBC Eo771 cell were investigated to assess the expression of Trib1 in TAMs and tumour microenvironment. The fluorescence staining of the tumours with anti-TRIB1 antibody and macrophage marker F4/80 demonstrated that about 40% of cells present in the tumour microenvironment express Trib1 and most of these cells were TAMs (**Figure 3.7F)** which implies the potential role of TRIB1 in TAMs.

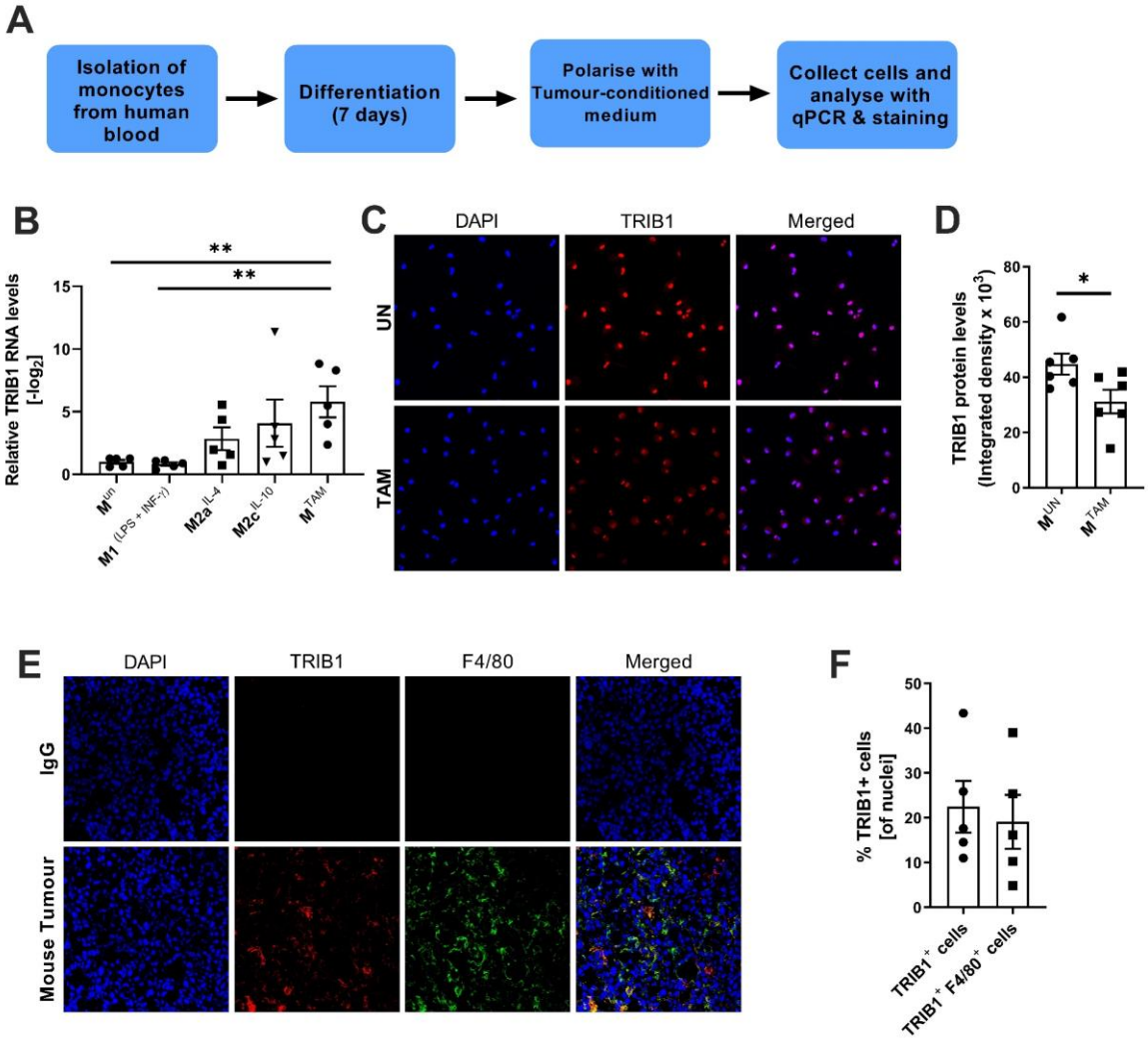

Figure 3.7. TRIB1 level is altered in TAMs *in vitro* and predominantly expressed in TAMs *in vivo*. The expression of mRNA and protein TRIB1 in TAMs were investigated both *in vivo* and *in vitro*. (A) *In vitro* TRIB1 level in TAMs was assessed using human MDMs stimulated with LPS and INF-γ (pro-inflammatory), IL-4 or IL-10 (anti-inflammatory), and the tumour-conditioned medium (TAMs) for 24 hours. Cells were then analysed with RT-qPCR and immunocytochemistry. (B) *TRIB1* RNA levels (relative to *GAPDH*) in human MDMs 24 hours after unstimulated (M^{UN}), stimulated with LPS and INF-γ ($M^{(LPS + INF-\gamma)}$, IL-4 (M^{IL-4}), IL-10 (M^{IL-10}), and tumour-conditioned medium (M^{TAM}). (C) Representative images of TRIB1 immunocytochemistry on human MDMs polarised to TAMs. Cells were stained with DAPI (blue) and TRIB1 (red). (D) The fluorescence intensity of TRIB1 protein levels in MDMs unstimulated and stimulated with the tumour-conditioned medium for 24 hours. Results of AVNOA and paired T-test are presented as *$p<0.05$ **$p<0.01$, and data represent mean±SEM of n=5-6donor/group. *In vivo* TRIB1 level in TAMs was assessed using fluorescence staining of TRIB1 and F4/80 on the primary tumours developed from wild-type (C57/BL3) animals. (E) Representative images of fluorescence staining on the primary tumours. Cells were stained with DAPI (blue) and TRIB1 (red), and TAMs were stained with F4/80 (green). (F) Quantification of cells with TRIB1 expression ($TRIB1^+$ cells) and TRIB1 expressing TAMs ($TRIB1^+$ $F4/80^+$ cells) relative to total cell counts. Data represent mean±SEM of n=5mice/group.

3.3.5 *TRIB1* regulates TAMs phenotype and function

Following the demonstration of *TRIB1* expression in TAMs, TRIB1-dependent regulation of TAM functions was investigated using *TRIB1* siRNA transfection of human MDMs for 24 hours prior to TAM polarisation and analysis of the altered cytokines and functionally important TAM genes, using RT-qPCR. The schematic flow chart of the study is shown in **Figure 3.8A**. In addition to cytokines, genes involved in the suppression of immune surveillance, angiogenesis, and metastasis were assessed. Expression of IL-8 in the tumour microenvironment has been reported to enhance breast cancer progression in clinical studies through alteration of immune cell composition and enhance the immunosuppressive state in the tumour microenvironment (David et al., 2016). IL-10 in pre-tumours promotes immunosuppression via upregulation of TNF, IL-1, IL-12, and chemokine expression, and downregulation of CD80 and CD86 on tumour cells, as well as initiating angiogenesis through inhibition of MMPs (Sheikhpour et al., 2018). IL-15 is involved in T-cell infiltration (Robinson and Schluns, 2017) whilst PD-L1 expressed on the surface of antigen-presenting cells, and tumour cells bind to PD-1 on the surface of T-cells and inhibit their proliferation, cytokine generation and release, and cytotoxicity of T-cells (Wu et al., 2019). SPARC has a controversial role in cancer development and progression, depending on the surrounding stroma and type of cancer (Tai and Tang, 2008). In breast cancer, SPARC expression significantly reduces metastasis-free survival, with 2.34 times higher risk of mortality and poor prognosis but it was also reported to inhibit breast cancer bone metastasis (Ma et al., 2017). VEGF is involved in angiogenesis and vasculogenesis, where the production of this cytokine is important in the development of a solid tumour and the VEGF enhanced tumour growth and metastatic potential *in vivo* (Verheul and Pinedo, 2000). The assessment of the expression of these cytokines and genes in *TRIB1* knockdown MDMs treated with tumour-

conditioned medium ($TAM^{TRIB1KD}$) revealed a trend for increased *IL-15* expression (**Figure 3.8D**) as well as a significant increase in *IL-8* (**Figure 3.8B**), *IL-10* (**Figure 3.8C**), *PD-L1* (**Figure 3.8E**), *SPARC* (**Figure 3.8F**), and *VEGF* (**Figure 3.8G**) RNA levels in $TAM^{TRIB1KD}$, compared to control group. Other cytokines were not altered between control and TRIB1 knockdown TAMs (**Supplementary figure 6**).

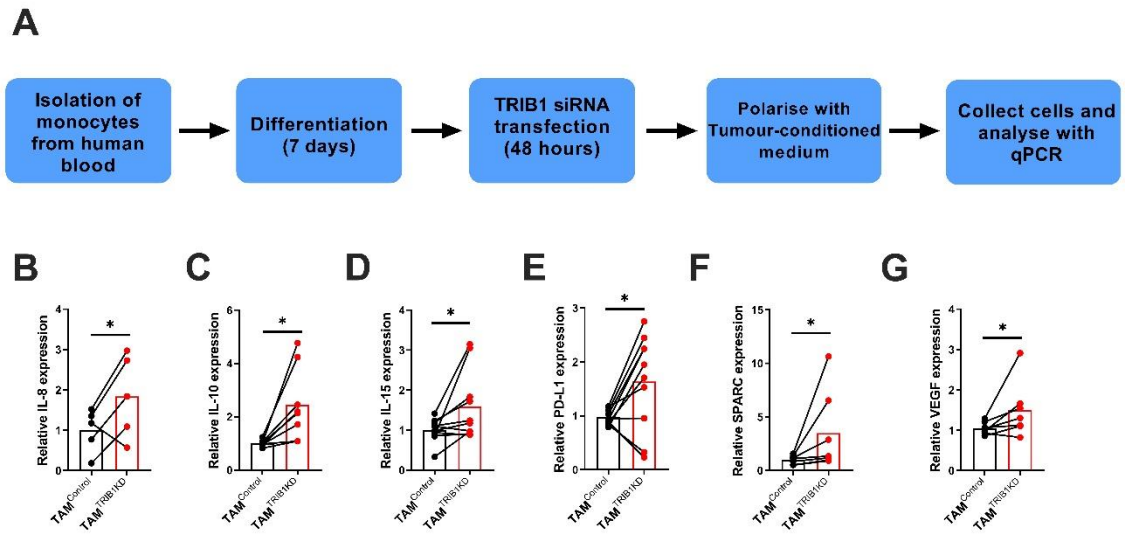

Figure 3.8. Myeloid *TRIB1* knockdown modulates functional cytokines and genes in TAMs *in vitro*. The regulation of TAM functions depending on *TRIB1* level *in vitro* was assessed using transient knockdown of *TRIB1* in human MDMs with siRNA transfection. (A) Human MDMs isolated and differentiated from blood were transfected with either control or *TRIB1* siRNA for 48 hours and polarised to TAMs using the tumour-conditioned medium for 24 hours. Cells were then analysed using RT-qPCR. RNA levels of *IL-8* (B), *IL-10* (C), *PD-L1* (E), *SPARC* (F), and *VEGF* (G) 72 hours after control or *TRIB1* siRNA transfection and polarisation. Results of paired T-test are presented as *p<0.05, and data represent the mean of n=5-8donor/group.

3.4 Discussion

The regulation of macrophage phenotype by TRIB1 was reported by a number of papers (Satoh et al., 2013, Shiraishi et al., 2016, Arndt et al., 2018, Johnston et al., 2019a). It was also observed previously in our lab where regulation of *Trib1* in myeloid cells altered composition of macrophage phenotype in the liver *in vivo*, and *TRIB1* high human MDMs upregulated anti-inflammatory markers compared to *TRIB1* low MDMs but not in monocytes

as discussed above in this chapter, which implies the distinct role of *TRIB1* in monocytes and macrophages (Johnston, 2017). Further analysis of regulatory functions altered between *TRIB1* high and low human monocytes and MDMs confirmed the specific role of *TRIB1* in macrophages where top 10 upregulated pathways in *TRIB1* high MDMs were not altered in *TRIB1* high monocytes. The *in vitro* transient knockdown of *TRIB1* in MDMs isolated from human blood also demonstrated a significant overexpression of pro-inflammatory cytokines *IL-1β*, and *IL-8* but unaltered anti-inflammatory markers *MRC1* and *SCARB1*, in line with published literature and previous work in the lab, where the knockout of *Trib1* in mice significantly reduced the number of anti-inflammatory macrophages in spleen and liver and significantly increased pro-inflammatory macrophages in the liver.

The expression of TRIB1 in breast cancer was assessed by *in silico* analysis of published human breast cancer patient datasets provided on the cBioportal website (https://www.cbioportal.org/). The analysis demonstrated that among different cancer types, breast cancer aligns at third-highest cancer with alteration in TRIB1 gene with 13.28% of reported cases; mostly amplification of the gene, and a significant reduction in the overall survival of patients with TRIB1 alterations. The *in silico* analysis of gene expression microarray datasets of human breast tissues provided on the GENT2 website (http://gent2.appex.kr/gent2/) revealed paradoxical expression of *TRIB1* in breast cancer tissues compared to normal tissues where a significant reduction of *TRIB1* in breast cancer was observed in one platform, but the difference was lost with the microarray generated from a different platform, perhaps due to the increased number of samples in the normal breast tissues which normalised the results. In other hands, *TRIB1* RNA expression between different breast cancer subtypes demonstrated that TNBC expresses highest *TRIB1* compared to other breast cancer tissues. Similar was observed *in vitro* in breast cancer cell lines which

observed high expression of TRIB1 protein in different subtypes of breast cancer but exceptionally high in the TNBC cell lines, which suggests a vital role for TRIB1 in breast cancer development and aggressiveness.

The expression of TRIB1 in TAMs was also assessed both *in vitro* and *in vivo* using RT-qPCR and fluorescence staining. The assessment of *TRIB1* mRNA levels in human MDMs polarised to TAMs using the tumour-conditioned medium revealed overexpression of *TRIB1* in TAMs, compared to unpolarised and pro-inflammatory macrophages. Controversially, however, expression of TRIB1 protein level observed in TAMs through immunocytochemistry demonstrated a significant reduction of TRIB1 levels compared to unpolarised MDMs. The contentious expression of mRNA and protein levels were also observed in breast cancer with the member of Tribbles family, TRIB3, where Wennemers *et al*. (2011) reported significant overexpression of *TRIB3* in breast cancer patients and the expression correlates with breast cancer prognosis (Wennemers et al., 2011b) but the protein level of TRIB3 in the patients did not correlate with *TRIB3* mRNA levels, which suggested potential distinct transcriptional and translational mechanisms regulating TRIB3 protein levels (Wennemers et al., 2011a). The gene-specific correlation of RNA and protein levels using proteomics and transcriptomics across human tissues and cell lines also revealed no correlation between transcript and protein levels without gene-specific RNA-to-protein conversion factors independent of the cells and tissues but suggested potential universal RNA to protein ratio across cells from different origin (Edfors et al., 2016), which could explain the difference between TRIB1 mRNA and protein levels in TAMs. *In vivo* analysis of primary breast tumours from wild-type animals also demonstrated that ~10-45% of cells present in the tumour microenvironment expressed Trib1 and mostly from TAMs, which implies the potential role of *Trib1* in TAMs.

The regulation of TAM functions via *TRIB1* was tested using the transient knockdown of *TRIB1* with siRNA transfection in human MDMs polarised to TAMs and assessment of altered cytokine and chemokines. The analysis of altered cytokines and chemokines in $TAM^{TRIB1KD}$ revealed that *TRIB1* knockdown in TAMs significantly increases the expression of *IL-8* and *IL-10* which have previously been shown to promote the suppression of immune surveillance (David et al., 2016, Sheikhpour et al., 2018), a trend of increased *IL-15* expression which enhances T-cell infiltration into the tumour (Robinson and Schluns, 2017) but with a significant increase of *PD-L1* expression which disrupts T-cell proliferation and function (Wu et al., 2019). $TAM^{TRIB1KD}$ also demonstrated a significant increase of *SPARC* and *VEGF* expression, which are essential for breast cancer growth and angiogenesis (Verheul and Pinedo, 2000). However, the *SPARC* expression also inhibits breast cancer metastasis to bone (Ma et al., 2017), which suggest *TRIB1* expression in TAMs modulate oncogenic functions through alteration of cytokines and chemokines produced in TAMs.

Chapter 4. Overexpression of myeloid *Trib1* enhances breast tumour growth and modifies the tumour immune microenvironment

4.1 Introduction

In the tumour microenvironment, regulation of macrophage phenotype plays an essential role in tumorigenesis. Previous papers suggested that the cytokines expressed by pro-inflammatory TAMs initiate immune responses mediated by NK cells, T_H1 cells, cytotoxic T lymphocytes and NO production via *NOS2* promotes cytotoxicity and apoptosis using the activation of aconitase and ribonucleotide reductase or mitochondrial cytochrome C release (Choudhari et al., 2013, Paul et al., 2019, Quaranta and Schmid, 2019). In contrast, anti-inflammatory TAMs are generally reported as oncogenic macrophages. About 70% of TAMs in lung cancer reported to be anti-inflammatory TAMs positive for the macrophage marker CD68 and an anti-inflammatory marker CD163, and in stage II of colorectal cancer, tumours infiltrated high numbers of anti-inflammatory macrophages to enhance their growth (Ma et al., 2010, Pinto et al., 2019).

Chapter 3 demonstrated *TRIB1* dependent regulation of macrophage phenotypes and the overexpression of *TRIB1* in different cancer types, especially in breast cancer, which implies the potential oncogenicity of *TRIB1* in breast cancer via alteration of macrophage phenotypes. Recent studies also reported the oncogenic role of *TRIB1* in prostate cancer, where the overexpression of *TRIB1* in the prostate tumour tissue was observed compared to non-tumour prostatic tissues or adjacent non-malignant tissues (Moya et al., 2018). The expression of *TRIB1* in prostate cancer cells enhanced the infiltration of angiogenesis promoting, $CD163^+$ macrophages into the tumour and also drove the macrophage phenotype

towards $CD163^{+}$ expressing macrophages potentially through *IKB-zeta* expression (Liu et al., 2019b).

Therefore, in this chapter, the role of myeloid *Trib1* in the murine mammary tumour growth will be assessed by the injection of cancer cells into the mammary fat pads of $Trib1^{mTg}$ animals and investigate the myeloid *Trib1* dependent tumour growth and alteration of the TAMs in the tumour microenvironment.

4.2 Hypothesis and aims

This chapter tests the hypothesis that overexpression of myeloid *Trib1* enhances breast tumour growth in a murine mammary cancer model via alteration of TAM phenotype within the tumour microenvironment.

1. *In vivo* development of mammary cancer model with myeloid *Trib1* overexpressing mice
2. Investigation of the myeloid *Trib1* induced tumour development
3. Post-mortem analysis of myeloid *Trib1* overexpression induced alteration of the tumour microenvironment

4.3 Results

4.3.1 Myeloid *Trib1* overexpression facilitates triple-negative breast tumour growth *in vivo*

To determine the role of *Trib1* in breast cancer development, we have used the C57BL/6N female mice with myeloid-specific *Trib1* overexpression ($Trib1^{mTg}$) using the SV40 transcriptional terminator cassette inserted at the *Rosa26* locus. The expression of *Cre* recombinase with *Lyz2* promotor enabled the transcription of *Trib1* transgene which resulted

in the significant increase of *Trib1* RNA levels in BMDMs and blood monocytes but did not alter the number of white blood cells, lymphocytes, monocytes, macrophages, and neutrophils in mice (Johnston et al., 2019b). Genotypes of mice were confirmed using the *Trib1* and *Lyz2Cre* PCR with the DNA extracted from mouse ear clips (**Figure 4.1**). *Trib1*^{mTg} mice were housed and bred at the University of Sheffield Biological Service Unit and maintained according to the University of Sheffield code of ethics and Home Office regulations. All the works were carried out under personal license I2AB6392A and Home Office project license PPL70/8670.

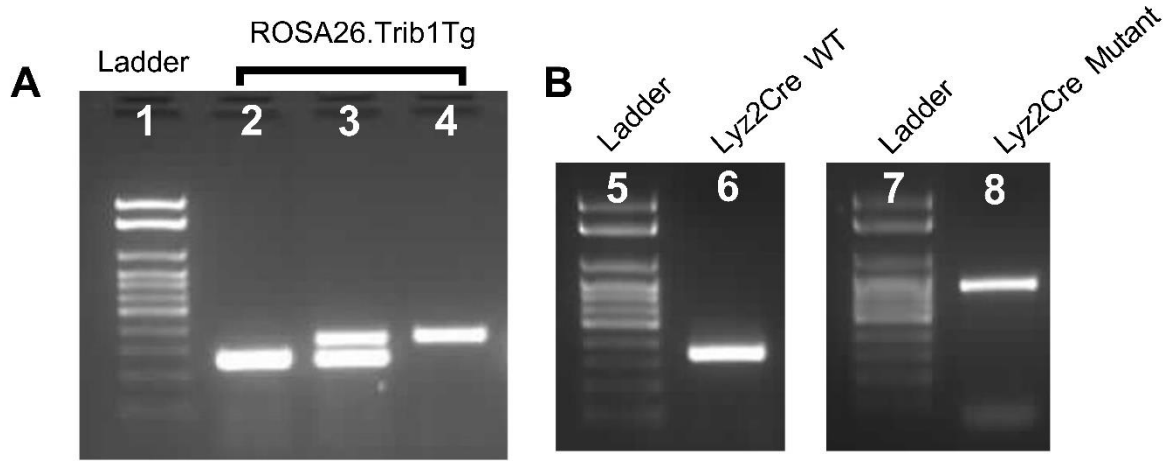

Figure 4.1. Example of *Trib1*^{mTg} (*ROSA26.Trib1Tg x Lyz2Cre*) genotyping PCR. (A) Demonstrates the example of *ROSA26.Trib1Tg* PCR gel. Lane 2 represents the homozygous mutation of *ROSA26* alleles, and the band is located at 263bp. Bands in lane 3 represent the heterozygous mutation of *ROSA26* allele which shows both mutated and wild-type alleles at 263bp and 353bp. (B) Demonstrates the PCR gel of *Lyz2Cre* genotyping results. Lane 6 with band located at 350bp represents animals without *Cre* in *Lyz2* alleles, and lane 8 with band located at 700bp represents the mutation of both *Lyz2* alleles with *Cre* expression.

The Eo771 cell line was used to develop breast cancer in mice because as it is derived from C57 black mice and in syngeneic mouse models, orthotopic transplantation gives advantages to mimic the human breast cancer development and can easily develop tumours within weeks (Le Naour et al., 2020). At 8-9weeks of age, $3x10^5$ Eo771 cells were injected to the nipple of *Trib1*^{mTg} mice, monitored and weighed routinely every two days. The tumour was also

measured with a calliper every two days, and once the tumour reached 15mm in diameter, mice were culled, and the tumour and other tissues were collected for post-mortem analysis. The schematics of the study shown in **Figure 4.2A**. The study consisted of n=12-15 animals in wild-type (*Trib1*^{mWT}) and *Trib1*^{mTg} groups.

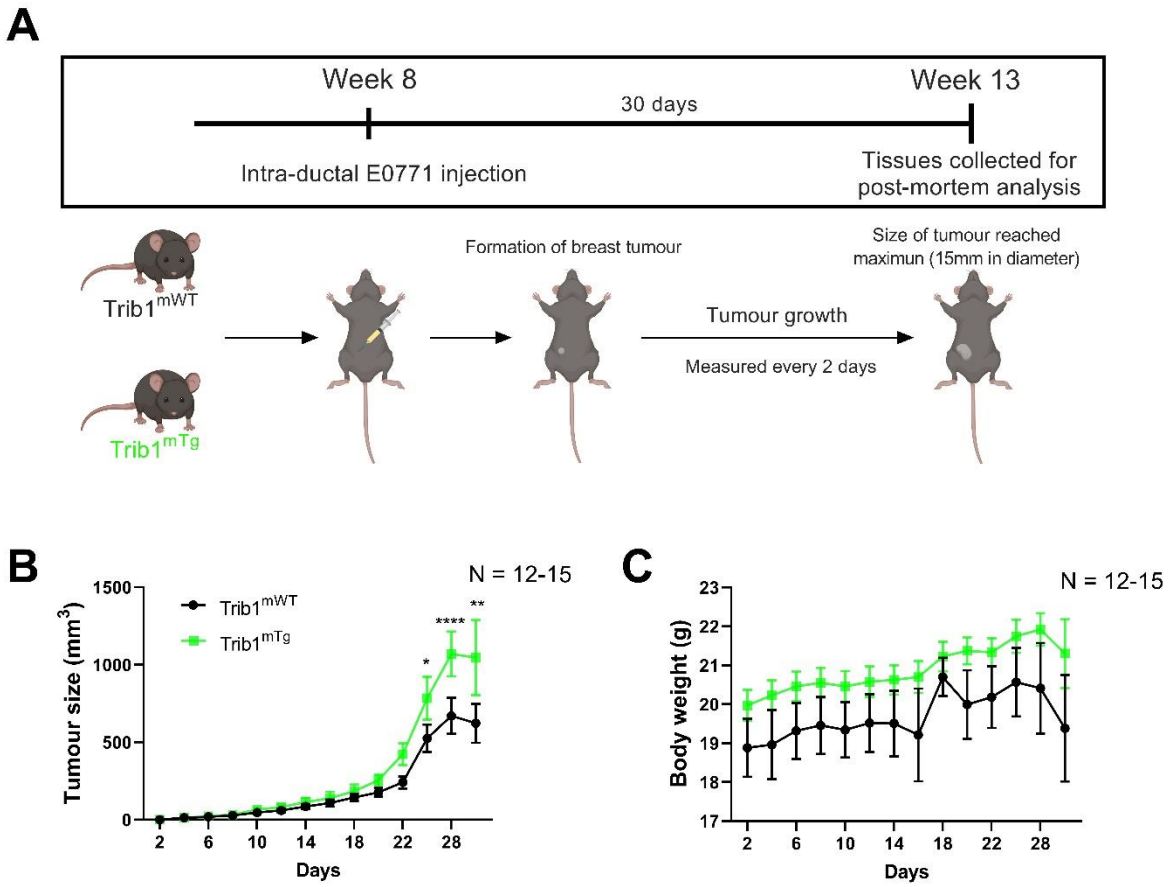

Figure 4.2. Overexpression of myeloid *Trib1* accelerates murine Eo771 tumour growth *in vivo*. (A) Represents the schematic diagram of *in vivo* injection of cancer cells into the nipple of *Trib1*^{mWT} and *Trib1*^{mTg} animals. Eo771 cells were injected into the nipple of animals at 8-9 weeks of age and monitored the body weight and tumour growth for every 2 days until the size of tumour reached 15mm in diameter. (B) The tumour growth in *Trib1*^{mWT} and *Trib1*^{mTg} animals after cancer cell injection. (C) The changes in body weight during the experiment. Results of two-way ANOVA are presented as *p<0.05 **p<0.01 ***p<0.001, and data represent mean±SEM of n=12-15mice/group.

The tumour was grown for approx. 30 days after injection when the *Trib1*^{mTg} tumour reached 15mm in diameter, and both *Trib1*^{mTg} and *Trib1*^{mWT} animals were culled. The growth curve of the tumour demonstrated a significant acceleration of *Trib1*^{mTg} tumour growth from 24 days

after injection until the end of the experiment (**Figure 4.2B**). The body weight of animals did not alter significantly over time, but on average, *Trib1*^{mTg} females had higher weight compared to *Trib1*^{mWT} female animals (**Figure 4.2C**).

4.3.2 Myeloid *Trib1* overexpression reduces infiltration of macrophages in breast tumours

To investigate the mechanisms of accelerated tumour growth in *Trib1*^{mTg} animals, TAM phenotype was assessed with immunofluorescence staining of frozen mouse tumour sections and imaged with x40 Nikon A1 confocal microscope (**Figure 4.3A**) or with x20 Af6000 widefield microscope (**Figure 4.3E**). F4/80 was used to detect TAMs in the tumour as it is a well-known macrophage marker expressed by a broad range of macrophages including Kupffer cells, bronchoalveolar macrophages, and microglial cells (Hume et al., 1984). CD31 and carbonic anhydrase IX (CA9) were stained together with F4/80 to determine the location of macrophages in the tumour microenvironment. CD31 or platelet/endothelial cell adhesion molecule 1 is highly expressed on endothelial cells and blood vessels involved in the interaction of leukocytes and endothelium (Goncharov et al., 2017). CA9 is an enzyme induced by hypoxia. In the tumour microenvironment, CA9 is associated with aggressive tumour behaviour and poor prognosis (Pastorekova and Gillies, 2019). The number of F4/80^{+} TAMs present in the tumour microenvironment were quantified using ImageJ and observed the reduction of macrophage infiltration into the *Trib1*^{mTg} tumour microenvironment (**Figure 4.3B**). Quantification of the number of CD31^{+} cells (**Figure 4.3C**) and CD31^{+} F4/80^{+} PV TAMs (**Figure 4.3D**) did not show any difference between *Trib1*^{mWT} and *Trib1*^{mTg} animals. However, the assessment of CA9^{+} F4/80^{+} hypoxic TAMs demonstrated a significant

reduction of hypoxic TAMs (~45% reduction) in the *Trib1*^{mTg} tumour microenvironment (**Figure 4.3F**).

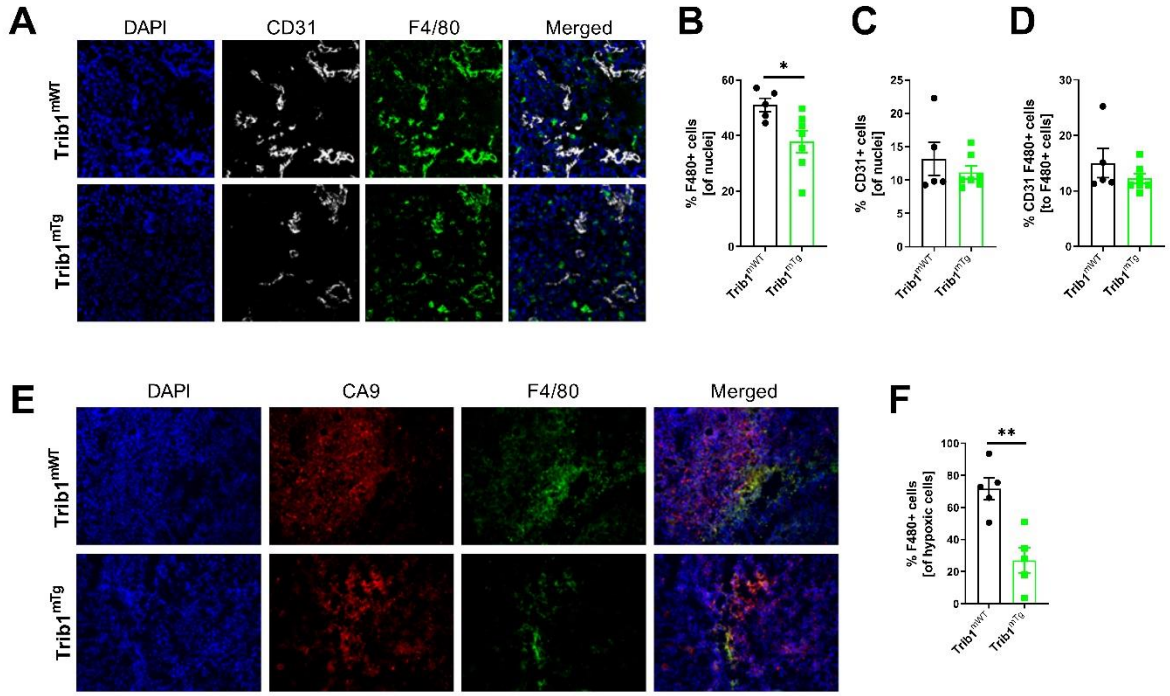

Figure 4.3. Infiltration of macrophages altered in *Trib1*^{mTg} tumours. Primary tumours developed in *Trib1*^{mWT} and *Trib1*^{mTg} animals were stained with macrophage marker F4/80 to assess the TAMs in the tumour microenvironment. (A) Representative images of staining PVM. Cells were stained with DAPI (blue), vessels are stained with CD31 (white), and TAMs are stained with F4/80 (green). Quantification of total macrophages (F4/80+ cells)(B), endothelial cells (CD31+ cells)(C), and PVM (F4/80+ CD31+ cells) in the tumours from *Trib1*^{mWT} and *Trib1*^{mTg} animals. (E) Representative images of staining hypoxic TAMs. Cells were stained with DAPI (blue), the hypoxic area was stained with CA9 (red), and TAMs are stained with F4/80 (green). (F) Quantification of TAMs in the hypoxic area relative to total cells in hypoxia. Results of unpaired T-test are presented as *p<0.05 **p<0.01, and data represent mean±SEM of n=5-7mice/group.

4.3.3 The overexpression of myeloid *Trib1* modulates the phenotype of TAMs

Previous reports emphasised the importance of macrophage phenotype in tumour growth. Therefore, TAM phenotype in the tumour microenvironment of our model was assessed by immunofluorescence staining using NOS2 and MR. NOS2 or nitric oxide synthase is a pro-inflammatory marker used in the study as NOS produces a large amount of endogenous NO and macrophages and other tissues express the isoform of NOS (NOS2) in response to pro-

inflammatory mediators (Luiking et al., 2010). NOS2 is highly expressed in macrophages and monocytes from patients with infectious or inflammatory diseases; these cells show antimicrobial action and enhance host resistance (MacMicking et al., 1997). CD206 or MR (C-type mannose receptor 1) was used to detect the anti-inflammatory marker, as it was reported that several types of tissue-resident macrophages express MR and the depletion increased the pro-inflammatory responses (Orecchioni et al., 2019). MR is known to bind and internalise glycoproteins and collagen ligands (Madsen et al., 2013), but the function of MR in macrophages is not yet fully understood. Potentially, MR in macrophages plays a role in the clearance of inflammatory molecules from the blood and produces hepatocyte growth factor in injured muscle, helping muscle fibre regeneration (Roszer, 2015b). Triple staining of F4/80, CD31 and NOS2 or MR on the frozen tumour sections were imaged with x40 Nikon A1 confocal microscope as shown in **Figure 4.4A** and **Figure 4.4D**. The number of F4/80 positive macrophages with NOS2 or MR and CD31 were quantified using ImageJ, and the percentage of pro-inflammatory and anti-inflammatory macrophages in the tumour microenvironment was assessed with ImageJ. Overexpression of myeloid *Trib1* significantly reduced the number of pro-inflammatory macrophages (F4/80+ NOS2+)(**Figure 4.4B**) and pro-inflammatory PVM (F4/80+ NOS2+ CD31+)(**Figure 4.4C**) in the $Trib1^{mTg}$ tumours but did not alter the number of anti-inflammatory macrophages (F4/80+ MR+)(**Figure 4.4E-F**).

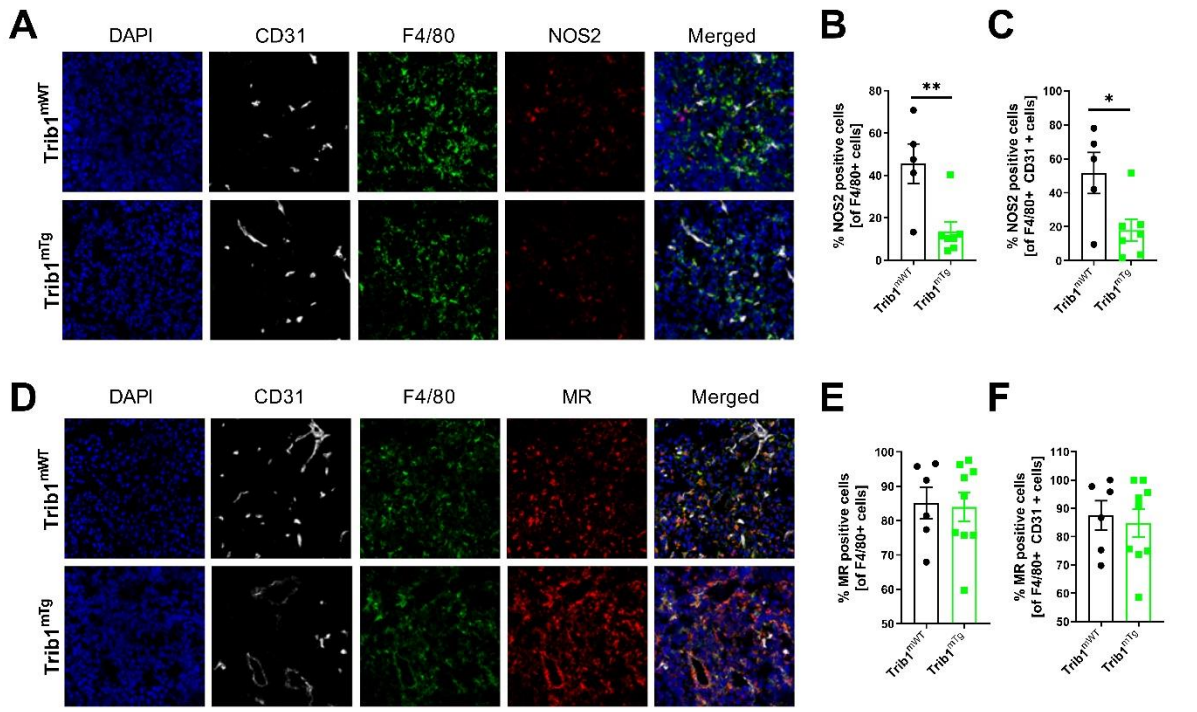

Figure 4.4. Myeloid *Trib1* reduces TAM polarisation towards pro-inflammatory phenotype. Primary tumours from *Trib1*^{mTg} and *Trib1*^{mWT} animals were stained with F4/80 and polarisation markers NOS2 (pro-inflammatory) and MR (anti-inflammatory) to investigate the phenotype of TAMs in the tumour. (A) Representative images of F4/80, CD31, and NOS2 staining. Cells were stained with DAPI (blue) and pro-inflammatory marker NOS2 (red), endothelial cells were stained with CD31 (white), and TAMs were stained with F4/80 (green). Quantification of NOS2+ F4/80+ pro-inflammatory TAMs relative to total TAMs (B) and NOS2+ F4/80+ CD31+ pro-inflammatory PVM relative to total PV TAMs (C). (D) Representative images of F4/80, CD31, and MR staining in the tumours. Cells were stained with DAPI (blue) and anti-inflammatory marker MR (red), endothelial cells were stained with Cd31 (white), and TAMs were stained with F4/80 (green). Quantification of MR+ F4/80+ anti-inflammatory TAMs relative to total TAMs (E) and MR+ F4/80+ CD31+ anti-inflammatory PV TAMs relative to total PV TAMs (F). Results of unpaired T-test are presented as *p<0.05 **p<0.01, and data represent mean±SEM of n=5-7mice/group.

4.3.4 Myeloid *Trib1* altered T-cell infiltration and the density of T-cell subtypes

In the tumour microenvironment, T-cells are essential for their anti-tumour effects, and the number of T-cells present in the tumour correlates with a better response to therapy and prognosis. In addition, previous studies demonstrated that the dynamic cell-cell interaction between T-cells and macrophages is essential for the activation of T-cells (Underhill et al., 1999). Therefore, the number of T-cells present in the tumour microenvironment and the activation of T-cells were examined by CD3 staining and the triple staining of CD3, CD4,

and CD8 on the frozen tumour sections from *Trib1*^{mTg} and *Trib1*^{mWT} animals. The latter provides an indication of the subsets of T-cell within the tumour microenvironment. Both CD3 staining and triple staining were imaged with x40 Nikon A1 confocal microscope as shown in **Figure 4.5A** and **Figure 4.5C** and the images were analysed with ImageJ. Quantification of $CD3^+$ T-cells demonstrated the significant reduction of T-cell infiltration into the tumour microenvironment in *Trib1*^{mTg} animals compared to the tumour from *Trib1*^{mWT} animals (**Figure 4.5B**). The further assessment of T-cell subtypes by triple staining demonstrated the significant reduction of $CD3^+/CD4^+$ naïve T-cells (**Figure 4.5D**) and $CD3^+/CD8^+$cytotoxic T-cells (**Figure 4.5E**), and increased $CD3^+/CD4^-/CD8^-$ T-cells (**Figure 4.5G**) within the *Trib1*^{mTg} tumours but the difference was not observed with T-cells positive for both CD4 and CD8 (**Figure 4.5F**).

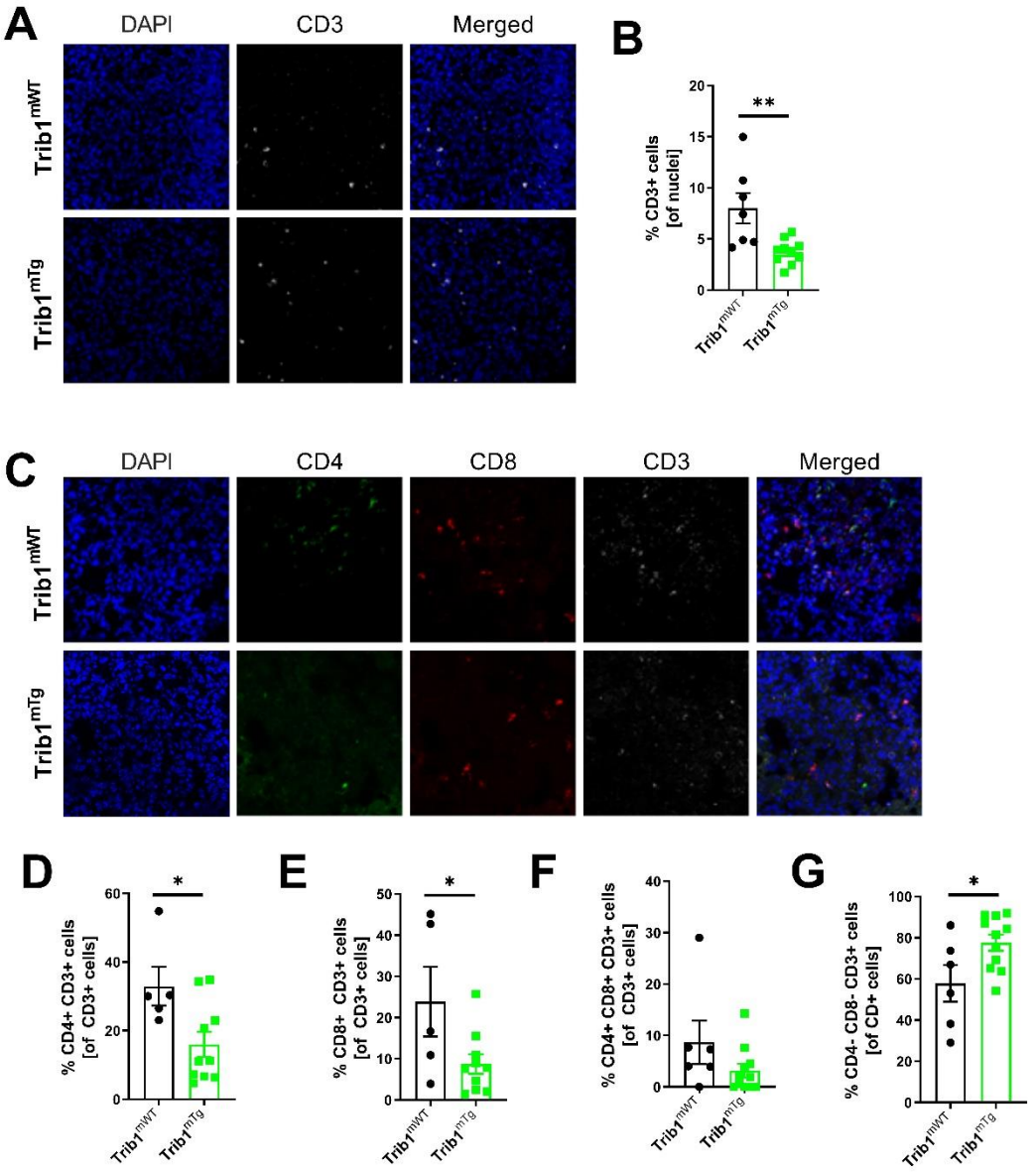

Figure 4.5. Tumours from *Trib1^{mTg}* animals inhibited T-cell infiltration and altered T-cell subtypes. T-cells in the primary tumours from *Trib1^{mWT}* and *Trib1^{mTg}* were assessed using fluorescence staining of CD3. (A) Representative images of CD3 staining on the tumours from *Trib1^{mWT}* and *Trib1^{mTg}* animals. Cells were stained with DAPI (blue), and T-cells were stained with CD3 (white). (B) Quantification of CD3+ T-cells in the tumour microenvironment relative to total cells. Staining of CD3 with CD4 (naïve T-cell marker) and CD8 (cytotoxic T-cell marker) was also performed to analyse the changes of T-cell subtypes. (C) Representative images of CD3, CD4, and CD8 triple staining. Cells were stained with DAPI (blue), and T-cells were stained with CD3 (white) with Naïve T-cell marker CD4 (green), and cytotoxic T-cell marker CD8 (red). Quantification of CD3+ CD4+ naïve T-cells (D), CD3+ CD8+ cytotoxic T-cells (E), CD3+ CD4+ CD8+ double-positive T-cells (F), and CD3+ CD4- CD8- double-negative T-cells (G) relative to total CD3+ T-cell numbers. Results of unpaired T-test are presented as *p,0.05 **p<0.01, and data represent mean±SEM of n=5-8mice/group.

4.3.5 *Trib1* alters *IL-15* in BMDMs regulating T-cell infiltration

The mechanism of myeloid *Trib1* regulating T-cell infiltration into the tumour was investigated using RT-qPCR on BMDMs and fluorescence staining of primary tumours from $Trib1^{mWT}$ and $Trib1^{mTg}$ animals. IL-15 is a cytokine expressed mainly by myeloid cells with many overlapping functions as IL-12 to promote anti-tumour responses by stimulating the tumour-specific T-cell responses, and increase cellular growth, decrease apoptosis, and enhance immune cell activation and migration, which is essential in the development, function, and survival of T-cells (Robinson and Schluns, 2017). The interaction of IL-15 and TRIB1 was observed in the microarray data of comparing *TRIB1* high, and low human monocytes and macrophages were in macrophages, high *TRIB1* expression significantly decreased *IL-15* expression in human MDMs (**Figure 4.6A**). The negative correlation of *Trib1* and *IL-15* mRNA was further confirmed in mouse BMDMs from $Trib1^{mWT}$ and $Trib1^{mTg}$ animals, where BMDMs from $Trib1^{mTg}$ animals demonstrated a significant decrease of *IL-15* expression (**Figure 4.6B**). Staining of IL-15 and F4/80 in tumours from $Trib1^{mWT}$ and $Trib1^{mTg}$ animals also revealed a significant reduction of IL-15 expressing TAMs in the tumours from $Trib1^{mTg}$ animals (**Figure 4.6D**). The representative images of staining for F4/80 and IL-15 are shown in **Figure 4.6C.**

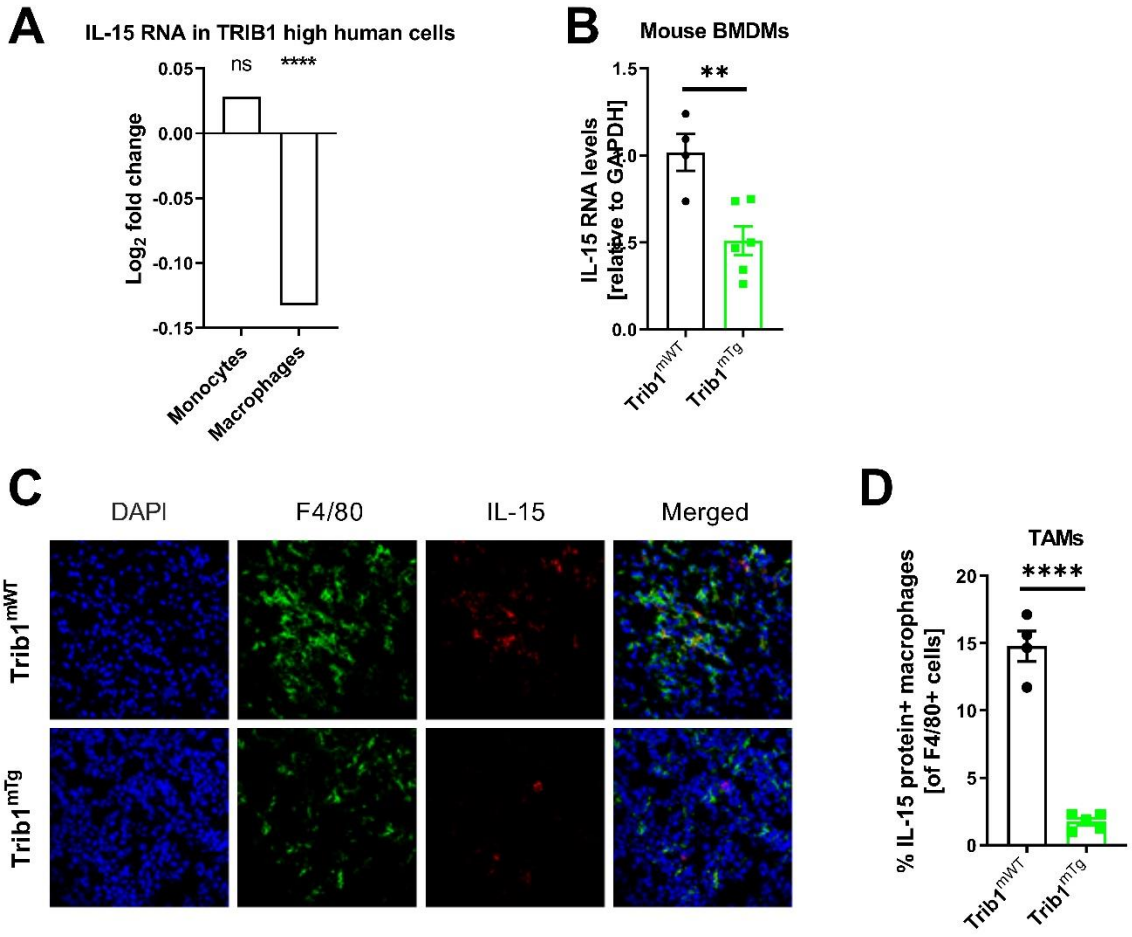

Figure 4.6. *IL-15* expression in macrophages negatively correlates with myeloid *Trib1* levels. The regulation of T-cell infiltration by TAMs was investigated using microarray from Cardiogenics Consortium Transcriptomic data set, RT-qPCR, and fluorescence staining of IL-15. (A) *IL-15* RNA expression in *TRIB1* high and low human monocytes and macrophages from the microarray dataset. Results of FDR adjusted p-values are presented as ****p<0.0001. (B) *IL-15* RNA expression in mouse BMDMs from *Trib1*^{mWT} and *Trib1*^{mTg} animals. (C) Representative images of F4/80 and IL-15 staining on the tumours from *Trib1*^{mWT} and *Trib1*^{mTg} animals. Cells were stained with DAPI (blue) and IL-15 (red), and TAMs were stained with F4/80 (green). (D) Quantification of TAMs expressing IL-15 in the tumour microenvironment relative to the total number of TAMs. Results of unpaired T-test are presented **p<0.01 ****p<0.0001, and data represent mean±SEM of n=4-6mice/group.

4.3.6 Overexpression of myeloid *Trib1* enhanced the development of pulmonary metastasis

The development of a secondary tumour is classified as the final stage of tumour progression and crucial for cancer treatment and patient survival. Cancer Research UK reported that there is a decrease of long-term survival of patients with stage IV breast cancer to about 26%,

compared to stage II (90%) and stage III (72%) breast cancer patients (CancerResearchUK, 2020). Macrophages play an essential role in metastasis progression and cancer cell survival in the blood vessels. Therefore, to assess the role of myeloid *Trib1*-dependent macrophage regulation in metastasis, the secondary tumour developed in other organs were investigated. Lung and liver tissues were analysed in this study since they are the metastatic sites preferred by breast cancer cells and previous experiments with Eo771 cells demonstrated a high prevalence of lung metastasis in mice. The organs collected from $Trib1^{mWT}$ and $Trib1^{mTg}$ animals were sectioned and stained with H&E. The slides were imaged using a Hamamatsu slide scanner at Sheffield Institute for Translational Neuroscience. The scanned images were analysed using ImageScope software to quantify the number and size of the secondary tumours in lung and liver, as shown in **Figure 4.7A**. The number of metastases observed in the liver (**Figure 4.7D**) was similar between $Trib1^{mTg}$ and $Trib1^{mWT}$ animals. However, $Trib1^{mTg}$ lung had a significantly higher number of metastases (**Figure 4.7B**) with increased secondary tumour area compared to the $Trib1^{mWT}$ lungs (**Figure 4.7C**). In contrast, the total area of liver metastasis was similar between $Trib1^{mTg}$ and $Trib1^{mWT}$ animals (**Figure 4.7E**).

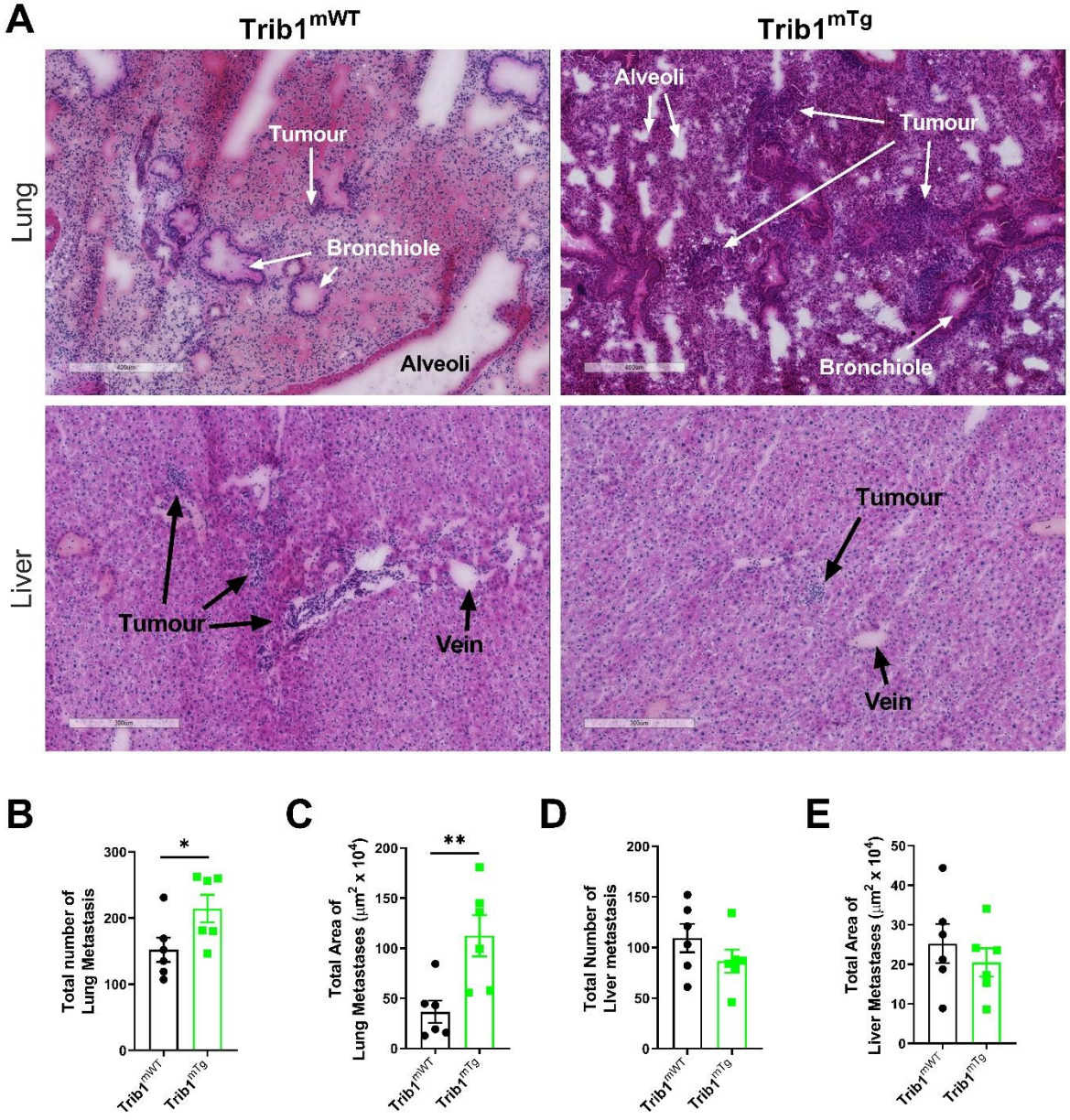

Figure 4.7. Myeloid *Trib1* accelerates the development of secondary tumour in the lung. The development of secondary tumours in the lung and liver were investigated using H&E staining of lung and liver tissues from *Trib1*^{mWT} and *Trib1*^{mTg} animals injected with cancer cells at the nipple. The slides were imaged with Hammatsu slide scanner at the Sheffield Institute for Translational Neuroscience. (A) Representative images of lung and liver tissues from *Trib1*^{mWT} and *Trib1*^{mTg} animals. The number and size of secondary tumours were analysed using ImageScope software. Quantification of secondary tumours in the lung (B) and liver (D) and the total area of metastasis in the lung (C) and liver (E) of *Trib1*^{mWT} and *Trib1*^{mTg} animals. Results of unpaired T-test are presented as *p<0.05 **p<0.01, and data represent mean±SEM of n=6mice/group.

4.4 Discussion

The previous chapter demonstrated that the human breast cancer cell lines express *TRIB1,* and among the breast cancer cell subtypes, TNBC cells expressed the highest *TRIB1* level compared to other subtypes. It was also reported that the expression of *TRIB1* is essential for the progression of cell cycle and the knockdown of *TRIB1* in the breast cancer cell lines promoted apoptosis (Gendelman et al., 2017), which implies the importance of *TRIB1* in breast tumour growth. Therefore, to assess the role of myeloid *TRIB1* in the development of breast cancer growth, $Trib1^{mTg}$ animals that overexpress *Trib1* in the myeloid-specific cells were developed as described in (Johnston et al., 2019a). The development of breast cancer in $Trib1^{mTg}$ animals using Eo771 cells demonstrated that Trib1 overexpression in myeloid cells accelerates mammary tumour growth significantly at a late stage of tumour growth, from day 26 (**Figure 4.2B**).

Post-mortem analysis of tumours was performed to assess the mechanisms of accelerated tumour growth using fluorescence staining. Staining of macrophages demonstrated the reduction in TAM numbers in $Trib1^{mTg}$ tumours, compared to $Trib1^{mWT}$ tumours. This finding is in contrast to previous studies that reported knockout of TRIB1 using siRNA in the mouse macrophage cell line (RAW264.7) significantly inhibited the migration of macrophages in both presence and absence of chemoattractant (Liu et al., 2013), and the number of $CD68^+$ macrophages in the tumour positively correlated with decreased overall survival in colon cancer (Pinto et al., 2019). The difference perhaps is due to the complexity of *in vivo* development of tumour regulating the macrophage infiltration compared to the *in vitro* experiments, changes of cytokine and chemokine expressions in *Trib1* high macrophages in response to cancer development, and the difference between the cancer types. Further staining of F4/80 with CD31 and CA9 revealed a similar number of $CD31^+$ $F4/80^+$ PVM in

Trib1^{mWT} and *Trib1*^{mTg} tumours but a significant reduction of CA9^{+} F4/80^{+} hypoxic macrophages in the *Trib1*^{mTg} tumours.

TAMs enhance glycolysis via TNF expression and exacerbate tumour hypoxia via PGC-1α and AMP-activated protein kinase (AMPK) activation in the hypoxic areas; these TAMs have been reported to express both M1 and M2 macrophage markers (NOS2 and Arg1)(Jeong et al., 2019). Therefore, to investigate the relationship of hypoxic TAM reduction in the tumour microenvironment with macrophage phenotype, triple staining of F4/80, CD31, and NOS2 or MR was done on the frozen tumour sections. The analysis demonstrated that *Trib1*^{mTg} tumours had a significant reduction in NOS2^{+} F4/80^{+} pro-inflammatory TAMs or NOS2^{+} F4/80^{+} CD31^{+} perivascular pro-inflammatory TAMs in the *Trib1*^{mTg} tumour microenvironment but did not alter the MR^{+} F4/80^{+} anti-inflammatory TAM numbers. This suggests that the reduction of hypoxic TAMs in *Trib1*^{mTg} tumours are due to the myeloid *Trib1* dependent inhibition of pro-inflammatory TAMs, which as a consequence, reduced the number of TAMs expressing both pro- and anti-inflammatory phenotypes in the tumour microenvironment.

Reduction of hypoxic TAMs and NOS2^{+} MR^{+} F4/80^{+} TAMs in the tumour microenvironment also potentially explain the similar breast tumour growth between *Trib1*^{mWT} and *Trib1*^{mTg} animals until 22 days post-cancer injection. The reduction of hypoxic TAMs and NOS^{+} MR^{+} F4/80^{+} TAMs, which can exacerbate the hypoxia in the tumour, led to a reduction in hypoxic areas in the tumour, and as a consequence, reduced the hypoxic signals essential for the primary tumour growth. For instance, HIF-1α is crucial for cancer cell division, and the knockout of HIF-1α significantly decreased the proliferation of breast cancer cells *in vitro* and reduced about 60% of primary breast tumour volume *in vivo* (Schwab et al., 2012). In addition, Pinto *et al*. (2019) reported the abundant infiltration of

$CD80^+$ $CD68^+$ pro-inflammatory macrophages in the early development of colorectal cancer at T1 stage (Pinto et al., 2019), suggesting the importance of pro-inflammatory macrophages in the formation and the development of early cancer.

However, the presence of pro-inflammatory TAMs in the tumour microenvironment, in general, is anti-tumoral where the pro-inflammatory cytokines secreted by TAMs, such as *IL-12*, initiate immune responses mediated by NK cells, T_H1 cells, and cytotoxic T lymphocytes (Quatromoni and Eruslanov, 2012). It has also been reported that the abundant number of anti-inflammatory TAMs positively correlate with the better proliferation of *ERα* and *PR*-negative tumours (Lindsten et al., 2017), and anti-inflammatory TAMs facilitate the breast cancer migration and invasion via different signalling pathways including VEGF, CCL-18, and CHI3L1 (Little et al., 2019, Chen et al., 2017). Therefore, the reduction of hypoxic TAMs and pro-inflammatory TAMs in the $Trib1^{mTg}$ animals may postpone the formation and development of early breast tumour growth. However, at the same time, the inhibition of pro-inflammatory TAMs and the abundant number of anti-inflammatory TAMs may enhance breast tumour growth at the later stages.

In addition, staining of T-cells in the frozen tumour demonstrated a significant reduction of T-cell infiltration in the $Trib1^{mTg}$ tumours. Although the population of $CD4^+$ naïve T-cells and $CD8^+$ cytotoxic T-cells from the total pool of $CD3^+$ T-cells only demonstrated a trend of reduction in the $Trib1^{mTg}$ tumours, the absolute number of T-cells significantly decreased in the $Trib1^{mTg}$ tumour microenvironment which any further support the acceleration of tumour growth in $Trib1^{mTg}$ animals.

However, Jeong et al., (2019) reported that the depletion of TAMs in the tumour enhances the infiltration of both naïve and cytotoxic T-cells into the tumour microenvironment (Jeong et al., 2019), which is in contrast to our data. Therefore, to gain further insight into the

potential mechanisms behind altered myeloid *Trib1*-dependent T-cell infiltration, the Cardiogenics Consortium transcriptomic data set were analysed in collaboration with Professor Alison Goodall and Dr Stephen Hamby at the University of Leicester. The data set includes RNA profiles of monocytes from 758 donors and MDMs from 596 donors and compared the top and bottom quartile of individuals based on the *TRIB1* expression levels. The microarray analysis of human MDMs demonstrated a significant reduction of *IL-15* expression in *Trib1* high individuals. *IL-15* interacts with different lymphocytes, including NK cells and T-cells. Carrero et al., (2019) reported the enhanced number of tumour-infiltrating lymphocytes, especially cytotoxic T-cells positively correlates with *IL-15* expression in the tumour microenvironment, predominantly observed in myeloid cells, and the *IL-15* expression activates $CD8^+$ T-cells and promotes antitumour responses (Santana Carrero et al., 2019). The regulatory role of *Trib1* in the expression of *IL-15* was further observed in BMDMs isolated from $Trib1^{mTg}$ and $Trib1^{mWT}$ animals with a significant decrease in *IL-15* expression in $Trib1^{mTg}$ BMDMs. In addition, fluorescence staining of tumours from $Trib1^{mWT}$ and $Trib1^{mTg}$ animals revealed a significant reduction of IL-15 expressing TAMs in the tumours from $Trib1^{mTg}$ animals, which implies the reduction of T-cell infiltration into the tumours from $Trib1^{mTg}$ animals was through myeloid *Trib1*-dependent regulation of IL-15 expression in TAMs.

As discussed above, abundant anti-inflammatory TAMs are crucial for cancer migration, and the development of secondary tumour was observed using H&E staining. The number of metastasis to the liver did not change, but myeloid Trib1 overexpression enhanced the number of metastasis and the growth of the secondary tumour in the $Trib1^{mTg}$ lung probably due to the inhibition of pro-inflammatory TAM recruitment and the abundance of anti-inflammatory TAMs in the tumour microenvironment.

Chapter 5. Myeloid *Trib1* knockdown enhances breast tumour growth by disrupting monocyte and macrophage infiltration

5.1 Introduction

It has already been reported that TRIB1 is oncogenic in different cancer types (Wang et al., 2017c, Mashima et al., 2014, Yokoyama and Nakamura, 2011). Data from chapter 3 also demonstrated amplification of *TRIB1* gene in breast cancer patients and correlation of TRIB1 alteration and overall patient survival, as well as regulation of functional cytokine and chemokine expressions in TAMs depending on *TRIB1* levels, which supports the potential oncogenicity of *TRIB1* in breast cancer. Chapter 4 further analysed the oncogenic role of *Trib1* in $Trib1^{mTg}$ animals *in vivo*, where myeloid *Trib1* overexpression enhanced breast tumour growth through alteration of the tumour microenvironment compositions, especially TAM phenotype and T-cell infiltration which also enhanced the development of secondary tumour in the lung.

However, the role of *TRIB1* deficiency in tumour development remains to be investigated, and the literature so far has only reported anti-tumour aspects in *TRIB1* deficit tumours. Knockdown of *TRIB1* significantly reduced the proliferation and survival of breast cancer cells through enhancing the activity of P53 proteins (Miyajima et al., 2015), and downregulation of *TRIB1* via *miRNA-224* inhibited the progression of human prostate cancer (Lin et al., 2014). Targeting *TRIB1* via *miRNA-23A* was also reported to increase the *p53* expression in the hepatocellular carcinoma (HCC) cells, and *TRIB1* deficient HCC impeded the formation of tumour cells *in vivo* (Ye et al., 2017). In addition, Tang *et al.* (2015) reported enhanced sensitivity of radiotherapy in human glioma cells with inhibition of *TRIB1*

(Tang et al., 2015). However, although it was not directly mentioned in the paper, *miRNA-224* which target *TRIB1* was reported to promote nonsmall cell lung cancer (Cui et al., 2015), which demonstrates potential complexity of *TRIB1* deficiency in tumour development.

Therefore, following on from the previous chapter, the development of triple-negative breast tumours in myeloid *Trib1* deficient mice will be investigated by the injection of cancer cells through the nipple of *Trib1*^{mKO} animals for the assessment of tumour growth using callipers and post-mortem changes to TAMs as well as other cell types in the tumour microenvironment using multi-colour flow cytometry (**Table 5.1**) and immunofluorescence staining of frozen sections.

Table 5.1. Antibodies used in flow cytometry to detect cells in the tumour microenvironment.

Antibodies	Targets
F4/80	Tumour-associated macrophage
CD206	Anti-inflammatory marker
CD274	Pro-inflammatory marker
Ly-6C	Monocyte
NK1.1	NK cells
Ly-6G	Neutrophil
CD3	T-cells
CD4	Naive T-cells
CD8	Cytotoxic T-cells
CD279	PD-1

5.2 Hypothesis and aims

This chapter tests the hypothesis that myeloid *Trib1* is oncogenic and knockdown of myeloid *Trib1* reduces the development of triple-negative breast tumour growth in a murine breast tumour model.

1. *In vivo* development of breast cancer model with myeloid *Trib1* knockout mice
2. Investigation of the tumour development and the post-mortem analysis of the myeloid *Trib1* knockout tumour microenvironment with flow cytometry and fluorescence staining

5.3 Results

5.3.1 Knockdown of myeloid *Trib1* enhanced breast tumour growth *in vivo*

In parallel to Chapter 4, we have used the C57BL/6N female mice with myeloid-specific *Trib1* knockdown ($Trib1^{mKO}$) using the *loxP-Cre* splicing of *Trib1* exon 2 to investigate the role of *Trib1* knockdown in breast cancer development. The insertion of *loxP* around the second exon of *Trib1* and the expression of *Cre* recombinase with the *Lyz2* promotor, spliced the second exon which resulted in a significant decrease of *Trib1* expression in BMDMs without alteration of white blood cells, lymphocytes, monocytes, and neutrophil numbers in mice (Johnston et al., 2019a, Bauer et al., 2015). Genotypes of mice were confirmed using the *Trib1* and *Lyz2Cre* PCR with the DNA extracted from mouse ear clips (**Figure 5.1**). $Trib1^{mTg}$ mice were housed and bred at the University of Sheffield Biological Service Unit and maintained according to the University of Sheffield code of ethics and Home Office regulations. All the works were carried out under personal license I2AB6392A and Home Office project license PPL70/8670.

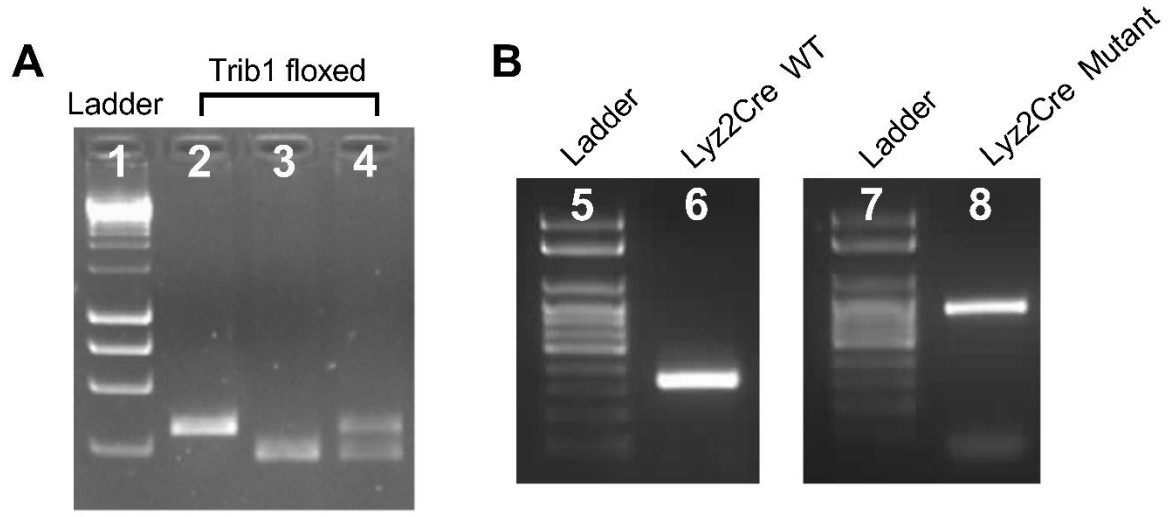

Figure 5.1. Example of *Trib1*^{mKO} (*Trib1 floxed x Lyz2Cre*) genotyping PCR. (A) Representative image of *Trib1 floxed* PCR gel. Lane 2 represents the homozygous mutation of *Trib1* alleles with a *loxP* insertion around the second exon (451bp). Lane 3 represents wild-type animals without *Trib1* mutation (374bp). Lane 4 represents heterozygous mutation of *Trib1* alleles with both *loxP* inserted and wild-type alleles at 374bp and 451bp. (B) Representative images of *Lyz2Cre* genotyping PCR results. Lane 6 represents animals without *Cre* in *Lyz2* alleles (350bp), and lane 8 represents the mutation of both *Lyz2* alleles with *Cre* expression.

As mentioned in the previous chapter, Eo771 cells were used to develop mammary tumour model on a myeloid-specific *Trib1* knockout C57BL/6 mouse. At 8-9 weeks of age, $3x10^5$ Eo771 cells were injected to the nipple of *Trib1*^{mKO} mice, monitored and weighed routinely every two days. The growth of tumour was measured with a calliper, and once the tumour reached 15mm in diameter, mice were culled, and the tumour and other tissue were collected for post-mortem analysis. The schematics of the study is shown in **Figure 5.2A**. The study consisted of n=5-9 animals in wild-type (*Trib1*^{mWT}) and *Trib1*^{mKO} groups.

The tumour was grown for approx. 22 days after injection when the *Trib1*^{mKO} tumour reached 15mm in diameter, and both *Trib1*^{mWT} and *Trib1*^{mKO} animals were culled. The analysis revealed a significant acceleration of tumour growth in *Trib1*^{mKO} animals compared to *Trib1*^{mWT} from 18 days after injection until the end of the experiment (**Figure 5.2B**). There was no significant difference observed in the bodyweight of *Trib1*^{mWT} and *Trib1*^{mKO} animals throughout the study (**Figure 5.2C**).

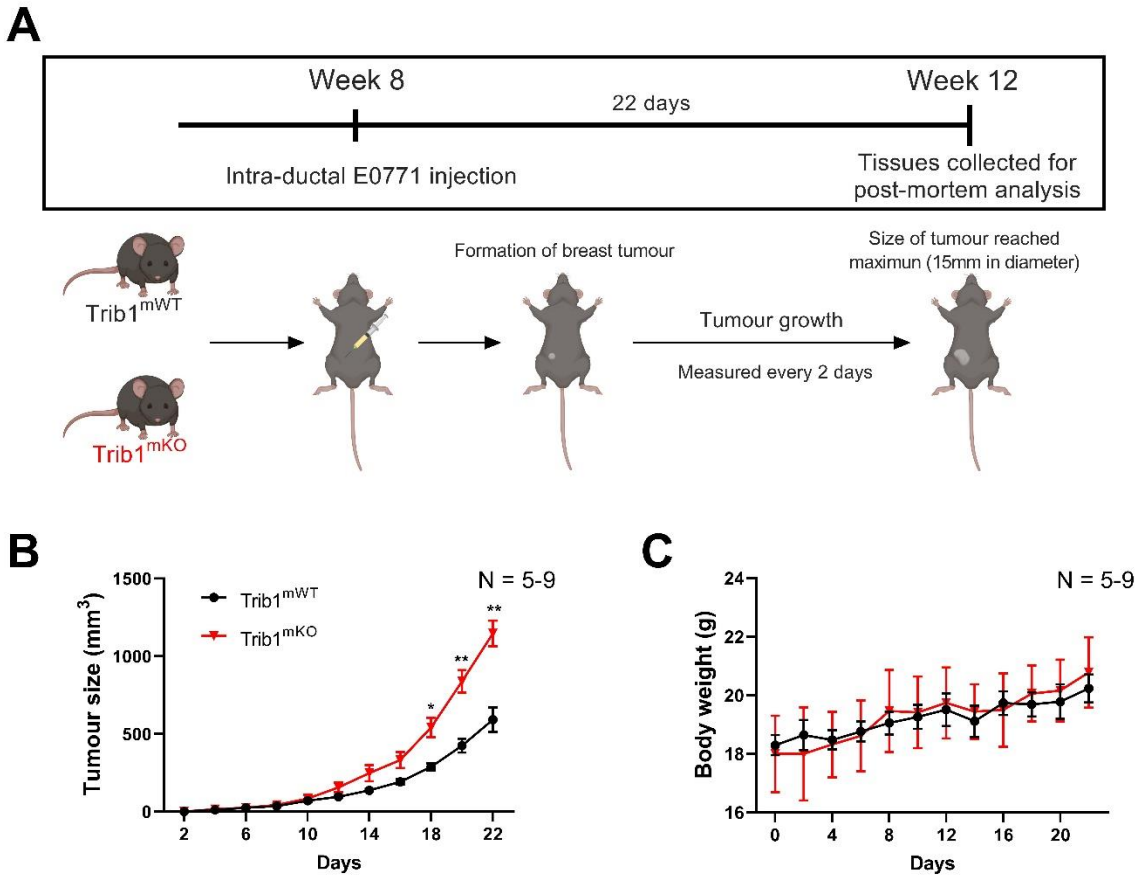

Figure 5.2. Myeloid *Trib1* knockout accelerates murine Eo771 tumour growth *in vivo*. (A) Schematic diagram of *in vivo* study. At 8-9weeks of age, both *Trib1*^{mWT} and *Trib1*^{mKO} animals were injected with Eo771 cells at the nipple and monitored the changes of body weight and tumour growth every two days. (B) Tumour growth of Eo771 cells in *Trib1*^{mWT} and *Trib1*^{mKO} animals. Both *Trib1*^{mWT} and *Trib1*^{mKO} animals were culled at 22 days after injection when *Trib1*^{mKO} tumours reached 15mm in diameter. (C) Changes in body weight throughout the study. Results of two-way ANOVA are presented as *p<0.05 **p<0.01, and data represent mean±SEM of n=5-9mice/group.

5.3.2 Myeloid *Trib1* knockdown disrupted infiltration of monocytes and macrophages into the tumour microenvironment

The tumours grown in *Trib1*^{mWT} and *Trib1*^{mKO} animals were analysed following collagenase dissociation of frozen tumour tissues and analysed by flow cytometry using the BD LSRII or fluorescence. This enabled the investigation of changes in the tumour microenvironment

composition when myeloid *Trib1* expression was decreased. The analysis of tumours by flow cytometry demonstrated that both tumours from *Trib1*^{mWT} and *Trib1*^{mKO} animals had a similar number of NK1.1+ NK cells (**Figure 5.3B**) and Ly-6G+ neutrophils (**Figure 5.3C**) with a wide variation in data between samples. Of note, the sample size was only small (n=3). However, a significant decrease of the total Ly-6C+ monocytes (**Figure 5.4B**) and F4/80+ TAMs (**Figure 5.4C**) was observed in the *Trib1*^{mKO} tumour microenvironment compared to *Trib1*^{mWT} tumours (~20% reduction in both monocytes and TAMs). Interestingly expression of the checkpoint markers PD-L1 was unchanged in TAMs (**Figure 5.4D**).

The tumour vasculature and the TAMs associated with the vessels were also assessed using the fluorescence staining of endothelial cell marker CD31 and macrophage marker F4/80 on frozen tumours from *Trib1*^{mWT} and *Trib1*^{mKO} animals. The analysis revealed that in the tumours from *Trib1*^{mKO}, there was a significant reduction of CD31+ F4/80+ PV TAMs compared to the tumours from *Trib1*^{mWT} animals (**Figure 5.5C**). The size of vessels was similar between the tumours from *Trib1*^{mWT} and *Trib1*^{mKO} animals (**Figure 5.5B**). The representative images of staining are shown in **Figure 5.5A**. In addition, the number of pro-inflammatory and anti-inflammatory TAMs in the tumour microenvironment was assessed by further analysis of F4/80+ TAMs with pro-inflammatory (PD-L1) and anti-inflammatory (CD206) markers using flow cytometry. PD-L1 is not a genuine pro-inflammatory marker but used in this chapter due to the limited number of antibodies allowed to run with flow cytometry, and the reduction of PD-L1 in macrophages induces pro-inflammatory phenotype (Lu et al., 2019). The analysis denoted a similar percentage of pro-inflammatory (**Figure 5.6B**) and anti-inflammatory (**Figure 5.6C**) TAMs between the tumours from *Trib1*^{mWT} and *Trib1*^{mKO} animals. The representative images of flow cytometry are shown in **Figure 5.3A**, **Figure 5.4A**, **Figure 5.6A**.

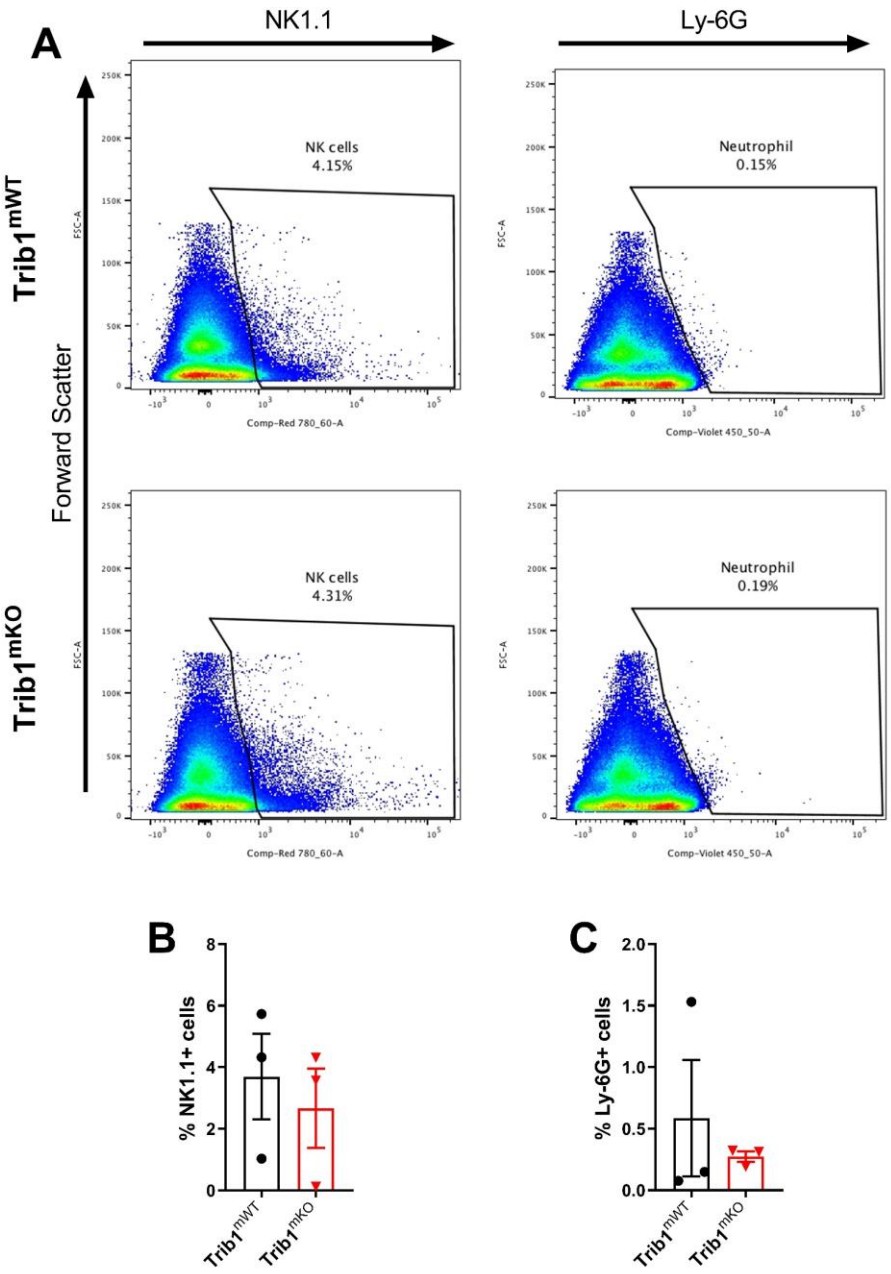

Figure 5.3. The number of NK cells and neutrophils were comparable between the tumours from *Trib1^{mWT}* and *Trib1^{mKO}* animals. Cells dissociated from primary tumours were stained with NK1.1 (NK cells) and Ly-6G (neutrophil), and viability was assessed with Live/Dead dead cell staining. The staining was analysed with BD LSRII, and the positive cells were gated with FlowJo. (A) Representative dot plots of NK cells and neutrophils. Percentage of NK1.1+ NK cells (B) and Ly-6G+ neutrophils (C) relative to viable cells. Data represent mean±SEM of n=3mice/group.

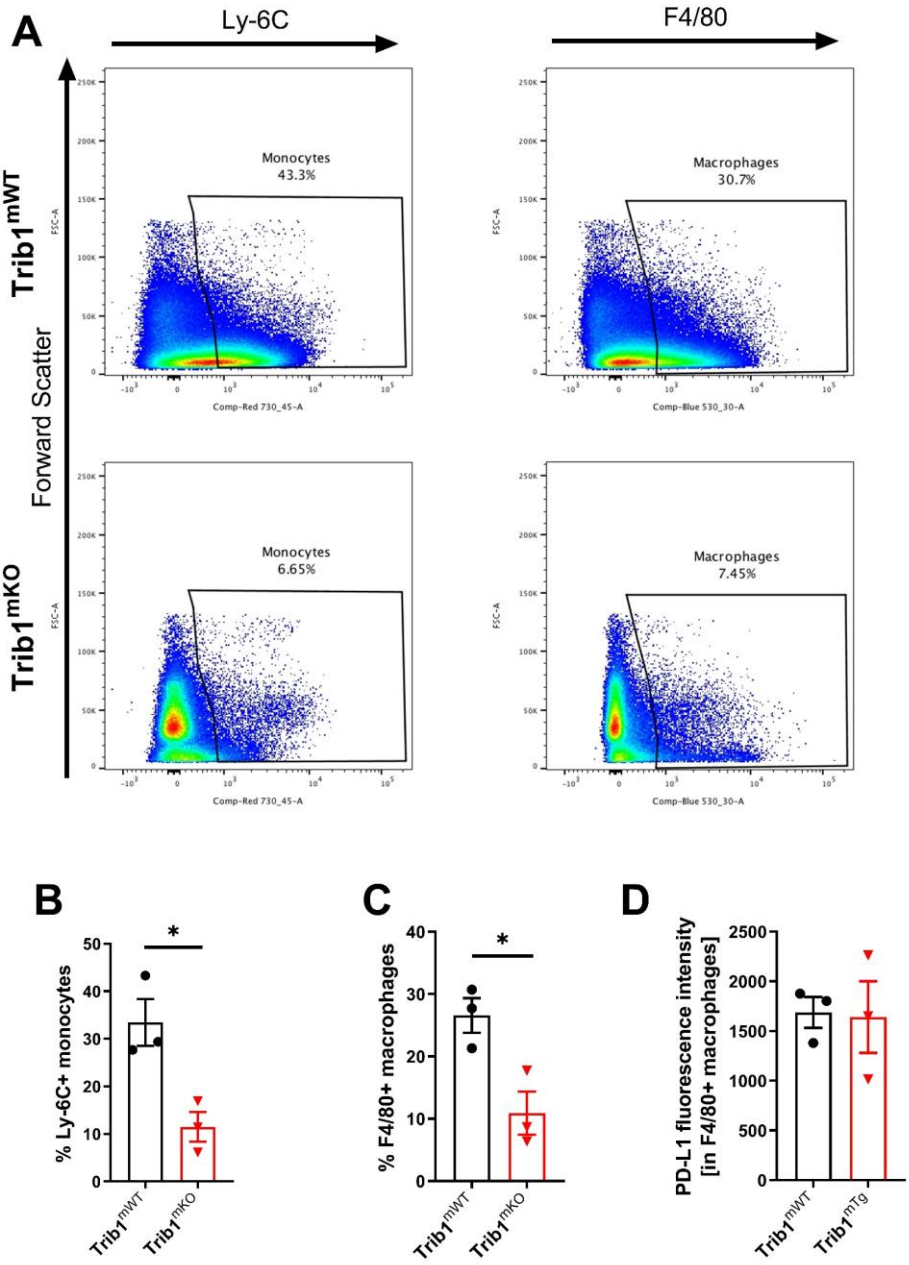

Figure 5.4. Reduced myeloid cell numbers in the tumour microenvironment in *Trib1^{mKO}* animals. (A) Representative images of monocytes and TAMs flow cytometry. Cells were stained with Ly-6C (monocytes) and F4/80 (TAMs), and viability was assessed with Live/Dead dead cell staining. The staining was analysed using BD LSRII, and the positive cells were gated with FlowJo. Percentage of Ly-6C+ monocytes (B) and F4/80+ TAMs (C) relative to the total number of viable cells. (D) PD-L1 expression level in F4/80+ TAMs from *Trib1^{mWT}* and *Trib1^{mKO}* animals. Results of unpaired T-test are presented as *p<0.05, and data represent mean±SEM of n=3mice/group.

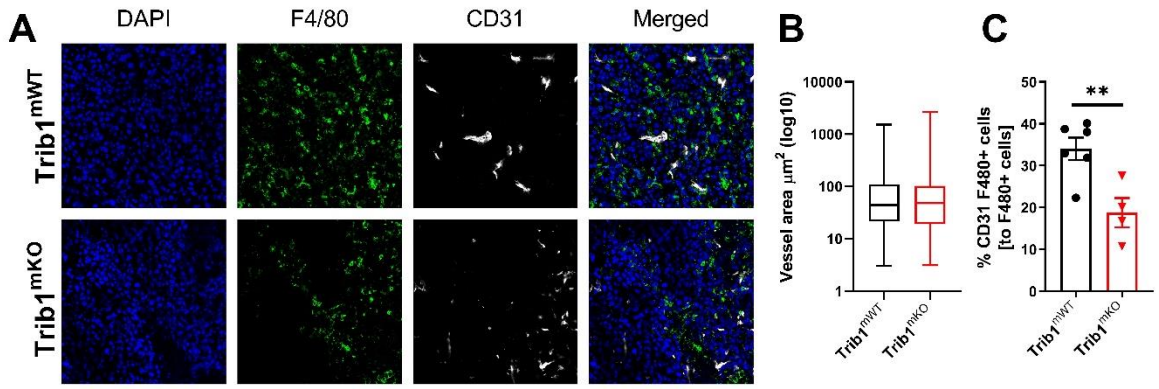

Figure 5.5. Reduction of PV TAMs in the tumours from *Trib1^{mKO}* animals. (A) Representative images of CD31 and F4/80 fluorescence staining with tumours from *Trib1^{mWT}* and *Trib1^{mKO}* animals. Cells were stained with DAPI (blue), TAMs were stained with F4/80 (green), and vessels were stained with CD31 (white). Images were taken with Nikon A1 confocal microscope and analysed using ImageJ. (B) Area of vessels in tumours from *Trib1^{mWT}* and *Trib1^{mKO}* animals. (C) Quantification of CD31+ F4/80+ PV TAMs in the tumour microenvironment relative to the total number of F4/80+ TAMs. Result of unpaired T-test is presented as **p<0.01, and data represent mean±SEM of n=4-6mice/group.

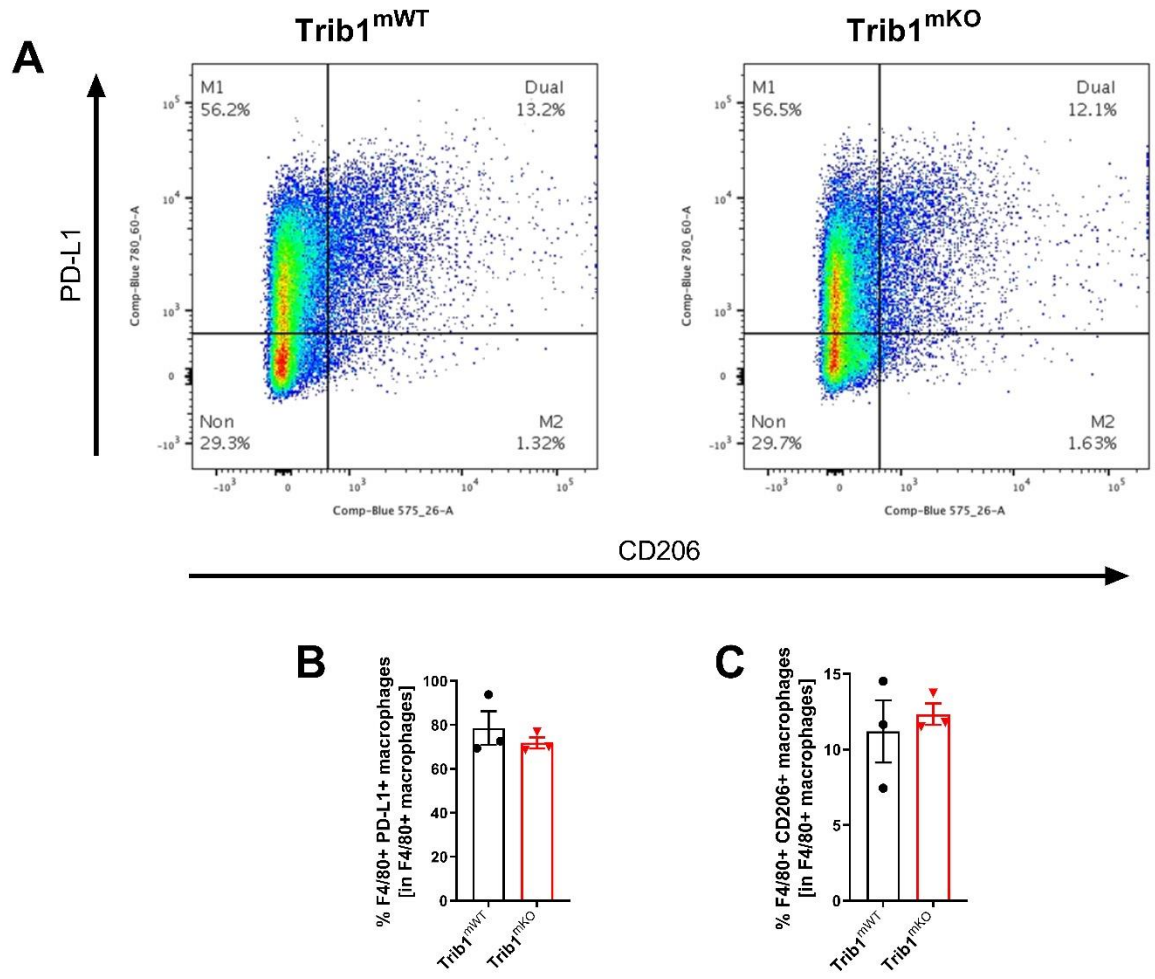

Figure 5.6. Knockdown of myeloid *Trib1* did not alter the percentage of pro-inflammatory and anti-inflammatory TAMs in the tumours from *Trib1*^{mWT} and *Trib1*^{mKO} animals. (A) Representative dot plots of pro-inflammatory and anti-inflammatory TAMs flow cytometry analysis. Cells dissociated from tumour tissues were stained with Live/Dead viability dye to select live cells, TAMs were stained with F4/80, and the phenotype of TAMs was assessed using pro-inflammatory marker PD-L1 and anti-inflammatory marker CD206. The staining was analysed using BD LSRII, and the positive cells were gated with FlowJo. Percentage of PD-L1+ pro-inflammatory (B) and CD206+ anti-inflammatory TAMs (C) relative to the total number of TAMs in the tumour microenvironment. Data represent mean±SEM of n=3mice/group.

5.3.3 Knockdown of myeloid *Trib1* did not impact on T-cell infiltration

The total number of T-cells and the subtypes were investigated using staining of cells dissociated from tumour tissues with T-cell marker CD3, cytotoxic T-cell marker CD8, and naïve T-cell marker CD4 and analysed with flow cytometry. In relation to PD-L1 expression in TAMs, PD1 was also stained and analysed with flow cytometry to assess the expression of

PD1 in T-cells. The analysis demonstrated a trend of increased T-cell infiltration in the tumours from *Trib1*^{mKO} animals, but the difference was due to the wide variation of the amount of T-cell infiltration in *Trib1*^{mKO} animals (**Figure 5.7B**). A similar number of PD1 expressing T-cells (**Figure 5.7C**) and the level of PD1 expression in T-cells (**Figure 5.7D**) were observed between the tumours from *Trib1*^{mWT} and *Trib1*^{mKO} animals. Further analysis of CD3+ CD8+ cytotoxic T-cells and PD1 expression of these cells also demonstrated no significant difference in the total number of cytotoxic T-cells (**Figure 5.8B**), number of PD1 expressing cytotoxic T-cells (**Figure 5.8C**), and the level of PD1 expression in the CD3+ CD8+ cytotoxic T-cells (**Figure 5.8D**). Identically, a similar number of CD3+ CD4+ naïve T-cells (**Figure 5.8F**) and PD1 expressing naïve T-cells (**Figure 5.8G**) were observed between *Trib1*^{mWT} and *Trib1*^{mKO} tumours. However, a trend of reduced PD1 expression level was observed in the tumours from *Trib1*^{mKO} animals (**Figure 5.8H**).

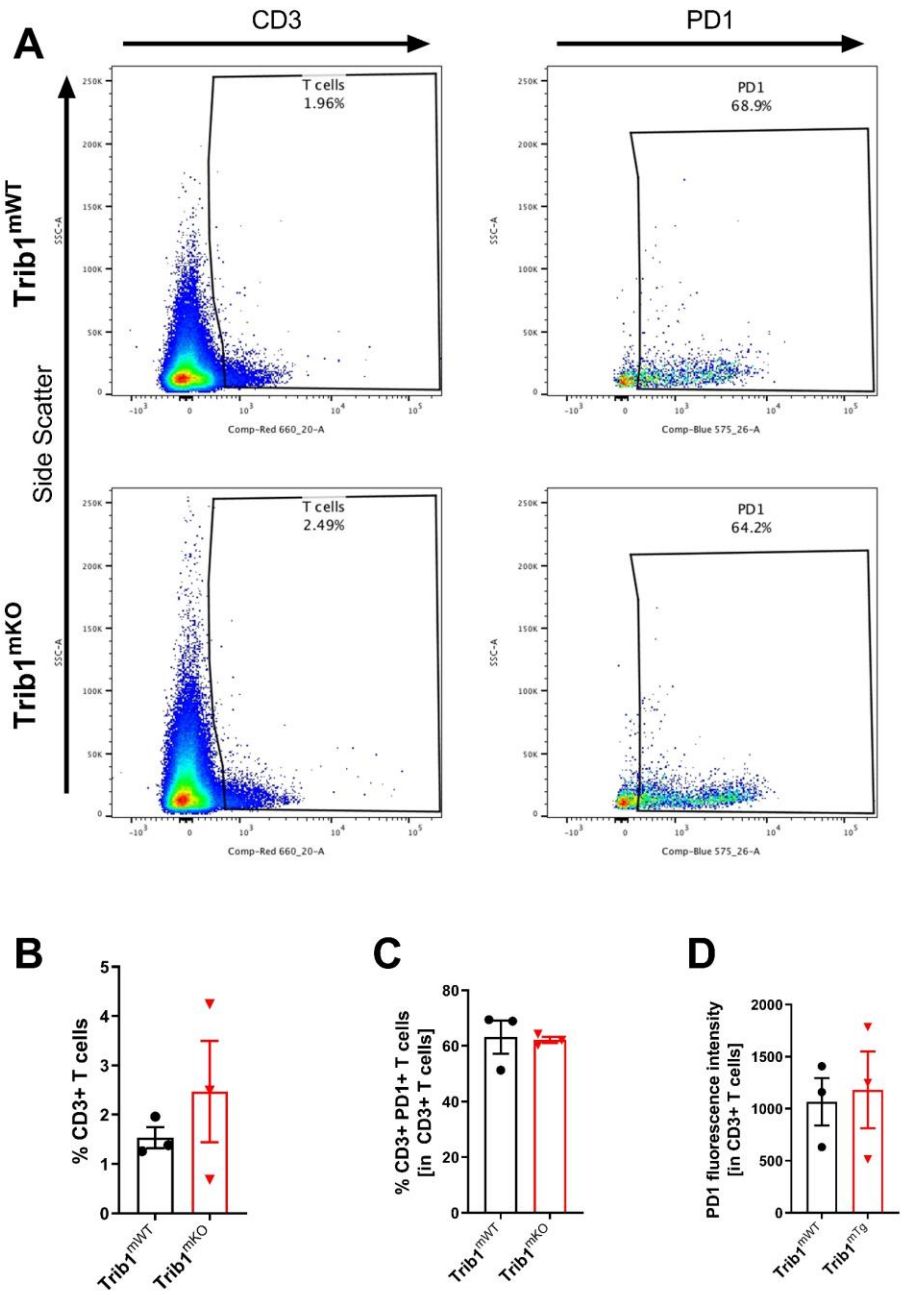

Figure 5.7. Knockdown of myeloid *Trib1* did not alter the number of T-cells and PD1 expression in T-cells. (A) Representative images of CD3 and PD1 flow cytometry. Cells extracted from tumour tissues were stained with Live/Dead viability dye to identify the live cells, and T-cells were stained with CD3 and PD1. The staining was analysed using BD LSRII, and the positive cells were gated with FlowJo. Percentage of total CD3+ T-cells (B) and PD1+ CD3+ PD1 expressing T-cells (C) relative to the total number of live cells. (D) Level of PD1 expression in CD3+ T-cells. Data represent mean±SEM of n=3mice/group.

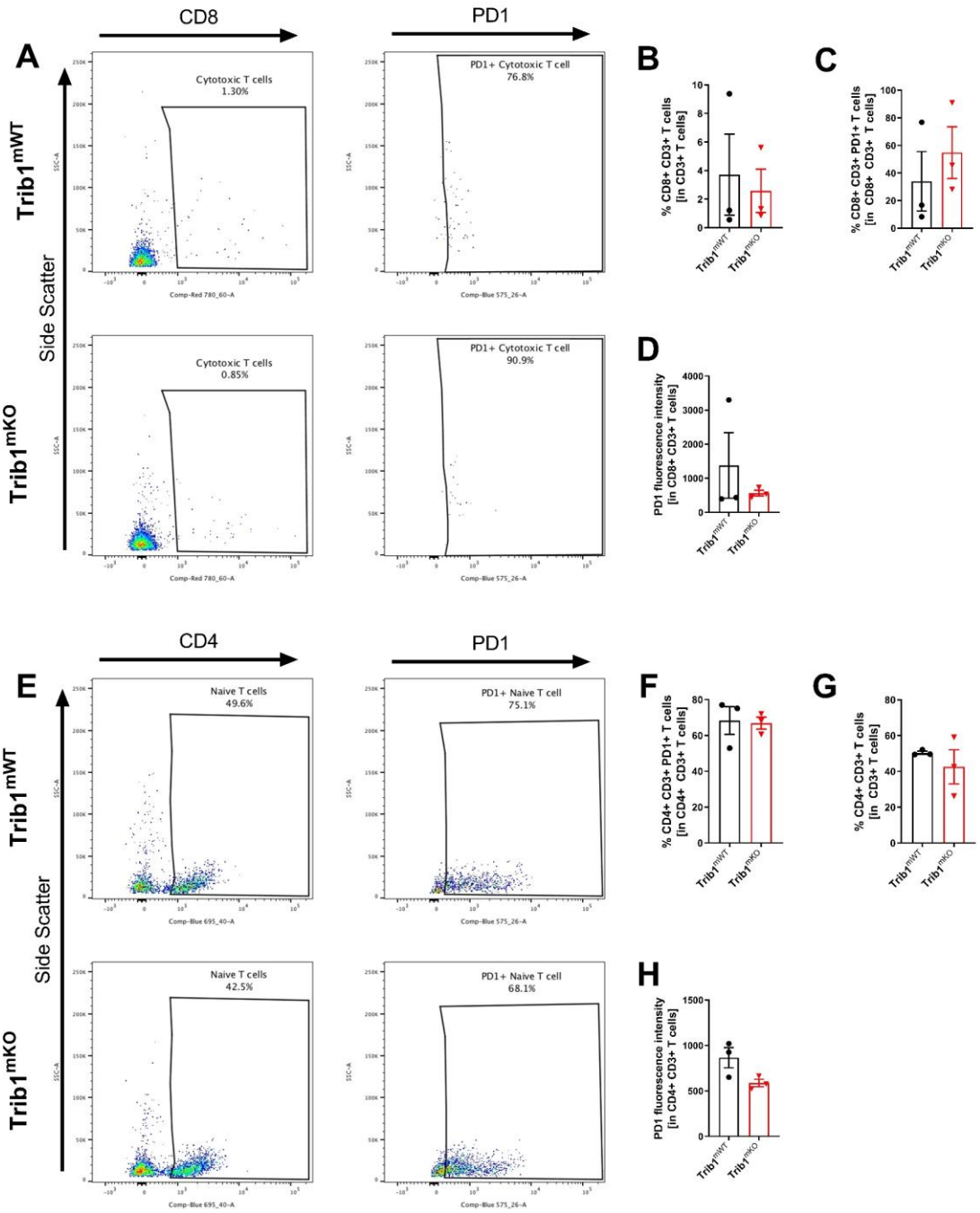

Figure 5.8. Myeloid *Trib1* does not influence the subtype of T-cells and PD1 expression. (A) Representative images of CD3, CD8, and PD1 flow cytometry. Cells were stained with CD3 to identify T-cells and further stained with CD8 and PD1 to assess the number of cytotoxic T-cells and PD1 expression. Percentages of cytotoxic T-cells relative to the number of total T-cells (A), and PD1 expressing cytotoxic T-cells relative to total cytotoxic T-cells (B). (C) PD1 expression level in CD3+ CD8+ cytotoxic T-cells. (E) Representative images of CD3, CD4, and PD1 flow cytometry. Cells were stained with CD3 to identify T-cells and further stained with CD4 and PD1 to assess the number of naïve T-cells and PD1 expression. Percentages of naïve T-cells relative to total T-cells (F), and PD1 expressing naïve T-cells relative to total naïve T-cells (G). (H) PD1 expression level in CD3+ CD4+ naïve T-cells. Data represent mean±SEM of n=3mice/group.

5.4 Discussion

In solid cancer, including breast cancer, TRIB1 is reported as an oncogene which facilitate tumour development. It is reported that TRIB1 is frequently amplified in cancers including breast, prostate, and colon cancers, and particularly in colon cancer, TRIB1 expression is positively correlated with poor prognosis and cancer metastasis(Wang et al., 2017c). TRIB1 is also associated with cell cycle arrest, and inhibition of TRIB1 increased the sensitivity of breast cancer cells to TRAIL-induced apoptosis (Gendelman et al., 2017). In addition, our study revealed that TRIB1 expression is involved in the aggressiveness of breast cancer and regulate oncogenic cytokine expressions in TAMs, and the overexpression of myeloid *Trib1* would accelerate breast tumour growth through inhibition of pro-inflammatory TAM polarisation and T-cell infiltration in the tumour microenvironment, which suggested the oncogenicity of TRIB1 in breast cancer. Therefore, we hypothesised TRIB1 as a potential target to inhibit tumorigenesis and to further identify the mechanism of myeloid TRIB1 in the breast cancer development, $Trib1^{mKO}$ animals with reduced *Trib1* expression in myeloid-specific cells as discussed in (Johnston et al., 2019a) were injected with mouse Eo771 cells to investigate the consequence of myeloid *Trib1* knockout in the tumour growth and formation of the tumour microenvironment. However, the development of Eo771 cells in $Trib1^{mKO}$ animals also demonstrated accelerated tumour growth compared to $Trib1^{mWT}$ animals, and interestingly faster than tumours grew in $Trib1^{mTg}$ animals as shown in chapter 4, which reached maximum tumour size at 22 days after injection (**Figure 5.2B**).

The mechanism behind the acceleration of tumour growth in $Trib1^{mKO}$ animals was initially investigated by the assessment of the tumour microenvironment with post-mortem analysis using flow cytometry and immunofluorescence staining. The assessment of tumour microenvironment revealed no difference in the population of NK cells and neutrophils

present in the tumours from *Trib1*^{mWT} and *Trib1*^{mKO} animals but observed a significant decrease of monocyte and macrophage numbers in *Trib1*^{mKO} tumours as well as reduction of CD31+ F4/80+ PV TAMs in the tumour microenvironment. However, regardless of TAM numbers, both TAMs from *Trib1*^{mWT} and *Trib1*^{mKO} tumours expressed a similar level of PD-L1 which was also observed *in vitro* transient *TRIB1* knockdown TAMs which shown overexpression of *PD-L1* when *TRIB1* was silenced with siRNA (**Chapter 3, figure3.8E**). PD-L1 expression in TAMs inhibits proliferation, cytokine generation and release, and cytotoxicity of T-cells by binding to PD1 in T-cells (Wu et al., 2019), which implies the reduction of TAM infiltration in *Trib1*^{mKO} tumours would not inhibit the oncogenic roles of TAMs. However, the ratio of TAM phenotypes between *Trib1*^{mWT} and *Trib1*^{mKO} animals was similar which suggest the acceleration of tumour growth in *Trib1*^{mKO} animal was not associated with the changes of TAM phenotype, especially with pro-inflammatory TAMs as shown in *Trib1*^{mTg} animals in Chapter 4. Therefore, we explored whether the acceleration of tumour growth in *Trib1*^{mKO} animals is due to the potential impairment of T-cell associated immune responses by TAMs irrelevant of the phenotypic changes.

The T-cells in the tumour microenvironment were evaluated using flow cytometry to assess the population of total T cells and demonstrated a wide variation of total T-cell numbers in *Trib1*^{mKO} animals. In addition, a comparable number of cytotoxic T-cells, naïve T-cells, and the level of PD1 expression in T-cells were observed between *Trib1*^{mWT} and *Trib1*^{mKO} animals which further confirms that in contrast to *Trib1*^{mTg} animals, infiltration of T-cells in *Trib1*^{mKO} animals does not influence tumour growth. Therefore, our flow cytometry and fluorescence staining data suggest a distinct mechanism in the development of tumours from *Trib1*^{mKO} animals compared to *Trib1*^{mTg} animals as the knockdown of myeloid *Trib1* does not alter

TAM phenotype or T-cell infiltration as in *Trib1*^{mTg} animals. *Trib1*^{mKO} also regulate macrophage infiltration but particularly PV TAMs in contrast to *Trib1*^{mTg} animals.

Chapter 6. General discussion

6.1 Summary

For many years, breast cancer had the highest incidence and mortality rate in women worldwide. Although rapid progress in molecular biology, systems biology, and genome science allowed to develop personalised medicine and treatments which significantly reduced the mortality rate from 1990, breast cancer is still the most common cause of cancer deaths with an increasing number of incidence in females. Upon development of cancer, both mutations in different genes and recruitment of neighbouring healthy cells are performed by cancer cells to initiate the formation of solid tumour, and TAMs are observed to consist ~50% of the breast tumour mass and accelerate tumour growth and promote resistance to the therapies. Therefore, increasing knowledge of breast cancer biology and mechanisms that underpin cancer development will lead to effective strategies to develop breast cancer treatments. In this study, we aimed to understand the mechanisms of oncogenicity in TAMs, particularly in relation to TRIB1 expression.

TRIB1, which is a pseudokinase protein that regulates MAPK signalling and C/EBPα, was initially emphasised for its role in myeloid cells, with TRIB1 being highly expressed in the myeloid lineages (Richmond and Keeshan, 2019) and the knockout of *Trib1* in mice showing reduction of anti-inflammatory macrophages in tissues (Satoh et al., 2013, Johnston, 2017). The regulation of macrophage phenotype by TRIB1 expression was also confirmed in our study via *in vitro* transient knockdown of *TRIB1* in the macrophages which demonstrated the significant increase of pro-inflammatory cytokines *IL-1β* and *IL-8* whilst the expression of anti-inflammatory cytokines were not altered (**Figure 3.3**). The *in silico* analysis of Cardiogenic Consortium transcriptomic data set also revealed that the top 10 functional roles

of macrophages modified based on the *TRIB1* expression was specific to macrophages and were not altered in monocytes (**Figure 3.2**) which supports the distinct TRIB1 dependent regulation of macrophages among myeloid cells.

Our study also revealed the oncogenicity of TRIB1 in breast cancer where *in silico* analysis of TRIB1 gene in breast cancer patients with published cancer genomics data sets cBioportal (https://www.cbioportal.org/) demonstrated the alteration of TRIB1 gene in the 13.28% of breast cancer patients among 1084 cases, mostly amplification of the gene (**Figure 3.4A**), and the patient with altered TRIB1 gene had significantly decreased overall survival (**Figure 3.4C**). It was also reported by a previous study that demonstrated a significant reduction of patient breast cancer-specific and overall survival with amplification of TRIB1 copy number (Gendelman et al., 2017). The microarrays of published human datasets from GENT2 (http://gent2.appex.kr/gent2/) also revealed the significant overexpression of *TRIB1* RNA level in the TNBC tissues compared to other subtypes (**Figure 3.5C**), and similar was observed in the breast cancer cell lines where the TNBC cells expressed high TRIB1 levels (**Figure 3.6**). In addition, although *TRIB1* RNA level between normal and breast cancer tissues with GENT2 demonstrated either reduction of *TRIB1* in breast cancer in the Affymetrix U133A platform (GPL96) or no difference in Affymetrix U133Plus2 platform (GPL570) (**Figure 3.5A and B**), comparing normal breast tissues with TNBCs shown a significant increase of *TRIB1* expression ($p<0.0001$) which implies that huge variations of *TRIB1* expression depending on breast cancer phenotypes and in the analysis of breast cancer in comparison with healthy tissues, it is essential to specify the cancer subtype to avoid misleading of data. Collectively, *in silico* analysis of two different published data sets in this study uncovered that TRIB1 is highly involved with the aggressiveness of breast cancer.

Similar to our *in silico* analysis, *in vitro* assessment of macrophages treated with tumour-conditioned medium, mimicking TAMs from the tumour microenvironment, exhibited a significant increase of *TRIB1* RNA levels in TAMs compared to unpolarised or M1 macrophage stimulated with LPS and INF-γ (**Figure 3.7A**). However, the level of TRIB1 protein in TAMs was significantly reduced compared to unpolarised macrophages (**Figure 3.7B-C**). The difference of RNA and protein level of the same gene is potentially caused by lack of gene-specific RNA-to-protein conversion factors independent of the cells and tissues (Edfors et al., 2016), and similar controversial expression of RNA and protein levels was reported with TRIB3 which observed significant overexpression of *TRIB3* in breast cancer patients and correlation of *TRIB3* expression with poor breast cancer prognosis whilst the protein level of TRIB3 was opposite (Wennemers et al., 2011b, Wennemers et al., 2011a). However, the fluorescence staining of the murine mammary tumours developed *in vivo* demonstrated most expressions of TRIB1 observed in the tumour microenvironment are from TAMs (**Figure 3.7D-F**), which denoted the importance of myeloid TRIB1 in breast tumour development.

Based on our findings in Chapter 3 which implied the importance of myeloid TRIB1 in breast cancer, we have developed a mammary cancer model with myeloid-specific *Trib1* overexpressing and knockout C57/BL6N mice to investigate the mechanisms of myeloid *Trib1* dependent breast cancer development. In order to develop the syngeneic mice model with our immunocompetent *Trib1* knockout and transgenic mice, we have used Eo771 cells to inject into the mammary fat pads and monitoring the tumour growth (**Figure 2.1**). The classification of Eo771 cell line still remains controversial, but among 30 publications considering Eo771 cells, only 3 articles reported ERα in Eo771 cells with much weaker expression compared to MCF-7 (considered ERα+), but the receptor was not found in the

nuclear compartment which could consider as Erα- (Le Naour et al., 2020). In addition, Eo771 cells are derived from C57 black mice which allow being used as syngeneic models, and orthotopically transplantation leads to large tumours within weeks.

Interestingly, measuring breast tumour growth on *Trib1*^{mTg} and *Trib1*^{mKO} animals demonstrated that both overexpression and knockout of myeloid *Trib1* promoted the breast tumour growth. However, *Trib1*^{mTg} animals accelerated at the later stage at 24 days (**Figure 4.2B**) compared to *Trib1*^{mKO} animals at 18 days (**Figure 5.2B**). In relation to our *in silico* data which show a significant increase of *TRIB1* expression in TNBC tissues compared to normal breast tissues with other breast cancer subtypes, acceleration of breast tumour growth with either overexpression or knockout of myeloid *Trib1* implies that regulation of *Trib1* level from the baseline will promote aggressiveness of breast cancer.

In order to determine whether alteration of *Trib1* expression from baseline will generate aggressiveness of breast cancer in distinct mechanisms, primary tumours developed in animals were collected for further analysis. The post-mortem analysis of tumours revealed that tumours from *Trib1*^{mTg} animals had a significant reduction of TAMs in the tumour microenvironment, especially hypoxic TAMs (**Figure 4.3**), with significant inhibition of TAM polarisation towards pro-inflammatory phenotypes (**Figure 4.4**). Hypoxic TAMs are distinguished as entrapped, less motile TAMs in the hypoxic area with pro-tumoral features facilitating cancer cell survival, angiogenesis, metastasis and immune suppression as described above. In addition, TAMs expressing both pro- and anti-inflammatory phenotypes are reported to exacerbate tumour hypoxia (Jeong et al., 2019) crucial for the tumour blood vessel formation and primary tumour growth (Muz et al., 2015). The sufficient infiltration of pro-inflammatory macrophages is also known to be essential for the early cancer formation

and development (Pinto et al., 2019), which could explain the delay of breast tumour growth in the *Trib1*^{mTg} animals compared to the *Trib1*^{mKO} animals.

However, the acceleration of mammary tumour growth in the *Trib1*^{mTg} animals compared to the *Trib1*^{mWT} animals could also be delineated by the inhibition of pro-inflammatory TAM polarisation as the cytokines expressed by pro-inflammatory TAMs initiate tumoricidal immune responses mediated by different immune cells (Quatromoni and Eruslanov, 2012). Furthermore, fluorescence staining of the tumour also demonstrated a significant reduction of T-cell number in *Trib1*^{mTg} tumours (**Figure 4.5**). It was reported that TAMs are involved in the T-cell infiltration (Jeong et al., 2019), and one of the contributors is IL-15 expression which is highly involved in the T-cell infiltration, development, and survival (Santana Carrero et al., 2019, Robinson and Schluns, 2017). The microarray of *TRIB1* high and low human monocytes and macrophages revealed a significant reduction of *IL-15* expression in *TRIB1* high macrophages (**Figure 4.6A**). Similar was also observed in murine BMDMs and tumour microenvironment from *Trib1*^{mTg} animals (**Figure 4.6B-D**) which confirmed that overexpression of myeloid *Trib1* reduced *Il-15* expression in TAMs and as a consequence, reduced T-cell infiltration and accelerated breast tumour growth.

Finally, post-mortem analysis of *Trib1*^{mKO} tumours also revealed a significant reduction of TAM (**Figure 5.4**), but in contrast to *Trib1*^{mTg} tumours, observed the decrease of PV TAM numbers compared to WT tumours (**Figure 5.5**), essential for the angiogenesis and metastasis of cancer. The number of TAM phenotypes, T-cells, and other immune cells was not changed between the tumours from *Trib1*^{mKO} and *Trib1*^{mWT} animals (**Figure 5.3, Figure 5.6, Figure 5.7, Figure 5.8**), but *in vitro* transient *TRIB1* knockdown of human macrophages polarised to TAMs demonstrated a significant increase of cytokines involved in the immune suppression and angiogenesis such as *IL-8, IL-10, PD-L1, SPARC* and *VEGF* (**Figure 3.8**). Although

previous paper reported the correlation of *TRIB1* and *IL-8* expression in breast cancer, we have observed overexpression of *IL-8* in *TRIB1* knockdown TAMs that is involved in the immune suppression and poor PD-L1 blockade (Yuen et al., 2020). In addition, *IL-10* suppresses immune surveillance, inhibit apoptosis and enhances migration of cancer cells (Sheikhpour et al., 2018, Chen et al., 2019a); *PD-L1* disrupts T cell proliferation and function (Wu et al., 2019); and *SPARC* and *VEGF* expressions are crucial for breast cancer growth and angiogenesis, which suggest the knockout of myeloid *Trib1* does not alter TAM phenotype nor other immune cell population in breast tumours but alter the expression of oncogenic cytokines in TAMs to accelerate breast tumour growth.

In summary, our findings suggest that *TRIB1* expression is associated with aggressiveness of breast cancer and regulation of myeloid *Trib1* in either way has distinct mechanisms in the tumour microenvironment to facilitate breast tumour growth (**Figure 6.1**). The overexpression of myeloid *Trib1* inhibits polarisation of pro-inflammatory TAMs and significantly reduce the *IL-15* expression, as a consequence, reduce infiltration of T cells into the tumour microenvironment and accelerate breast tumour growth. Whilst the myeloid *Trib1* knockout does not alter TAM phenotype nor infiltration of T cells but instead increases the expression of oncogenic cytokines in TAMs to accelerate tumour growth.

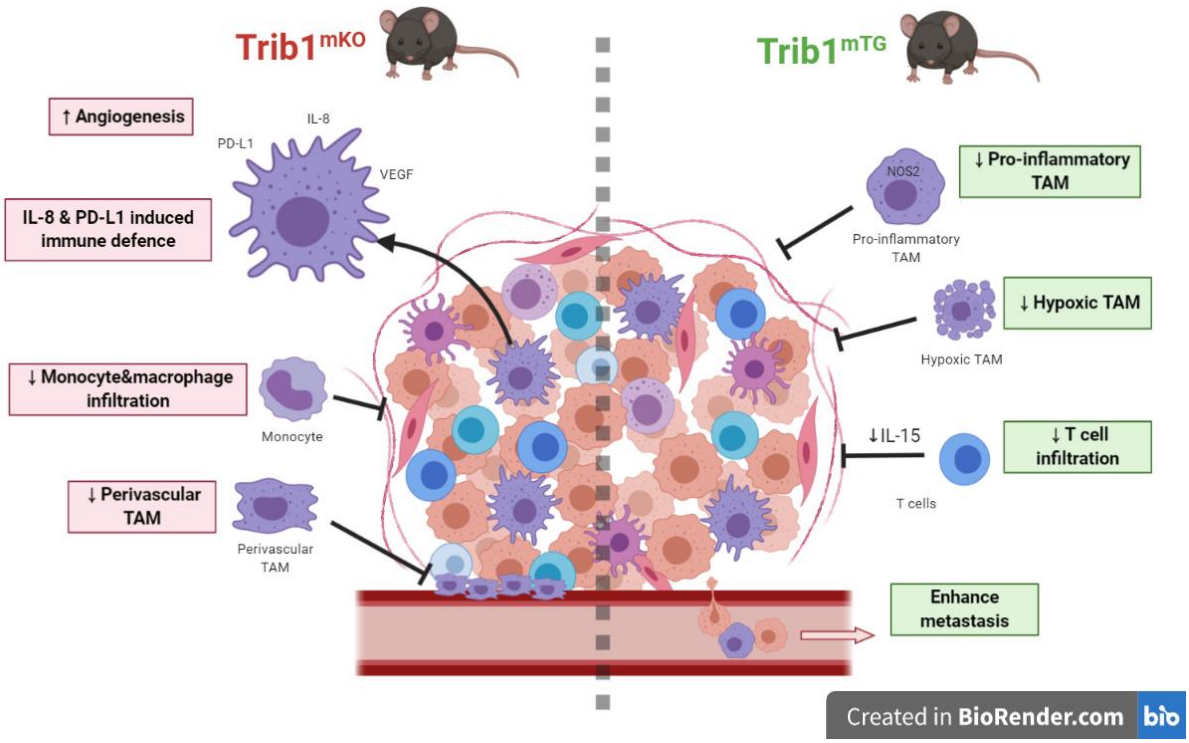

Figure 6.1. Myeloid *Trib1* has distinct roles in the formation of the tumour microenvironment. Schematic diagram of the tumour microenvironment alteration depending on the myeloid *Trib1* overexpression and knockout.

6.2 Limitations

Animal models provide critical insights into disease pathology, gene characterisation and investigating therapeutic agents which thereby highly used in the biomedical researches. Correspondingly, the project is highly involved with mouse model studies; therefore, the main limitation of the study is the lack of human patient data. To overcome the challenge, we attempted to use published human datasets available from the websites to develop the rationale of the project, as shown in chapter 3. However, it will be interesting to investigate the human patient samples to confirm the direct translation of the murine data. Another limitation regarding mouse model is the classification of Eo771 cells. As we have used C57/BL6N mice to modify the expression of myeloid *Trib1*, we required to develop cancer model on the immunocompetent host that requires breast cancer cells from the same host.

Therefore, although the classification of Eo771 was controversial, we have initially used this cell line as TNBC to develop cancer models as it was challenging to find the alternatives. However, it was confirmed in 2020 that Eo771 cells are luminal B mammary cancer cells. There were difficulties also with the recruitment of enough sample number as we bred specific mouse strains for the study which required specific genotype of the animal and time to grow the animals to a certain age to start the experiments. Moreover, we encountered major difficulties with breeding *Trib1*^{mKO} animals as they were not able to produce litters as other strains which unable to get enough samples to strengthen the data.

After the development of tumour models, limitations are also found in the post-mortem analysis. Although TAMs, T-cells, and other immune cells were assessed either with fluorescence staining or flow cytometry, there are other cells involved in the tumour development such as Tregs, fibroblasts, and B cells which were not investigated in this study. Flow cytometry allows multiple screening of antibodies at a single time, but the number of antibodies allowed to run depends on the number of lasers and detectors that inhibited to screen other antibodies. Analysing fluorescence staining also has limitations as due to the technical issues and efficiency, it is difficult to analyse the whole tissues. Therefore, 4-5-random areas were imaged and analysed, which has possibilities to have bias data.

The *in vitro* studies with human macrophages, especially investigating the tumour-conditioned medium treated macrophages, contains some limitations. Although it will be able to represent the human data with the ease to assess the response of cells depending on the conditional changes, it would be impossible to provide the complexity of interactions in tissues and tumour microenvironment. Therefore, treating conditioned medium to macrophages will polarise cells similar to TAMs, but it will react differently from the TAMs in the tumour microenvironment.

Finally, chapter 5 concludes the acceleration of tumour growth in the *Trib1*^{mKO} animals based on the *in vitro* human MDM data. As mentioned above, *in vitro* development of TAMs from human macrophages could not completely mimic the re-education of macrophages to TAMs in the tumour microenvironment. The difference in the species also lacks substantial evidence to confirm that the TAMs in the *Trib1*^{mKO} tumours will react as observed in the human MDMs.

6.3 Future work

Based on the findings in this thesis and the limitations, it would be useful to translate the current findings to human samples by investigating the human breast cancer tissues with fluorescence staining to confirm the regulatory role of myeloid TRIB1 in the breast tumour microenvironment. Chapter 3 briefly demonstrated the correlation of *TRIB1* expression and the aggressiveness of breast cancer by presenting the highest expression of *TRIB1* in TNBC tissues and the analysis of human patient tissues will provide further supporting evidence to denote the mechanism of modulating aggressiveness of different breast cancer subtypes depending on myeloid *TRIB1* expression. Furthermore, increasing N numbers of *in vivo* myeloid *Trib1* knockdown studies and analysis of the tumour microenvironment with flow cytometry, and isolating TAMs directly from *Trib1*^{mKO} tumours and investigating the functional cytokines involved in the tumour development using RT-qPCR or RNA-seq will strengthen the significance of changes in *Trib1*^{mKO} tumours and confirms the mechanism of accelerated breast tumour growth in *Trib1*^{mKO} animals.

Chapter 4 briefly mentioned the potential regulation of metastasis via myeloid *Trib1* expression. In contrast to the *Trib1*^{mTg} tumours, *Trib1*^{mKO} tumours also had a significant reduction of PV TAMs, which raise a new question of whether the metastatic stage of breast

tumour will be affected by myeloid *Trib1*. Therefore, it would be interesting to investigate the myeloid *Trib1* dependent secondary tumour development in the lung and the liver and further develop another project to establish metastasis cancer models on the $Trib1^{mTg}$ and $Trib1^{mKO}$ animals and analyse the mechanism of the myeloid *Trib1* dependent metastasis. This could be done by resection of the primary mammary tumour or in seeding models where the tumour cells are injected via the circulation to establish metastasis.

Translating the data for the clinical application would also be exciting work in the future. Current findings revealed that myeloid *Trib1* expression consists of two distinct mechanisms to regulate breast tumour growth and aggressiveness. If we have reliable evidence regarding metastasis, developing *TRIB1* as a marker to classify breast cancer will enable us to specify the patients to appropriate therapies. If we get data regarding the interaction of myeloid *TRIB1* and other immune cells such as T-cells, it would be interesting to research *TRIB1* as a potential therapeutic target to antagonise or agonise combination with other therapies based on the expression levels to maximise the response rate and reduce resistance.

Finally, the research in this thesis was done only with Eo771 cells that is confirmed as luminal B mammary cancer cells. Therefore, based on the published human datasets in chapter 3 demonstrating highest *TRIB1* expression in TNBCs compared to other breast cancer subtypes, it would be beneficial in future to analyse the role of myeloid *TRIB1* in the TNBC development.

Chapter 7. References

ALTOMARE, D. A. & TESTA, J. R. 2005. Perturbations of the AKT signaling pathway in human cancer. *Oncogene,* 24**,** 7455-7464.

AMIT-COHEN, B.-C., RAHATAND, M. M. & RAHAT, M. A. 2013. Tumor cell-macrophage interactions increase angiogenesis through secretion of EMMPRIN. *Frontiers in Physiology,* 4.

ANFRAY, UMMARINO, ANDÓN & ALLAVENA 2019. Current Strategies to Target Tumor-Associated-Macrophages to Improve Anti-Tumor Immune Responses. *Cells,* 9**,** 46.

ARNDT, L., DOKAS, J., GERICKE, M., KUTZNER, C. E., MULLER, S., JEROMIN, F., THIERY, J. & BURKHARDT, R. 2018. Tribbles homolog 1 deficiency modulates function and polarization of murine bone marrow-derived macrophages. *J Biol Chem,* 293**,** 11527-11536.

ARNOLD, L., HENRY, A., PORON, F., BABA-AMER, Y., VAN ROOIJEN, N., PLONQUET, A., GHERARDI, R. K. & CHAZAUD, B. 2007. Inflammatory monocytes recruited after skeletal muscle injury switch into antiinflammatory macrophages to support myogenesis. *Journal of Experimental Medicine,* 204**,** 1057-1069.

ARWERT, E. N., HARNEY, A. S., ENTENBERG, D., WANG, Y., SAHAI, E., POLLARD, J. W. & CONDEELIS, J. S. 2018. A Unidirectional Transition from Migratory to Perivascular Macrophage Is Required for Tumor Cell Intravasation. *Cell Reports,* 23**,** 1239-1248.

ASANO, K., KIKUCHI, K. & TANAKA, M. 2018. CD169 macrophages regulate immune responses toward particulate materials in the circulating fluid. *The Journal of Biochemistry,* 164**,** 77-85.

AZAMJAH, N., SOLTAN-ZADEH, Y. & ZAYERI, F. 2019. Global Trend of Breast Cancer Mortality Rate: A 25-Year Study. *Asian Pac J Cancer Prev,* 20**,** 2015-2020.

BALKWILL, F. R., CAPASSO, M. & HAGEMANN, T. 2012. The tumor microenvironment at a glance. *Journal of Cell Science,* 125**,** 5591-5596.

BASKAR, R., DAI, J., WENLONG, N., YEO, R. & YEOH, K.-W. 2014. Biological response of cancer cells to radiation treatment. *Frontiers in Molecular Biosciences,* 1.

BAUER, R. C., SASAKI, M., COHEN, D. M., CUI, J., SMITH, M. A., YENILMEZ, B. O., STEGER, D. J. & RADER, D. J. 2015. Tribbles-1 regulates hepatic lipogenesis through posttranscriptional regulation of C/EBPalpha. *J Clin Invest,* 125**,** 3809-18.

BOYETTE, L. B., MACEDO, C., HADI, K., ELINOFF, B. D., WALTERS, J. T., RAMASWAMIL, B., CHALASANI, G., TABOAS, J. M., LAKKIS, F. G. & METES, D. M. 2017. Phenotype, function, and differentiation potential of human monocyte subsets. *Plos One,* 12.

BRYANT, C. D. 2011. The blessings and curses of C57BL/6 substrains in mouse genetic studies. *Annals of the New York Academy of Sciences,* 1245**,** 31-33.

BURCOMBE, R. 2017. Current treatment of HER 2+ metastatic breast cancer. *British journal of nursing : BJN.,* 26**,** S7-S14.

BUROTTO, M., CHIOU, V. L., LEE, J.-M. & KOHN, E. C. 2014. The MAPK Pathway Across Different Malignancies: A New Perspective. *Cancer,* 120**,** 3446-3456.

CAMPS, J., NGUYEN, Q. T., PADILLA-NASH, H. M., KNUTSEN, T., MCNEIL, N. E., WANGSA, D., HUMMON, A. B., GRADE, M., RIED, T. & DIFILIPPANTONIO,

M. J. 2009. Integrative genomics reveals mechanisms of copy number alterations responsible for transcriptional deregulation in colorectal cancer. *Genes Chromosomes Cancer,* 48**,** 1002-17.

CANCERRESEARCHUK. 2020. *Breast cancer survival statistics* [Online]. Cancer Research UK. [Accessed].

CARBOGNIN, L., MIGLIETTA, F., PARIS, I. & DIECI, M. V. 2019. Prognostic and Predictive Implications of PTEN in Breast Cancer: Unfulfilled Promises but Intriguing Perspectives. *Cancers,* 11**,** 1401.

CAUX, C., RAMOS, R. N., PRENDERGAST, G. C., BENDRISS-VERMARE, N. & MENETRIER-CAUX, C. 2016. A Milestone Review on How Macrophages Affect Tumor Growth. *Cancer Research,* 76**,** 6439-6442.

CERAMI, E., GAO, J., DOGRUSOZ, U., GROSS, B. E., SUMER, S. O., AKSOY, B. A., JACOBSEN, A., BYRNE, C. J., HEUER, M. L., LARSSON, E., ANTIPIN, Y., REVA, B., GOLDBERG, A. P., SANDER, C. & SCHULTZ, N. 2012. The cBio cancer genomics portal: an open platform for exploring multidimensional cancer genomics data. *Cancer Discov,* 2**,** 401-4.

CEVEY, Á. C., PENAS, F. N., ALBA SOTO, C. D., MIRKIN, G. A. & GOREN, N. B. 2019. IL-10/STAT3/SOCS3 Axis Is Involved in the Anti-inflammatory Effect of Benznidazole. *Frontiers in Immunology,* 10.

CHAVEZ-GALAN, L., OLLEROS, M. L., VESIN, D. & GARCIA, I. 2015. Much more than M1 and M2 macrophages, there are also CD169(+) and TCR+ macrophages. *Frontiers in Immunology,* 6.

CHEN, F., ZHUANG, X., LIN, L., YU, P., WANG, Y., SHI, Y., HU, G. & SUN, Y. 2015. New horizons in tumor microenvironment biology: challenges and opportunities. *Bmc Medicine,* 13.

CHEN, H., LI, M., SANCHEZ, E., SOOF, C. M., BUJARSKI, S., NG, N., CAO, J., HEKMATI, T., ZAHAB, B., NOSRATI, J. D., WEN, M., WANG, C. S., TANG, G., XU, N., SPEKTOR, T. M. & BERENSON, J. R. 2020. JAK1/2 pathway inhibition suppresses M2 polarization and overcomes resistance of myeloma to lenalidomide by reducing TRIB1, MUC1, CD44, CXCL12, and CXCR4 expression. *Br J Haematol,* 188**,** 283-294.

CHEN, L., SHI, Y., ZHU, X., GUO, W., ZHANG, M., CHE, Y., TANG, L., YANG, X., YOU, Q. & LIU, Z. 2019a. IL-10 secreted by cancer-associated macrophages regulates proliferation and invasion in gastric cancer cells via c-Met/STAT3 signaling. *Oncology Reports*.

CHEN, Y., SONG, Y., DU, W., GONG, L., CHANG, H. & ZOU, Z. 2019b. Tumor-associated macrophages: an accomplice in solid tumor progression. *Journal of Biomedical Science,* 26.

CHEN, Y., ZHANG, S., WANG, Q. & ZHANG, X. 2017. Tumor-recruited M2 macrophages promote gastric and breast cancer metastasis via M2 macrophage-secreted CHI3L1 protein. *J Hematol Oncol,* 10**,** 36.

CHISTIAKOV, D. A., BOBRYSHEV, Y. V. & OREKHOV, A. N. 2015. Changes in transcriptome of macrophages in atherosclerosis. *Journal of Cellular and Molecular Medicine,* 19**,** 1163-1173.

CHOUDHARI, S. K., CHAUDHARY, M., BAGDE, S., GADBAIL, A. R. & JOSHI, V. 2013. Nitric oxide and cancer: a review. *World Journal of Surgical Oncology,* 11.

CLAIRE, ALLISON & JEFFREY 2016. The Multifaceted Role of Perivascular Macrophages in Tumors. *Cancer Cell,* 30**,** 18-25.

CLARK, A. R. & TOKER, A. 2014. Signalling specificity in the Akt pathway in breast cancer. *Biochemical Society Transactions,* 42**,** 1349-1355.

COLEGIO, O. R., NGOC-QUYNH, C., SZABO, A. L., CHU, T., RHEBERGEN, A. M., JAIRAM, V., CYRUS, N., BROKOWSKI, C. E., EISENBARTH, S. C., PHILLIPS, G. M., CLINE, G. W., PHILLIPS, A. J. & MEDZHITOV, R. 2014. Functional polarization of tumour-associated macrophages by tumour-derived lactic acid. *Nature,* 513**,** 559-+.

CUI, R., MENG, W., SUN, H. L., KIM, T., YE, Z., FASSAN, M., JEON, Y. J., LI, B., VICENTINI, C., PENG, Y., LEE, T. J., LUO, Z., LIU, L., XU, D., TILI, E., JIN, V., MIDDLETON, J., CHAKRAVARTI, A., LAUTENSCHLAEGER, T. & CROCE, C. M. 2015. MicroRNA-224 promotes tumor progression in nonsmall cell lung cancer. *Proc Natl Acad Sci U S A,* 112**,** E4288-97.

CUNARD, R. 2013. Mammalian tribbles homologs at the crossroads of endoplasmic reticulum stress and Mammalian target of rapamycin pathways. *Scientifica,* 2013**,** 750871-750871.

DAURKIN, I., ERUSLANOV, E., STOFFS, T., PERRIN, G. Q., ALGOOD, C., GILBERT, S. M., ROSSER, C. J., SU, L.-M., VIEWEG, J. & KUSMARTSEV, S. 2011. Tumor-Associated Macrophages Mediate Immunosuppression in the Renal Cancer Microenvironment by Activating the 15-Lipoxygenase-2 Pathway. *Cancer Research,* 71**,** 6400-6409.

DAVID, J. M., DOMINGUEZ, C., HAMILTON, D. H. & PALENA, C. 2016. The IL-8/IL-8R Axis: A Double Agent in Tumor Immune Resistance. *Vaccines (Basel),* 4.

DAVIES, L. C., JENKINS, S. J., ALLEN, J. E. & TAYLOR, P. R. 2013. Tissue-resident macrophages. *Nature Immunology,* 14**,** 986-995.

DE BEULE, N., DE VEIRMAN, K., MAES, K., DE BRUYNE, E., MENU, E., BRECKPOT, K., DE RAEVE, H., VAN RAMPELBERGH, R., VAN GINDERACHTER, J. A., SCHOTS, R., VAN VALCKENBORGH, E. & VANDERKERKEN, K. 2017. Tumour-associated macrophage-mediated survival of myeloma cells through STAT3 activation. *Journal of Pathology,* 241**,** 534-546.

DONG, S., XIA, J., WANG, H., SUN, L., WU, Z., BIN, J., LIAO, Y., LI, N. & LIAO, W. 2016. Overexpression of TRIB3 promotes angiogenesis in human gastric cancer. *Oncology Reports,* 36**,** 2339-2348.

DREESEN, O. & BRIVANLOU, A. H. 2007. Signaling pathways in cancer and embryonic stem cells. *Stem Cell Reviews,* 3**,** 7-17.

DUGAST, E., KISS-TOTH, E., SOULILLOU, J. P., BROUARD, S. & ASHTON-CHESS, J. 2013. The Tribbles-1 Protein in Humans: Roles and Functions in Health and Disease. *Current Molecular Medicine,* 13**,** 80-85.

DUQUE, G. A. & DESCOTEAUX, A. 2014. Macrophage cytokines: involvement in immunity and infectious diseases. *Frontiers in Immunology,* 5**,** 1-12.

EDFORS, F., DANIELSSON, F., HALLSTROM, B. M., KALL, L., LUNDBERG, E., PONTEN, F., FORSSTROM, B. & UHLEN, M. 2016. Gene-specific correlation of RNA and protein levels in human cells and tissues. *Mol Syst Biol,* 12**,** 883.

ELIYATKIN, N., YALCIN, E., ZENGEL, B., AKTAŞ, S. & VARDAR, E. 2015. Molecular Classification of Breast Carcinoma: From Traditional, Old-Fashioned Way to A New Age, and A New Way. *Journal of Breast Health,* 11**,** 59-66.

EPELMAN, S., LAVINE, K. J. & RANDOLPH, G. J. 2014. Origin and Functions of Tissue Macrophages. *Immunity,* 41**,** 21-35.

ESTKO, M., BAUMGARTNER, S., URECH, K., KUNZ, M., REGUEIRO, U., HEUSSER, P. & WEISSENSTEIN, U. 2015. Tumour cell derived effects on monocyte/macrophage polarization and function and modulatory potential of Viscum album lipophilic extract in vitro. *BMC Complementary and Alternative Medicine,* 15.

EYERS, P. A., KEESHAN, K. & KANNAN, N. 2017. Tribbles in the 21st Century: The Evolving Roles of Tribbles Pseudokinases in Biology and Disease. *Trends in Cell Biology,* 27**,** 284-298.

FANG, J. Y. & RICHARDSON, B. C. 2005. The MAPK signalling pathways and colorectal cancer. *Lancet Oncology,* 6**,** 322-327.

FANTOZZI, A. & CHRISTOFORI, G. 2006. Mouse models of breast cancer metastasis. *Breast Cancer Research,* 8.

FENG, Y., DAI, X., LI, X., WANG, H., LIU, J., ZHANG, J., DU, Y. & XIA, L. 2012. EGF signalling pathway regulates colon cancer stem cell proliferation and apoptosis. *Cell Proliferation,* 45**,** 413-419.

FENG, Y., SPEZIA, M., HUANG, S., YUAN, C., ZENG, Z., ZHANG, L., JI, X., LIU, W., HUANG, B., LUO, W., LIU, B., LEI, Y., DU, S., VUPPALAPATI, A., LUU, H. H., HAYDON, R. C., HE, T. C. & REN, G. 2018. Breast cancer development and progression: Risk factors, cancer stem cells, signaling pathways, genomics, and molecular pathogenesis. *Genes Dis,* 5**,** 77-106.

FERRANTE, C. J., PINHAL-ENFIELD, G., ELSON, G., CRONSTEIN, B. N., HASKO, G., OUTRAM, S. & LEIBOVICH, S. J. 2013. The Adenosine-Dependent Angiogenic

Switch of Macrophages to an M2-Like Phenotype is Independent of Interleukin-4 Receptor Alpha (IL-4R alpha) Signaling. *Inflammation,* 36**,** 921-931.

FITZMAURICE, C., COLLABORATION, G. B. D. C., ALLEN, C., BARBER, R. M., BARREGARD, L., BHUTTA, Z. A., BRENNER, H., DICKER, D. J., CHIMED-ORCHIR, O., DANDONA, R., DANDONA, L., FLEMING, T., FOROUZANFAR, M. H., HANCOCK, J., HAY, R. J., HUNTER-MERRILL, R., HUYNH, C., HOSGOOD, H. D., JOHNSON, C. O., JONAS, J. B., KHUBCHANDANI, J., KUMAR, G. A., KUTZ, M., LAN, Q., LARSON, H. J., LIANG, X., LIM, S. S., LOPEZ, A. D., MACINTYRE, M. F., MARCZAK, L., MARQUEZ, N., MOKDAD, A. H., PINHO, C., POURMALEK, F., SALOMON, J. A., SANABRIA, J. R., SANDAR, L., SARTORIUS, B., SCHWARTZ, S. M., SHACKELFORD, K. A., SHIBUYA, K., STANAWAY, J., STEINER, C., SUN, J., TAKAHASHI, K., VOLLSET, S. E., VOS, T., WAGNER, J. A., WANG, H., WESTERMAN, R., ZEEB, H., ZOECKLER, L., ABD-ALLAH, F., AHMED, M. B., ALABED, S., ALAM, N. K., ALDHAHRI, S. F., ALEM, G., ALEMAYOHU, M. A., ALI, R., AL-RADDADI, R., AMARE, A., AMOAKO, Y., ARTAMAN, A., ASAYESH, H., ATNAFU, N., AWASTHI, A., SALEEM, H. B., BARAC, A., BEDI, N., BENSENOR, I., BERHANE, A., BEMABE, E., BETSU, B., BINAGWAHO, A., BONEYA, D., CAMPOS-NONATO, I., CASTANEDA-ORJUELA, C., CATALA-LOPEZ, F., CHIANG, P., CHIBUEZE, C., CHITHEER, A., CHOI, J.-Y., COWIE, B., DAMTEW, S., DAS NEVES, J., DEY, S., DHARMARATNE, S., DHILLON, P., DING, E., DRISCOLL, T., EKWUEME, D., ENDRIES, A. Y., FARVID, M., FARZADFAR, F., FERNANDES, J., FISCHER, F., GHIWOT, T. T., GEBRU, A., GOPALANI, S., et al. 2017. Global, Regional, and National Cancer Incidence,

Mortality, Years of Life Lost, Years Lived With Disability, and Disability-Adjusted Life-years for 32 Cancer Groups, 1990 to 2015 A Systematic Analysis for the Global Burden of Disease Study. *Jama Oncology,* 3**,** 524-548.

FRAGOMENI, S. M., SCIALLIS, A. & JERUSS, J. S. 2018. Molecular Subtypes and Local-Regional Control of Breast Cancer. *Surg Oncol Clin N Am,* 27**,** 95-120.

FRANKLIN, R. A., LIAO, W., SARKAR, A., KIM, M. V., BIVONA, M. R., LIU, K., PAMER, E. G. & LI, M. O. 2014. The cellular and molecular origin of tumor-associated macrophages. *Science,* 344**,** 921-925.

GALLI, S. J., BORREGAARD, N. & WYNN, T. A. 2011. Phenotypic and functional plasticity of cells of innate immunity: macrophages, mast cells and neutrophils. *Nature Immunology,* 12**,** 1035-1044.

GAO, J., AKSOY, B. A., DOGRUSOZ, U., DRESDNER, G., GROSS, B., SUMER, S. O., SUN, Y., JACOBSEN, A., SINHA, R., LARSSON, E., CERAMI, E., SANDER, C. & SCHULTZ, N. 2013. Integrative analysis of complex cancer genomics and clinical profiles using the cBioPortal. *Sci Signal,* 6**,** pl1.

GENDELMAN, R., XING, H., MIRZOEVA, O. K., SARDE, P., CURTIS, C., FEILER, H. S., MCDONAGH, P., GRAY, J. W., KHALIL, I. & KORN, W. M. 2017. Bayesian Network Inference Modeling Identifies TRIB1 as a Novel Regulator of Cell-Cycle Progression and Survival in Cancer Cells. *Cancer Research,* 77**,** 1575-1585.

GENSEL, J. C. & ZHANG, B. 2015. Macrophage activation and its role in repair and pathology after spinal cord injury. *Brain Research,* 1619**,** 1-11.

GHOSH, A., SARKAR, S., BANERJEE, S., BEHBOD, F., TAWFIK, O., MCGREGOR, D., GRAFF, S. & BANERJEE, S. K. 2018. MIND model for triple-negative breast cancer

in syngeneic mice for quick and sequential progression analysis of lung metastasis. *PLOS ONE,* 13**,** e0198143.

GINHOUX, F. & GUILLIAMS, M. 2016. Tissue-Resident Macrophage Ontogeny and Homeostasis. *Immunity,* 44**,** 439-449.

GONCHAROV, N. V., NADEEV, A. D., JENKINS, R. O. & AVDONIN, P. V. 2017. Markers and Biomarkers of Endothelium: When Something Is Rotten in the State. *Oxid Med Cell Longev,* 2017**,** 9759735.

GONG, Z., MA, J., SU, H., GUO, T., CAI, H., CHEN, Q., ZHAO, X., QI, J. & DU, J. 2018. Interleukin-1 receptor antagonist inhibits angiogenesis in gastric cancer. *International Journal of Clinical Oncology,* 23**,** 659-670.

GORDON, S. & MARTINEZ, F. O. 2010. Alternative Activation of Macrophages: Mechanism and Functions. *Immunity,* 32**,** 593-604.

GRIVENNIKOV, S., KARIN, E., TERZIC, J., MUCIDA, D., YU, G. Y., VALLABHAPURAPU, S., SCHELLER, J., ROSE-JOHN, S., CHEROUTRE, H., ECKMANN, L. & KARIN, M. 2009. IL-6 and Stat3 Are Required for Survival of Intestinal Epithelial Cells and Development of Colitis-Associated Cancer. *Cancer Cell,* 15**,** 103-113.

GUILLIAMS, M., BRUHNS, P., SAEYS, Y., HAMMAD, H. & LAMBRECHT, B. N. 2014. The function of Fc gamma receptors in dendritic cells and macrophages. *Nature Reviews Immunology,* 14**,** 94-108.

GUILLIAMS, M., MILDNER, A. & YONA, S. 2018. Developmental and Functional Heterogeneity of Monocytes. *Immunity,* 49**,** 595-613.

GUO, Q., JIN, Z., YUAN, Y., LIU, R., XU, T., WEI, H., XU, X., HE, S., CHEN, S., SHI, Z., HOU, W. & HUA, B. 2016. New Mechanisms of Tumor-Associated Macrophages on

Promoting Tumor Progression: Recent Research Advances and Potential Targets for Tumor Immunotherapy. *Journal of immunology research,* 2016**,** 9720912-9720912.

GUO, X. C., ZHAO, Y., YAN, H., YANG, Y. C., SHEN, S. Y., DAI, X. M., JI, X. Y., JI, F. B., GONG, X. G., LI, L., BAI, X. L., FENG, X. H., LIANG, T. B., JI, J. F., CHEN, L., WANG, H. Y. & ZHAO, B. 2017. Single tumor-initiating cells evade immune clearance by recruiting type II macrophages. *Genes & Development,* 31**,** 247-259.

GUO, Y. J., PAN, W. W., LIU, S. B., SHEN, Z. F., XU, Y. & HU, L. L. 2020. ERK/MAPK signalling pathway and tumorigenesis (Review). *Experimental and Therapeutic Medicine.*

HARBECK, N. & GNANT, M. 2017. Breast cancer. *The Lancet,* 389**,** 1134-1150.

HARBECK, N., PENAULT-LLORCA, F., CORTES, J., GNANT, M., HOUSSAMI, N., POORTMANS, P., RUDDY, K., TSANG, J. & CARDOSO, F. 2019. Breast cancer. *Nature Reviews Disease Primers,* 5.

HAYASHI, T., MOMOTA, M., KURODA, E., KUSAKABE, T., KOBARI, S., MAKISAKA, K., OHNO, Y., SUZUKI, Y., NAKAGAWA, F., LEE, M. S. J., COBAN, C., ONODERA, R., HIGASHI, T., MOTOYAMA, K., ISHII, K. J. & ARIMA, H. 2018. DAMP-Inducing Adjuvant and PAMP Adjuvants Parallelly Enhance Protective Type-2 and Type-1 Immune Responses to Influenza Split Vaccination. *Frontiers in Immunology,* 9.

HEINIG, M., PETRETTO, E., WALLACE, C., BOTTOLO, L., ROTIVAL, M., LU, H., LI, Y., SARWAR, R., LANGLEY, S. R., BAUERFEIND, A., HUMMEL, O., LEE, Y. A., PASKAS, S., RINTISCH, C., SAAR, K., COOPER, J., BUCHAN, R., GRAY, E. E., CYSTER, J. G., CARDIOGENICS, C., ERDMANN, J., HENGSTENBERG, C., MAOUCHE, S., OUWEHAND, W. H., RICE, C. M., SAMANI, N. J.,

SCHUNKERT, H., GOODALL, A. H., SCHULZ, H., ROIDER, H. G., VINGRON, M., BLANKENBERG, S., MUNZEL, T., ZELLER, T., SZYMCZAK, S., ZIEGLER, A., TIRET, L., SMYTH, D. J., PRAVENEC, M., AITMAN, T. J., CAMBIEN, F., CLAYTON, D., TODD, J. A., HUBNER, N. & COOK, S. A. 2010. A trans-acting locus regulates an anti-viral expression network and type 1 diabetes risk. *Nature,* 467**,** 460-4.

HENZE, A.-T. & MAZZONE, M. 2016. The impact of hypoxia on tumor-associated macrophages. *Journal of Clinical Investigation,* 126**,** 3672-3679.

HETTINGER, J., RICHARDS, D. M., HANSSON, J., BARRA, M. M., JOSCHKO, A.-C., KRIJGSVELD, J. & FEUERER, M. 2013. Origin of monocytes and macrophages in a committed progenitor. *Nature Immunology,* 14**,** 821-+.

HILL, R., MADUREIRA, P. A., FERREIRA, B., BAPTISTA, I., MACHADO, S., COLAÇO, L., DOS SANTOS, M., LIU, N., DOPAZO, A., UGUREL, S., ADRIENN, A., KISS-TOTH, E., ISBILEN, M., GURE, A. O. & LINK, W. 2017. TRIB2 confers resistance to anti-cancer therapy by activating the serine/threonine protein kinase AKT. *Nature Communications,* 8**,** 14687.

HOLEN, I., SPEIRS, V., MORRISSEY, B. & BLYTH, K. 2017. In vivomodels in breast cancer research: progress, challenges and future directions. *Disease Models & Mechanisms,* 10**,** 359-371.

HORST, D., CHEN, J., MORIKAWA, T., OGINO, S., KIRCHNER, T. & SHIVDASANI, R. A. 2012. Differential WNT Activity in Colorectal Cancer Confers Limited Tumorigenic Potential and Is Regulated by MAPK Signaling. *Cancer Research,* 72**,** 1547-1556.

HOU, Z., GUO, K., SUN, X., HU, F., CHEN, Q., LUO, X., WANG, G., HU, J. & SUN, L. 2018. TRIB2 functions as novel oncogene in colorectal cancer by blocking cellular senescence through AP4/p21 signaling. *Molecular Cancer,* 17.

HUA, F., MU, R., LIU, J., XUE, J., WANG, Z., LIN, H., YANG, H., CHEN, X. & HU, Z. 2011. TRB3 interacts with SMAD3 promoting tumor cell migration and invasion. *Journal of Cell Science,* 124**,** 3235-3246.

HUANG, C.-Y., ZHOU, Q.-Y., HU, Y., WEN, Y., QIU, Z.-W., LIANG, M.-G., MO, J.-L., XU, J.-H., SUN, C., LIU, F.-B. & CHEN, X.-L. 2017. Hepatocyte growth factor is a prognostic marker in patients with colorectal cancer: a meta-analysis. *Oncotarget,* 8**,** 23459-23469.

HUGHES, R., QIAN, B.-Z., ROWAN, C., MUTHANA, M., KEKLIKOGLOU, I., OLSON, O. C., TAZZYMAN, S., DANSON, S., ADDISON, C., CLEMONS, M., GONZALEZ-ANGULO, A. M., JOYCE, J. A., DE PALMA, M., POLLARD, J. W. & LEWIS, C. E. 2015a. Perivascular M2 Macrophages Stimulate Tumor Relapse after Chemotherapy. *Cancer Research,* 75**,** 3479-3491.

HUGHES, R., QIAN, B. Z., ROWAN, C., MUTHANA, M., KEKLIKOGLOU, I., OLSON, O. C., TAZZYMAN, S., DANSON, S., ADDISON, C., CLEMONS, M., GONZALEZ-ANGULO, A. M., JOYCE, J. A., DE PALMA, M., POLLARD, J. W. & LEWIS, C. E. 2015b. Perivascular M2 Macrophages Stimulate Tumor Relapse after Chemotherapy. *Cancer Res,* 75**,** 3479-91.

HULTGREN, E. M., PATRICK, M. E., EVANS, R. L., STOOS, C. T. & EGLAND, K. A. 2017. SUSD2 promotes tumor-associated macrophage recruitment by increasing levels of MCP-1 in breast cancer. *Plos One,* 12.

HUME, D. A., PERRY, V. H. & GORDON, S. 1984. The mononuclear phagocyte system of the mouse defined by immunohistochemical localisation of antigen F4/80: macrophages associated with epithelia. *Anat Rec,* 210**,** 503-12.

HUSZNO, J. & GRZYBOWSKA, E. 2018. mutations and SNPs as prognostic and predictive factors in patients with breast cancer. *Oncol Lett,* 16**,** 34-40.

IQBAL, S. & KUMAR, A. 2015. Characterization of In vitro Generated Human Polarized Macrophages. *J Clin Cell Immunol,* 6:380.

ITALIANI, P. & BORASCHI, D. 2014. From monocytes to M1/M2 macrophages: phenotypical vs. functional differentiation. *Frontiers in Immunology,* 5.

IWAMOTO, S., BOONVISUT, S., MAKISHIMA, S., ISHIZUKA, Y., WATANABE, K. & NAKAYAMA, K. 2015. The role of TRIB1 in lipid metabolism; from genetics to pathways. *Biochemical Society Transactions,* 43**,** 1063-1068.

JACKSON, H. W., FISCHER, J. R., ZANOTELLI, V. R. T., ALI, H. R., MECHERA, R., SOYSAL, S. D., MOCH, H., MUENST, S., VARGA, Z., WEBER, W. P. & BODENMILLER, B. 2020. The single-cell pathology landscape of breast cancer. *Nature,* 578**,** 615-620.

JEONG, H., KIM, S., HONG, B. J., LEE, C. J., KIM, Y. E., BOK, S., OH, J. M., GWAK, S. H., YOO, M. Y., LEE, M. S., CHUNG, S. J., DEFRENE, J., TESSIER, P., PELLETIER, M., JEON, H., ROH, T. Y., KIM, B., KIM, K. H., JU, J. H., KIM, S., LEE, Y. J., KIM, D. W., KIM, I. H., KIM, H. J., PARK, J. W., LEE, Y. S., LEE, J. S., CHEON, G. J., WEISSMAN, I. L., CHUNG, D. H., JEON, Y. K. & AHN, G. O. 2019. Tumor-Associated Macrophages Enhance Tumor Hypoxia and Aerobic Glycolysis. *Cancer Res,* 79**,** 795-806.

JETTEN, N., VERBRUGGEN, S., GIJBELS, M. J., POST, M. J., DE WINTHER, M. P. J. & DONNERS, M. M. P. C. 2014. Anti-inflammatory M2, but not pro-inflammatory M1 macrophages promote angiogenesis in vivo. *Angiogenesis,* 17**,** 109-118.

JOHNSTON, J. M. 2017. *Regulation of macrophage polarisation by TRIB1 and its consequences in metabolic homeostasis and atherosclerosis.* PhD, University of Sheffield.

JOHNSTON, J. M., ANGYAL, A., BAUER, R. C., HAMBY, S., SUVARNA, S. K., BAIDZAJEVAS, K., HEGEDUS, Z., DEAR, T. N., TURNER, M., CARDIOGENICS, C., WILSON, H. L., GOODALL, A. H., RADER, D. J., SHOULDERS, C. C., FRANCIS, S. E. & KISS-TOTH, E. 2019a. Myeloid Tribbles 1 induces early atherosclerosis via enhanced foam cell expansion. *Sci Adv,* 5**,** eaax9183.

JOHNSTON, J. M., ANGYAL, A., BAUER, R. C., HAMBY, S., SUVARNA, S. K., BAIDŽAJEVAS, K., HEGEDUS, Z., DEAR, T. N., TURNER, M., WILSON, H. L., GOODALL, A. H., RADER, D. J., SHOULDERS, C. C., FRANCIS, S. E., KISS-TOTH, E. & CONSORTIUM, C. 2019b. Myeloid Tribbles 1 induces early atherosclerosis via enhanced foam cell expansion. *Sci Adv,* 5**,** eaax9183.

JORDAN, K. R., KAPOOR, P., SPONGBERG, E., TOBIN, R. P., GAO, D., BORGES, V. F. & MCCARTER, M. D. 2017. Immunosuppressive myeloid-derived suppressor cells are increased in splenocytes from cancer patients. *Cancer Immunology Immunotherapy,* 66**,** 503-513.

KANG, M. J., KIM, J. E., PARK, J. W., CHOI, H. J., BAE, S. J., KIM, K. S., JUNG, Y.-S., CHO, J.-Y., HWANG, D. Y. & SONG, H. K. 2019. Comparison of responsiveness to cancer development and anti-cancer drug in three different C57BL/6N stocks. *Laboratory Animal Research,* 35.

KARNEVI, E., ANDERSSON, R. & ROSENDAHL, A. H. 2014. Tumour-educated macrophages display a mixed polarisation and enhance pancreatic cancer cell invasion. *Immunology and Cell Biology,* 92**,** 543-552.

KAZI, M., TRIVEDI, T., KOBAWALA, T. & GHOSH, N. 2016. The Potential of Wnt Signaling Pathway in Cancer: A Focus on Breast Cancer. *Cancer Translational Medicine,* 2**,** 55-60.

KE, X., ZHANG, S., WU, M., LOU, J., ZHANG, J., XU, T., HUANG, L., HUANG, P., WANG, F. & PAN, S. 2016. Tumor-associated macrophages promote invasion via Toll-like receptors signaling in patients with ovarian cancer. *International Immunopharmacology,* 40**,** 184-195.

KECHAGIOGLOU, P., PAPI, R. M., PROVATOPOULOU, X., KALOGERA, E., PAPADIMITRIOU, E., GRIGOROPOULOS, P., NONNI, A., ZOGRAFOS, G., KYRIAKIDIS, D. A. & GOUNARIS, A. 2014. Tumor suppressor PTEN in breast cancer: heterozygosity, mutations and protein expression. *Anticancer Res,* 34**,** 1387-400.

KEESHAN, K., VIEUGUE, P., CHAUDHURY, S., RISHI, L., GAILLARD, C., LIANG, L., GARCIA, E., NAKAMURA, T., OMIDVAR, N. & KOGAN, S. C. 2016. Co-operative leukemogenesis in acute myeloid leukemia and acute promyelocytic leukemia reveals C/EBP alpha as a common target of TRIB1 and PML/RARA. *Haematologica,* 101**,** 1228-1236.

KIM, E. K. & CHOI, E.-J. 2010. Pathological roles of MAPK signaling pathways in human diseases. *Biochimica Et Biophysica Acta-Molecular Basis of Disease,* 1802**,** 396-405.

KIM, J. & BAE, J.-S. 2016. Tumor-Associated Macrophages and Neutrophils in Tumor Microenvironment. *Mediators of Inflammation*.

KIRBY, A. C., RAYNES, J. G. & KAYE, P. M. 2006. CD11b regulates recruitment of alveolar macrophages but not pulmonary dendritic cells after pneumococcal challenge. *Journal of Infectious Diseases,* 193**,** 205-213.

KOH, T. J. & DIPIETRO, L. A. 2011. Inflammation and wound healing: the role of the macrophage. *Expert Reviews in Molecular Medicine,* 13.

LAPENNA, A., DE PALMA, M. & LEWIS, C. E. 2018. Perivascular macrophages in health and disease. *Nature Reviews Immunology,* 18**,** 689-702.

LAWRENCE, M. C., JIVAN, A., SHAO, C., DUAN, L., GOAD, D., ZAGANJOR, E., OSBORNE, J., MCGLYNN, K., STIPPEC, S., EARNEST, S., CHEN, W. & COBB, M. H. 2008. The roles of MAPKs in disease. *Cell Research,* 18**,** 436-442.

LE NAOUR, A., ROSSARY, A. & VASSON, M. P. 2020. EO771, is it a well-characterized cell line for mouse mammary cancer model? Limit and uncertainty. *Cancer Medicine,* 9**,** 8074-8085.

LEE, B., QIAO, L., LU, M., YOO, H. S., CHEUNG, W., MAK, R., SCHAACK, J., FENG, G.-S., CHI, N.-W., OLEFSKY, J. M. & SHAO, J. 2014. C/EBP alpha regulates macrophage activation and systemic metabolism. *American Journal of Physiology-Endocrinology and Metabolism,* 306**,** E1144-E1154.

LI, H., JIANG, T., LI, M.-Q., ZHENG, X.-L. & ZHAO, G.-J. 2018. Transcriptional Regulation of Macrophages Polarization by MicroRNAs. *Frontiers in Immunology,* 9.

LI, S., SHEN, Y., WANG, M., YANG, J., LV, M., LI, P. & CHEN, Z. 2017. Loss of PTEN expression in breast cancer: association with clinicopathological characteristics and prognosis. *Oncotarget,* 8**,** 32043-32054.

LIN, H. H., FAUNCE, D. E., STACEY, M., TERAJEWICZ, A., NAKAMURA, T., ZHANG-HOOVER, J., KERLEY, M., MUCENSKI, M. L., GORDON, S. & STEIN-

STREILEIN, J. 2005. The macrophage F4/80 receptor is required for the induction of antigen-specific efferent regulatory T cells in peripheral tolerance. *Journal of Experimental Medicine,* 201**,** 1615-1625.

LIN, L., CHEN, Y.-S., YAO, Y.-D., CHEN, J.-Q., CHEN, J.-N., HUANG, S.-Y., ZENG, Y.-J., YAO, H.-R., ZENG, S.-H., FU, Y.-S. & SONG, E.-W. 2015. CCL18 from tumor-associated macrophages promotes angiogenesis in breast cancer. *Oncotarget,* 6**,** 34758-34773.

LIN, Y., XU, J. & LAN, H. 2019. Tumor-associated macrophages in tumor metastasis: biological roles and clinical therapeutic applications. *Journal of Hematology & Oncology,* 12.

LIN, Z.-Y., HUANG, Y.-Q., ZHANG, Y.-Q., HAN, Z.-D., HE, H.-C., LING, X.-H., FU, X., DAI, Q.-S., CAI, C., CHEN, J.-H., LIANG, Y.-X., JIANG, F.-N., ZHONG, W.-D., WANG, F. & WU, C.-L. 2014. MicroRNA-224 inhibits progression of human prostate cancer by downregulating TRIB1. *International Journal of Cancer,* 135**,** 541-550.

LINDSTEN, T., HEDBRANT, A., RAMBERG, A., WIJKANDER, J., SOLTERBECK, A., ERIKSSON, M., DELBRO, D. & ERLANDSSON, A. 2017. Effect of macrophages on breast cancer cell proliferation, and on expression of hormone receptors, uPAR and HER-2. *Int J Oncol,* 51**,** 104-114.

LITTLE, A. C., PATHANJELI, P., WU, Z., BAO, L., GOO, L. E., YATES, J. A., OLIVER, C. R., SOELLNER, M. B. & MERAJVER, S. D. 2019. IL-4/IL-13 Stimulated Macrophages Enhance Breast Cancer Invasion Via Rho-GTPase Regulation of Synergistic VEGF/CCL-18 Signaling. *Front Oncol,* 9**,** 456.

LIU, T., HAN, C., WANG, S., FANG, P., MA, Z., XU, L. & YIN, R. 2019a. Cancer-associated fibroblasts: an emerging target of anti-cancer immunotherapy. *Journal of Hematology & Oncology,* 12.

LIU, Y.-C., ZOU, X.-B., CHAI, Y.-F. & YAO, Y.-M. 2014. Macrophage Polarization in Inflammatory Diseases. *International Journal of Biological Sciences,* 10**,** 520-529.

LIU, Y.-H., TAN, K. A. L., MORRISON, I. W., LAMB, J. R. & ARGYLE, D. J. 2013. Macrophage migration is controlled by Tribbles 1 through the interaction between C/EBP beta and TNF-alpha. *Veterinary Immunology and Immunopathology,* 155**,** 67-75.

LIU, Z. Z., HAN, Z. D., LIANG, Y. K., CHEN, J. X., WAN, S., ZHUO, Y. J., CAI, Z. D., DENG, Y. L., LIN, Z. Y., MO, R. J., HE, H. C. & ZHONG, W. D. 2019b. TRIB1 induces macrophages to M2 phenotype by inhibiting IKB-zeta in prostate cancer. *Cell Signal,* 59**,** 152-162.

LONG, M. E., EDDY, W. E., GONG, K.-Q., LOVELACE-MACON, L. L., MCMAHAN, R. S., CHARRON, J., LILES, W. C. & MANICONE, A. M. 2017. MEK1/2 Inhibition Promotes Macrophage Reparative Properties. *Journal of Immunology,* 198**,** 862-872.

LU, D., NI, Z., LIU, X., FENG, S., DONG, X., SHI, X., ZHAI, J., MAI, S., JIANG, J., WANG, Z., WU, H. & CAI, K. 2019. Beyond T Cells: Understanding the Role of PD-1/PD-L1 in Tumor-Associated Macrophages. *Journal of Immunology Research,* 2019**,** 1-7.

LUIKING, Y. C., ENGELEN, M. P. & DEUTZ, N. E. 2010. Regulation of nitric oxide production in health and disease. *Curr Opin Clin Nutr Metab Care,* 13**,** 97-104.

LV, R., BAO, Q. & LI, Y. 2017. Regulation of M1-type and M2-type macrophage polarization in RAW264.7 cells by Galectin-9. *Molecular Medicine Reports,* 16**,** 9111-9119.

MA, J., GAO, S., XIE, X., SUN, E., ZHANG, M., ZHOU, Q. & LU, C. 2017. SPARC inhibits breast cancer bone metastasis and may be a clinical therapeutic target. *Oncol Lett,* 14**,** 5876-5882.

MA, J., LIU, L., CHE, G., YU, N., DAI, F. & YOU, Z. 2010. The M1 form of tumor-associated macrophages in non-small cell lung cancer is positively associated with survival time. *Bmc Cancer,* 10.

MACMICKING, J., XIE, Q. W. & NATHAN, C. 1997. Nitric oxide and macrophage function. *Annu Rev Immunol,* 15**,** 323-50.

MADSEN, D. H., LEONARD, D., MASEDUNSKAS, A., MOYER, A., JURGENSEN, H. J., PETERS, D. E., AMORNPHIMOLTHAM, P., SELVARAJ, A., YAMADA, S. S., BRENNER, D. A., BURGDORF, S., ENGELHOLM, L. H., BEHRENDT, N., HOLMBECK, K., WEIGERT, R. & BUGGE, T. H. 2013. M2-like macrophages are responsible for collagen degradation through a mannose receptor-mediated pathway. *J Cell Biol,* 202**,** 951-66.

MAEDA, H. & KHATAMI, M. 2018. Analyses of repeated failures in cancer therapy for solid tumors: poor tumor-selective drug delivery, low therapeutic efficacy and unsustainable costs. *Clinical and Translational Medicine,* 7**,** 11.

MANNING, H. C., BUCK, J. R. & COOK, R. S. 2016. Mouse Models of Breast Cancer: Platforms for Discovering Precision Imaging Diagnostics and Future Cancer Medicine. *Journal of Nuclear Medicine,* 57**,** 60S-68S.

MANTOVANI, A. & LOCATI, M. 2016. Macrophage Metabolism Shapes Angiogenesis in Tumors. *Cell Metabolism,* 24**,** 653-654.

MANTOVANI, A., MARCHESI, F., MALESCI, A., LAGHI, L. & ALLAVENA, P. 2017. Tumour-associated macrophages as treatment targets in oncology. *Nature Reviews Clinical Oncology,* 14**,** 399-416.

MARTINEZ, F. O. & GORDON, S. 2014. The M1 and M2 paradigm of macrophage activation: time for reassessment. *F1000Prime Reports,* 6.

MARTINEZ, F. O., GORDON, S., LOCATI, M. & MANTOVANI, A. 2006. Transcriptional profiling of the human monocyte-to-macrophage differentiation and polarization: New molecules and patterns of gene expression. *Journal of Immunology,* 177**,** 7303-7311.

MASHIMA, T., SOMA-NAGAE, T., MIGITA, T., KINOSHITA, R., IWAMOTO, A., YUASA, T., YONESE, J., ISHIKAWAE, Y. & SEIMIYA, H. 2014. TRIB1 Supports Prostate Tumorigenesis and Tumor-Propagating Cell Survival by Regulation of Endoplasmic Reticulum Chaperone Expression. *Cancer Research,* 74**,** 4888-4897.

MCCANN, K. E. & HURVITZ, S. A. 2018. Advances in the use of PARP inhibitor therapy for breast cancer. *Drugs in Context,* 7**,** 1-30.

MCCLEARY-WHEELER, A. L., MCWILLIAMS, R. & FERNANDEZ-ZAPICO, M. E. 2012. Aberrant signaling pathways in pancreatic cancer: A two compartment view. *Molecular Carcinogenesis,* 51**,** 25-39.

MELLMAN, I., KOCH, T., HEALEY, G., HUNZIKER, W., LEWIS, V., PLUTNER, H., MIETTINEN, H., VAUX, D., MOORE, K. & STUART, S. 1988. Structure and function of Fc receptors on macrophages and lymphocytes. *Journal of cell science. Supplement,* 9**,** 45-65.

MILLS, C. D., KINCAID, K., ALT, J. M., HEILMAN, M. J. & HILL, A. M. 2000. M-1/M-2 macrophages and the Th1/Th2 paradigm. *Journal of Immunology,* 164**,** 6166-6173.

MIYAJIMA, C., INOUE, Y. & HAYASHI, H. 2015. Pseudokinase tribbles 1 (TRB1) negatively regulates tumor-suppressor activity of p53 through p53 deacetylation. *Biol Pharm Bull,* 38**,** 618-24.

MORALES, L., NEVEN, P. & PARIDAENS, R. 2005. Choosing between an aromatase inhibitor and tamoxifen in the adjuvant setting. *Current Opinion in Oncology,* 17**,** 559-565.

MORENO-ASPITIA, A. & PEREZ, E. A. 2009. Treatment options for breast cancer resistant to anthracycline and taxane. *Mayo Clinic Proceedings.,* 84**,** 533-545.

MOYA, L., LAI, J., HOFFMAN, A., SRINIVASAN, S., PANCHADSARAM, J., CHAMBERS, S., CLEMENTS, J. A., BATRA, J. & AUSTRALIAN PROSTATE CANCER, B. 2018. Association Analysis of a Microsatellite Repeat in the TRIB1 Gene With Prostate Cancer Risk, Aggressiveness and Survival. *Front Genet,* 9**,** 428.

MURPHY, J. M., NAKATANI, Y., JAMIESON, S. A., DAI, W., LUCET, I. S. & MACE, P. D. 2015. Molecular Mechanism of CCAAT-Enhancer Binding Protein Recruitment by the TRIB1 Pseudokinase. *Structure,* 23**,** 2111-2121.

MURRAY, P. J., ALLEN, J. E., BISWAS, S. K., FISHER, E. A., GILROY, D. W., GOERDT, S., GORDON, S., HAMILTON, J. A., IVASHKIV, L. B., LAWRENCE, T., LOCATI, M., MANTOVANI, A., MARTINEZ, F. O., MEGE, J.-L., MOSSER, D. M., NATOLI, G., SAEIJ, J. P., SCHULTZE, J. L., SHIREY, K. A., SICA, A., SUTTLES, J., UDALOVA, I., VAN GINDERACHTER, J. A., VOGEL, S. N. & WYNN, T. A. 2014. Macrophage Activation and Polarization: Nomenclature and Experimental Guidelines. *Immunity,* 41**,** 14-20.

MUZ, B., DE LA PUENTE, P., AZAB, F. & AZAB, A. K. 2015. The role of hypoxia in cancer progression, angiogenesis, metastasis, and resistance to therapy. *Hypoxia***,** 83.

NEWTON, K. & DIXIT, V. M. 2012. Signaling in Innate Immunity and Inflammation. *Cold Spring Harbor Perspectives in Biology,* 4.

NIE, W., YU, T., SANG, Y. X. & GAO, X. 2017. Tumor-promoting effect of IL-23 in mammary cancer mediated by infiltration of M2 macrophages and neutrophils in tumor microenvironment. *Biochemical and Biophysical Research Communications,* 482**,** 1400-1406.

NORIEGA-GUERRA, H. & FREITAS, V. 2018. Extracellular Matrix Influencing HGF/c-MET Signaling Pathway: Impact on Cancer Progression. *International Journal of Molecular Sciences,* 19**,** 3300.

NOVAK, M. L. & KOH, T. J. 2013. Macrophage phenotypes during tissue repair. *Journal of Leukocyte Biology,* 93**,** 875-881.

NOY, R. & POLLARD, J. W. 2014. Tumor-Associated Macrophages: From Mechanisms to Therapy. *Immunity,* 41**,** 49-61.

OBEID, E., NANDA, R., FU, Y.-X. & OLOPADE, O. I. 2013. The role of tumor-associated macrophages in breast cancer progression. *International Journal of Oncology,* 43**,** 5-12.

OHAMA, H., ASAI, A., ITO, I., SUZUKI, S., KOBAYASHI, M., HIGUCHI, K. & SUZUKI, F. 2015. M2b Macrophage Elimination and Improved Resistance of Mice with Chronic Alcohol Consumption to Opportunistic Infections. *American Journal of Pathology,* 185**,** 420-431.

OLINGY, C. E., SAN EMETERIO, C. L., OGLE, M. E., KRIEGER, J. R., BRUCE, A. C., PFAU, D. D., JORDAN, B. T., PEIRCE, S. M. & BOTCHWEY, E. A. 2017. Non-

classical monocytes are biased progenitors of wound healing macrophages during soft tissue injury. *Scientific Reports,* 7.

ORECCHIONI, M., GHOSHEH, Y., PRAMOD, A. B. & LEY, K. 2019. Macrophage Polarization: Different Gene Signatures in M1(LPS+) vs. Classically and M2(LPS-) vs. Alternatively Activated Macrophages. *Front Immunol,* 10**,** 1084.

PANDY, J. G. P., BALOLONG-GARCIA, J. C., CRUZ-ORDINARIO, M. V. B. & QUE, F. V. F. 2019. Triple negative breast cancer and platinum-based systemic treatment: a meta-analysis and systematic review. *BMC Cancer,* 19.

PARK, M. K., LEE, C. H. & LEE, H. 2018. Mouse models of breast cancer in preclinical research. *Laboratory Animal Research,* 34**,** 160.

PARK, S. J., YOON, B. H., KIM, S. K. & KIM, S. Y. 2019. GENT2: an updated gene expression database for normal and tumor tissues. *BMC Med Genomics,* 12**,** 101.

PASTOREKOVA, S. & GILLIES, R. J. 2019. The role of carbonic anhydrase IX in cancer development: links to hypoxia, acidosis, and beyond. *Cancer Metastasis Rev,* 38**,** 65-77.

PAUL, S., CHHATAR, S., MISHRA, A. & LAL, G. 2019. Natural killer T cell activation increases iNOS+CD206- M1 macrophage and controls the growth of solid tumor. *Journal for ImmunoTherapy of Cancer,* 7.

PFEFFER, R. M. 2018. Radiotherapy for Breast Cancer: Curing the Cancer While Protecting the Heart. *Isr Med Assoc J,* 20**,** 582-583.

PINTO, M. L., RIOS, E., DURAES, C., RIBEIRO, R., MACHADO, J. C., MANTOVANI, A., BARBOSA, M. A., CARNEIRO, F. & OLIVEIRA, M. J. 2019. The Two Faces of Tumor-Associated Macrophages and Their Clinical Significance in Colorectal Cancer. *Front Immunol,* 10**,** 1875.

PONDÉ, N. F., ZARDAVAS, D. & PICCART, M. 2019. Progress in adjuvant systemic therapy for breast cancer. *Nature Reviews Clinical Oncology,* 16**,** 27-44.

POWELL, D. R. & HUTTENLOCHER, A. 2016. Neutrophils in the Tumor Microenvironment. *Trends in Immunology,* 37**,** 41-52.

PRIMA, V., KALIBEROVA, L. N., KALIBEROV, S., CURIEL, D. T. & KUSMARTSEV, S. 2017. COX2/mPGES1/PGE2 pathway regulates PD-L1 expression in tumor-associated macrophages and myeloid-derived suppressor cells. *Proceedings of the National Academy of Sciences,* 114**,** 1117-1122.

QUAIL, D. F. & JOYCE, J. A. 2013. Microenvironmental regulation of tumor progression and metastasis. *Nature Medicine,* 19**,** 1423-1437.

QUARANTA, V. & SCHMID, M. C. 2019. Macrophage-Mediated Subversion of Anti-Tumour Immunity. *Cells,* 8**,** 747.

QUATROMONI, J. G. & ERUSLANOV, E. 2012. Tumor-associated macrophages: function, phenotype, and link to prognosis in human lung cancer. *American Journal of Translational Research,* 4**,** 376-389.

RAHAT, M. A. & HEMMERLEIN, B. 2013. Macrophage-tumor cell interactions regulate the function of nitric oxide. *Frontiers in Physiology,* 4.

RHEE, I. 2016. Diverse macrophages polarization in tumor microenvironment. *Archives of Pharmacal Research,* 39**,** 1588-1596.

RIABOV, V., GUDIMA, A., WANG, N., MICKLEY, A., OREKHOV, A. & KZHYSHKOWSKA, J. 2014. Role of tumor assocaited macrophages in tumor angiogenesis and lymphangiogenesis. *Frontiers in Physiology,* 5.

RICHARDSON, E. T., SHUKLA, S., NAGY, N., BOOM, W. H., BECK, R. C., ZHOU, L., LANDRETH, G. E. & HARDING, C. V. 2015. ERK Signaling Is Essential for Macrophage Development. *Plos One,* 10.

RICHMOND, L. & KEESHAN, K. 2019. Pseudokinases: a tribble-edged sword. *The FEBS Journal*.

RICHMOND, L. & KEESHAN, K. 2020. Pseudokinases: a tribble-edged sword. *The FEBS Journal,* 287**,** 4170-4182.

ROBINSON, T. O. & SCHLUNS, K. S. 2017. The potential and promise of IL-15 in immuno-oncogenic therapies. *Immunol Lett,* 190**,** 159-168.

ROSZER, T. 2015a. Understanding the Mysterious M2 Macrophage through Activation Markers and Effector Mechanisms. *Mediators of Inflammation*.

ROSZER, T. 2015b. Understanding the Mysterious M2 Macrophage through Activation Markers and Effector Mechanisms. *Mediators Inflamm,* 2015**,** 816460.

ROTIVAL, M., ZELLER, T., WILD, P. S., MAOUCHE, S., SZYMCZAK, S., SCHILLERT, A., CASTAGNE, R., DEISEROTH, A., PROUST, C., BROCHETON, J., GODEFROY, T., PERRET, C., GERMAIN, M., ELEFTHERIADIS, M., SINNING, C. R., SCHNABEL, R. B., LUBOS, E., LACKNER, K. J., ROSSMANN, H., MUNZEL, T., RENDON, A., CARDIOGENICS, C., ERDMANN, J., DELOUKAS, P., HENGSTENBERG, C., DIEMERT, P., MONTALESCOT, G., OUWEHAND, W. H., SAMANI, N. J., SCHUNKERT, H., TREGOUET, D. A., ZIEGLER, A., GOODALL, A. H., CAMBIEN, F., TIRET, L. & BLANKENBERG, S. 2011. Integrating genome-wide genetic variations and monocyte expression data reveals trans-regulated gene modules in humans. *PLoS Genet,* 7**,** e1002367.

RUFFELL, B. & COUSSENS, L. M. 2015. Macrophages and Therapeutic Resistance in Cancer. *Cancer Cell,* 27**,** 462-472.

SAKAMOTO, K., SCHMIDT, J. W. & WAGNER, K.-U. 2015. Mouse Models of Breast Cancer. Springer New York.

SANMARCO, L. M., PONCE, N. E., VISCONTI, L. M., EBERHARDT, N., THEUMER, M. G., MINGUEZ, Á. R. & AOKI, M. P. 2017. IL-6 promotes M2 macrophage polarization by modulating purinergic signaling and regulates the lethal release of nitric oxide during Trypanosoma cruzi infection. *Biochimica et Biophysica Acta (BBA) - Molecular Basis of Disease,* 1863**,** 857-869.

SANTANA CARRERO, R. M., BECEREN-BRAUN, F., RIVAS, S. C., HEGDE, S. M., GANGADHARAN, A., PLOTE, D., PHAM, G., ANTHONY, S. M. & SCHLUNS, K. S. 2019. IL-15 is a component of the inflammatory milieu in the tumor microenvironment promoting antitumor responses. *Proceedings of the National Academy of Sciences,* 116**,** 599-608.

SATOH, T., KIDOYA, H., NAITO, H., YAMAMOTO, M., TAKEMURA, N., NAKAGAWA, K., YOSHIOKA, Y., MORII, E., TAKAKURA, N., TAKEUCHI, O. & AKIRA, S. 2013. Critical role of Trib1 in differentiation of tissue-resident M2-like macrophages. *Nature,* 495**,** 524-+.

SCHMID, M. C., KHAN, S. Q., KANEDA, M. M., PATHRIA, P., SHEPARD, R., LOUIS, T. L., ANAND, S., WOO, G., LEEM, C., FARIDI, M. H., GERAGHTY, T., RAJAGOPALAN, A., GUPTA, S., AHMED, M., VAZQUEZ-PADRON, R. I., CHERESH, D. A., GUPTA, V. & VARNER, J. A. 2018. Integrin CD11b activation drives anti-tumor innate immunity. *Nature Communications,* 9.

SCHUNKERT, H., KONIG, I. R., KATHIRESAN, S., REILLY, M. P., ASSIMES, T. L., HOLM, H., PREUSS, M., STEWART, A. F., BARBALIC, M., GIEGER, C., ABSHER, D., AHERRAHROU, Z., ALLAYEE, H., ALTSHULER, D., ANAND, S. S., ANDERSEN, K., ANDERSON, J. L., ARDISSINO, D., BALL, S. G., BALMFORTH, A. J., BARNES, T. A., BECKER, D. M., BECKER, L. C., BERGER, K., BIS, J. C., BOEKHOLDT, S. M., BOERWINKLE, E., BRAUND, P. S., BROWN, M. J., BURNETT, M. S., BUYSSCHAERT, I., CARDIOGENICS, CARLQUIST, J. F., CHEN, L., CICHON, S., CODD, V., DAVIES, R. W., DEDOUSSIS, G., DEHGHAN, A., DEMISSIE, S., DEVANEY, J. M., DIEMERT, P., DO, R., DOERING, A., EIFERT, S., MOKHTARI, N. E., ELLIS, S. G., ELOSUA, R., ENGERT, J. C., EPSTEIN, S. E., DE FAIRE, U., FISCHER, M., FOLSOM, A. R., FREYER, J., GIGANTE, B., GIRELLI, D., GRETARSDOTTIR, S., GUDNASON, V., GULCHER, J. R., HALPERIN, E., HAMMOND, N., HAZEN, S. L., HOFMAN, A., HORNE, B. D., ILLIG, T., IRIBARREN, C., JONES, G. T., JUKEMA, J. W., KAISER, M. A., KAPLAN, L. M., KASTELEIN, J. J., KHAW, K. T., KNOWLES, J. W., KOLOVOU, G., KONG, A., LAAKSONEN, R., LAMBRECHTS, D., LEANDER, K., LETTRE, G., LI, M., LIEB, W., LOLEY, C., LOTERY, A. J., MANNUCCI, P. M., MAOUCHE, S., MARTINELLI, N., MCKEOWN, P. P., MEISINGER, C., MEITINGER, T., MELANDER, O., MERLINI, P. A., MOOSER, V., MORGAN, T., MUHLEISEN, T. W., MUHLESTEIN, J. B., MUNZEL, T., MUSUNURU, K., NAHRSTAEDT, J., NELSON, C. P., NOTHEN, M. M., et al. 2011. Large-scale association analysis identifies 13 new susceptibility loci for coronary artery disease. *Nat Genet,* 43**,** 333-8.

SCHWAB, L. P., PEACOCK, D. L., MAJUMDAR, D., INGELS, J. F., JENSEN, L. C., SMITH, K. D., CUSHING, R. C. & SEAGROVES, T. N. 2012. Hypoxia-inducible factor 1alpha promotes primary tumor growth and tumor-initiating cell activity in breast cancer. *Breast Cancer Res,* 14**,** R6.

SHAPOURI-MOGHADDAM, A., MOHAMMADIAN, S., VAZINI, H., TAGHADOSI, M., ESMAEILI, S. A., MARDANI, F., SEIFI, B., MOHAMMADI, A., AFSHARI, J. T. & SAHEBKAR, A. 2018. Macrophage plasticity, polarization, and function in health and disease. *J Cell Physiol,* 233**,** 6425-6440.

SHEIKH, A., HUSSAIN, S. A., GHORI, Q., NAEEM, N., FAZIL, A., GIRI, S., SATHIAN, B., MAINALI, P. & AL TAMIMI, D. M. 2015. The Spectrum of Genetic Mutations in Breast Cancer. *Asian Pacific journal of cancer prevention.,* 16**,** 2177-2185.

SHEIKHPOUR, E., NOORBAKHSH, P., FOROUGHI, E., FARAHNAK, S., NASIRI, R. & NEAMATZADEH, H. 2018. A Survey on the Role of Interleukin-10 in Breast Cancer: A Narrative. *Rep Biochem Mol Biol,* 7**,** 30-37.

SHIEN, T. & IWATA, H. 2020. Adjuvant and neoadjuvant therapy for breast cancer. *Japanese Journal of Clinical Oncology,* 50**,** 225-229.

SHIOVITZ, S. & KORDE, L. A. 2015. Genetics of breast cancer: a topic in evolution. *Annals of Oncology,* 26**,** 1291-1299.

SHIRAISHI, M., SHINTANI, Y., SHINTANI, Y., ISHIDA, H., SABA, R., YAMAGUCHI, A., ADACHI, H., YASHIRO, K. & SUZUKI, K. 2016. Alternatively activated macrophages determine repair of the infarcted adult murine heart. *Journal of Clinical Investigation,* 126**,** 2151-2166.

SIN, W. C. & LIM, C. L. 2017. Breast cancer stem cells-from origins to targeted therapy. *Stem Cell Investig,* 4**,** 96.

SINGH, S., MEHTA, N., LILAN, J., BUDHTHOKI, M. B., CHAO, F. & YONG, L. 2017. Initiative action of tumor-associated macrophage during tumor metastasis. *Biochimie Open,* 4**,** 8-18.

SOARES-SILVA, M., DINIZ, F. F., GOMES, G. N. & BAHIA, D. 2016. The Mitogen-Activated Protein Kinase (MAPK) Pathway: Role in Immune Evasion by Trypanosomatids. *Frontiers in Microbiology,* 7.

SOLINAS, G., SCHIAREA, S., LIGUORI, M., FABBRI, M., PESCE, S., ZAMMATARO, L., PASQUALINI, F., NEBULONI, M., CHIABRANDO, C., MANTOVANI, A. & ALLAVENA, P. 2010. Tumor-Conditioned Macrophages Secrete Migration-Stimulating Factor: A New Marker for M2-Polarization, Influencing Tumor Cell Motility. *The Journal of Immunology,* 185**,** 642-652.

SOUBEYRAND, S., MARTINUK, A., THET, N., LAU, P. & MCPHERSON, R. 2016. Role of Tribbles Pseudokinase 1 (TRIB1) in human hepatocyte metabolism. *Biochimica Et Biophysica Acta-Molecular Basis of Disease,* 1862**,** 223-232.

SOUSA, S. & MAATTA, J. 2016. The role of tumour-associated macrophages in bone metastasis. *Journal of Bone Oncology,* 5**,** 135-138.

STRAMUCCI, L., PRANTEDA, A., STRAVATO, A., AMOREO, C. A., PENNETTI, A., DIODORO, M. G., BARTOLAZZI, A., MILELLA, M. & BOSSI, G. 2019. MKK3 sustains cell proliferation and survival through p38DELTA MAPK activation in colorectal cancer. *Cell Death & Disease,* 10.

SUGIE, T. 2018. Immunotherapy for metastatic breast cancer. *Chinese Clinical Oncology,* 7**,** 28-28.

TAHERIAN-FARD, A., SRIHARI, S. & RAGAN, M. A. 2015. Breast cancer classification: linking molecular mechanisms to disease prognosis. *Briefings in Bioinformatics,* 16**,** 461-474.

TAI, I. T. & TANG, M. J. 2008. SPARC in cancer biology: its role in cancer progression and potential for therapy. *Drug Resist Updat,* 11**,** 231-46.

TANG, B., WU, W., ZHANG, Q., SUN, Y., CUI, Y., WU, F., WEI, X., QI, G., LIANG, X., TANG, F., LI, Y. & FAN, W. 2015. Inhibition of tribbles protein-1 attenuates radioresistance in human glioma cells. *Sci Rep,* 5**,** 15961.

TARSOUNAS, M. & SUNG, P. 2020. The antitumorigenic roles of BRCA1–BARD1 in DNA repair and replication. *Nature Reviews Molecular Cell Biology,* 21**,** 284-299.

TESTA, J. R. & TSICHLIS, P. N. 2005. AKT signaling in normal and malignant cells. *Oncogene,* 24**,** 7391-7393.

THOMAS, G., TACKE, R., HEDRICK, C. C. & HANNA, R. N. 2015. Nonclassical Patrolling Monocyte Function in the Vasculature. *Arteriosclerosis Thrombosis and Vascular Biology,* 35**,** 1306-1316.

TOKER, A. & MARMIROLI, S. 2014. Signaling specificity in the Akt pathway in biology and disease. *Advances in Biological Regulation,* 55**,** 28-38.

TORRE, L. A., BRAY, F., SIEGEL, R. L., FERLAY, J., LORTET-TIEULENT, J. & JEMAL, A. 2015. Global cancer statistics, 2012. *CA Cancer J Clin,* 65**,** 87-108.

TOULANY, M. & RODEMANN, H. P. 2013. Potential of Akt mediated DNA repair in radioresistance of solid tumors overexpressing erbB-PI3K-Akt pathway. *Translational Cancer Research,* 2**,** 190-202.

TSCHOPP, J., MARTINON, F. & BURNS, K. 2003. NALPs: a novel protein family involved in inflammation. *Nat Rev Mol Cell Biol,* 4**,** 95-104.

TUNG, B., SCHADE, B., CARDIFF, R. D., AINA, O. H., SANGUIN-GENDREAU, V. & MULLER, W. J. 2017. beta-Catenin haploinsufficiency promotes mammary tumorigenesis in an ErbB2-positive basal breast cancer model. *Proceedings of the National Academy of Sciences of the United States of America,* 114**,** E707-E716.

UDALOVA, I. A., MANTOVANI, A. & FELDMANN, M. 2016. Macrophage heterogeneity in the context of rheumatoid arthritis. *Nature Reviews Rheumatology,* 12**,** 472-485.

UNDERHILL, D. M., BASSETTI, M., RUDENSKY, A. & ADEREM, A. 1999. Dynamic interactions of macrophages with T cells during antigen presentation. *J Exp Med,* 190**,** 1909-14.

URBAN, B. C., COLLARD, T. J., EAGLE, C. J., SOUTHERN, S. L., GREENHOUGH, A., HAMDOLLAH-ZADEH, M., GHOSH, A., POULSOM, R., PARASKEVA, C., SILVER, A. & WILLIAMS, A. C. 2016. BCL-3 expression promotes colorectal tumorigenesis through activation of AKT signalling. *Gut,* 65**,** 1151-1164.

VAN DE WIEL, M., DOCKX, Y., VAN DEN WYNGAERT, T., STROOBANTS, S., TJALMA, W. A. A. & HUIZING, M. T. 2017. Neoadjuvant systemic therapy in breast cancer: Challenges and uncertainties. *European Journal of Obstetrics & Gynecology and Reproductive Biology,* 210**,** 144-156.

VAN DEN BERG, T. K. & KRAAL, G. 2005. A function for the macrophage F4/80 molecule in tolerance induction. *Trends in Immunology,* 26**,** 506-509.

VEGA, A. 2013. Breast cancer genes: beyond BRCA1 and BRCA2. *Frontiers in Bioscience,* 18**,** 1358.

VELASCO, G. 2016. The complex relationship of Tribbles pseudokinase 1, PML/RARA and C/EBPalpha in leukemia: two possible couples but not a trio. *Haematologica,* 101**,** 1129-1130.

VERHEUL, H. M. & PINEDO, H. M. 2000. The role of vascular endothelial growth factor (VEGF) in tumor angiogenesis and early clinical development of VEGF-receptor kinase inhibitors. *Clin Breast Cancer,* 1 Suppl 1**,** S80-4.

VERONESI, U., BOYLE, P., GOLDHIRSCH, A., ORECCHIA, R. & VIALE, G. 2005. Breast cancer. *Lancet,* 365**,** 1727-41.

VORONOV, E., CARMI, Y. & APTE, R. N. 2014. The role IL-1 in tumor-mediated angiogenesis. *Frontiers in Physiology,* 5.

WADDELL, L. A., LEFEVRE, L., BUSH, S. J., RAPER, A., YOUNG, R., LISOWSKI, Z. M., MCCULLOCH, M. E. B., MURIUKI, C., SAUTER, K. A., CLARK, E. L., IRVINE, K. M., PRIDANS, C., HOPE, J. C. & HUME, D. A. 2018. ADGRE1 (EMR1, F4/80) Is a Rapidly-Evolving Gene Expressed in Mammalian Monocyte-Macrophages. *Frontiers in Immunology,* 9.

WAKS, A. G. & WINER, E. P. 2019. Breast Cancer Treatment. *JAMA,* 321**,** 288.

WANG, J. 2018. Neutrophils in tissue injury and repair. *Cell and Tissue Research,* 371**,** 531-539.

WANG, J., PARK, J.-S., WEI, Y., RAJURKAR, M., COTTON, L., JENNIFER, FAN, Q., LEWIS, C., BRIAN, JI, H. & MAO, J. 2013. TRIB2 Acts Downstream of Wnt/TCF in Liver Cancer Cells to Regulate YAP and C/EBPα Function. *Molecular Cell,* 51**,** 211-225.

WANG, L., LIU, X., REN, Y., ZHANG, J., CHEN, J., ZHOU, W., GUO, W., WANG, X., CHEN, H., LI, M., YUAN, X., ZHANG, X., YANG, J. & WU, C. 2017a. Cisplatin-enriching cancer stem cells confer multidrug resistance in non-small cell lung cancer via enhancing TRIB1/HDAC activity. *Cell Death & Disease,* 8.

WANG, M., ZHAO, J., ZHANG, L., WEI, F., LIAN, Y., WU, Y., GONG, Z., ZHANG, S., ZHOU, J., CAO, K., LI, X., XIONG, W., LI, G., ZENG, Z. & GUO, C. 2017b. Role of tumor microenvironment in tumorigenesis. *Journal of Cancer,* 8**,** 761-773.

WANG, Q., NI, H., LAN, L., WEI, X., XIANG, R. & WANG, Y. 2010. Fra-1 protooncogene regulates IL-6 expression in macrophages and promotes the generation of M2d macrophages. *Cell Research,* 20**,** 701-712.

WANG, S., GAO, X., SHEN, G., WANG, W., LI, J., ZHAO, J., WEI, Y.-Q. & EDWARDS, C. K. 2016a. Interleukin-10 deficiency impairs regulatory T cell-derived neuropilin-1 functions and promotes Th1 and Th17 immunity. *Scientific Reports,* 6**,** 24249.

WANG, Y., WU, N., PANG, B., TONG, D., SUN, D., SUN, H., ZHANG, C., SUN, W., MENG, X., BAI, J., CHEN, F., GENG, J., FU, S. & JIN, Y. 2017c. TRIB1 promotes colorectal cancer cell migration and invasion through activation MMP-2 via FAK/Src and ERK pathways. *Oncotarget,* 8**,** 47931-47942.

WANG, Z.-Y., ZHANG, J.-A., WU, X.-J., LIANG, Y.-F., LU, Y.-B., GAO, Y.-C., DAI, Y.-C., YU, S.-Y., JIA, Y., FU, X.-X., RAO, X., XU, J.-F. & ZHONG, J. 2016b. IL-6 Inhibition Reduces STAT3 Activation and Enhances the Antitumor Effect of Carboplatin. *Mediators of Inflammation,* 2016**,** 1-8.

WENNEMERS, M., BUSSINK, J., GREBENCHTCHIKOV, N., SWEEP, F. C. & SPAN, P. N. 2011a. TRIB3 protein denotes a good prognosis in breast cancer patients and is associated with hypoxia sensitivity. *Radiother Oncol,* 101**,** 198-202.

WENNEMERS, M., BUSSINK, J., SCHEIJEN, B., NAGTEGAAL, I. D., VAN LAARHOVEN, H. W., RALEIGH, J. A., VARIA, M. A., HEUVEL, J. J., ROUSCHOP, K. M., SWEEP, F. C. & SPAN, P. N. 2011b. Tribbles homolog 3

denotes a poor prognosis in breast cancer and is involved in hypoxia response. *Breast Cancer Res,* 13**,** R82.

WU, X., YANG, L., ZHENG, Z., LI, Z., SHI, J., LI, Y., HAN, S., GAO, J., TANG, C., SU, L. & HU, D. 2016. Src promotes cutaneous wound healing by regulating MMP-2 through the ERK pathway. *International Journal of Molecular Medicine,* 37**,** 639-648.

WU, Y., CHEN, W., XU, Z. P. & GU, W. 2019. PD-L1 Distribution and Perspective for Cancer Immunotherapy-Blockade, Knockdown, or Inhibition. *Front Immunol,* 10**,** 2022.

XU, D., CHEN, X., LI, X., MAO, Z., TANG, W., ZHANG, W., DING, L. & TANG, J. 2019. Addition of Capecitabine in Breast Cancer First-line Chemotherapy Improves Survival of Breast Cancer Patients. *J Cancer,* 10**,** 418-429.

YANG, C., HE, L., HE, P., LIU, Y., WANG, W., HE, Y., DU, Y. & GAO, F. 2015. Increased drug resistance in breast cancer by tumor-associated macrophages through IL-10/STAT3/bcl-2 signaling pathway. *Medical Oncology,* 32.

YANG, L. & ZHANG, Y. 2017. Tumor-associated macrophages: from basic research to clinical application. *Journal of Hematology & Oncology,* 10.

YANG, X., WANG, H. & JIAO, B. W. 2017. Mammary gland stem cells and their application in breast cancer. *Oncotarget,* 8**,** 10675-10691.

YANG, Z.-Y., YANG, L., XU, C.-W., WANG, X.-J. & LEI, L. 2020. An insertion mutation of ERBB2 enhances breast cancer cell growth and confers resistance to lapatinib through AKT signaling pathway. *Biology Open,* 9**,** bio047662.

YAO, W., BA, Q., LI, X., LI, H., ZHANG, S., YUAN, Y., WANG, F., DUAN, X., LI, J., ZHANG, W. & WANG, H. 2017. A Natural CCR2 Antagonist Relieves Tumor-

associated Macrophage-mediated Immunosuppression to Produce a Therapeutic Effect for Liver Cancer. *EBioMedicine,* 22**,** 58-67.

YE, S., XU, H., JIN, J., YANG, M., WANG, C., YU, Y. & CAO, X. 2012. The E3 Ubiquitin Ligase Neuregulin Receptor Degradation Protein 1 (Nrdp1) Promotes M2 Macrophage Polarization by Ubiquitinating and Activating Transcription Factor CCAAT/Enhancer-binding Protein beta (C/EBP beta). *Journal of Biological Chemistry,* 287**,** 26740-26748.

YE, Y., WANG, G., WANG, G., ZHUANG, J., HE, S., SONG, Y., NI, J., XIA, W. & WANG, J. 2017. The Oncogenic Role of Tribbles 1 in Hepatocellular Carcinoma Is Mediated by a Feedback Loop Involving microRNA-23a and p53. *Front Physiol,* 8**,** 789.

YOKOYAMA, T. & NAKAMURA, T. 2011. Tribbles in disease: Signaling pathways important for cellular function and neoplastic transformation. *Cancer Sci,* 102**,** 1115-22.

YU, J.-M., SUN, W., WANG, Z.-H., LIANG, X., HUA, F., LI, K., LV, X.-X., ZHANG, X.-W., LIU, Y.-Y., YU, J.-J., LIU, S.-S., SHANG, S., WANG, F., YANG, Z.-N., ZHAO, C.-X., HOU, X.-Y., LI, P.-P., HUANG, B., CUI, B. & HU, Z.-W. 2019. TRIB3 supports breast cancer stemness by suppressing FOXO1 degradation and enhancing SOX2 transcription. *Nature Communications,* 10.

YUAN, A., HSIAO, Y.-J., CHEN, H.-Y., CHEN, H.-W., HO, C.-C., CHEN, Y.-Y., LIU, Y.-C., HONG, T.-H., YU, S.-L., CHEN, J. J. W. & YANG, P.-C. 2015. Opposite Effects of M1 and M2 Macrophage Subtypes on Lung Cancer Progression. *Scientific Reports,* 5.

YUEN, K. C., LIU, L.-F., GUPTA, V., MADIREDDI, S., KEERTHIVASAN, S., LI, C., RISHIPATHAK, D., WILLIAMS, P., KADEL, E. E., KOEPPEN, H., CHEN, Y.-J., MODRUSAN, Z., GROGAN, J. L., BANCHEREAU, R., LENG, N., THASTROM, A., SHEN, X., HASHIMOTO, K., TAYAMA, D., VAN DER HEIJDEN, M. S., ROSENBERG, J. E., MCDERMOTT, D. F., POWLES, T., HEGDE, P. S., HUSENI, M. A. & MARIATHASAN, S. 2020. High systemic and tumor-associated IL-8 correlates with reduced clinical benefit of PD-L1 blockade. *Nature Medicine,* 26**,** 693-698.

ZANELLA, F., RENNER, O., GARCÍA, B., CALLEJAS, S., DOPAZO, A., PEREGRINA, S., CARNERO, A. & LINK, W. 2010. Human TRIB2 is a repressor of FOXO that contributes to the malignant phenotype of melanoma cells. *Oncogene,* 29**,** 2973-2982.

ZHAN, T., RINDTORFF, N. & BOUTROS, M. 2017. Wnt signaling in cancer. *Oncogene,* 36**,** 1461-1473.

ZHANG, H.-Y., LIANG, F., JIA, Z.-L., SONG, S.-T. & JIANG, Z.-F. 2013. PTEN mutation, methylation and expression in breast cancer patients. *Oncology Letters,* 6**,** 161-168.

ZHANG, M., LEE, A. V. & ROSEN, J. M. 2017a. The Cellular Origin and Evolution of Breast Cancer. *Cold Spring Harb Perspect Med,* 7.

ZHANG, M.-Z., WANG, X., WANG, Y., NIU, A., WANG, S., ZOU, C. & HARRIS, R. C. 2017b. IL-4/IL-13–mediated polarization of renal macrophages/dendritic cells to an M2a phenotype is essential for recovery from acute kidney injury. *Kidney International,* 91**,** 375-386.

ZHOU, H., LIAO, J., ALOOR, J., NIE, H., WILSON, B. C., FESSLER, M. B., GAO, H.-M. & HONG, J.-S. 2013. CD11b/CD18 (Mac-1) Is a Novel Surface Receptor for

Extracellular Double-Stranded RNA To Mediate Cellular Inflammatory Responses. *Journal of Immunology,* 190**,** 115-125.

ZHOU, J., CHEN, Q., ZOU, Y., CHEN, H., QI, L. & CHEN, Y. 2019. Stem Cells and Cellular Origins of Breast Cancer: Updates in the Rationale, Controversies, and Therapeutic Implications. *Front Oncol,* 9**,** 820.

Appendix 1. Confirmation of siRNA transfection

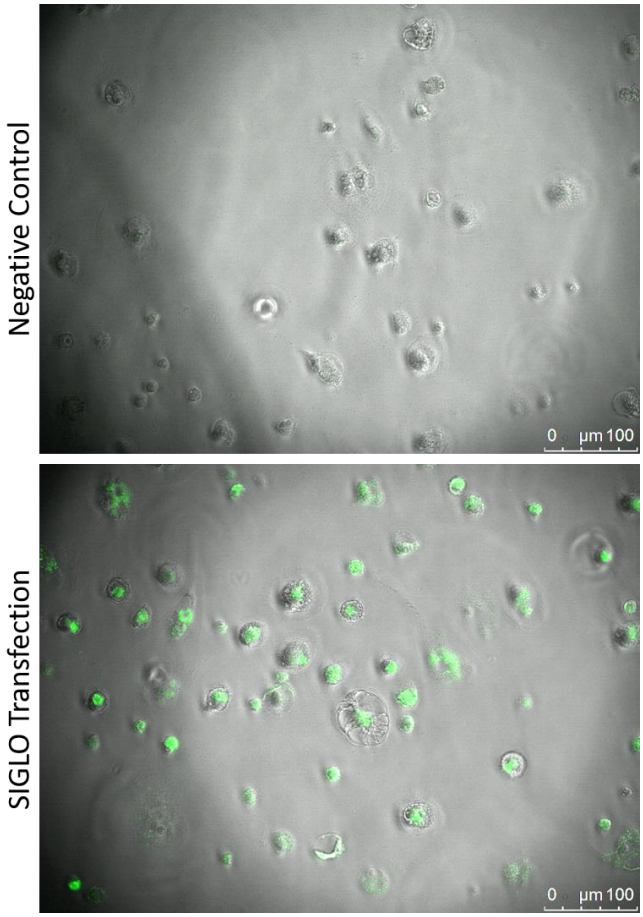

Supplementary figure 1. Transfection of siGLO on macrophages with Viromer Green. In order to evaluate the efficiency of transfection in primary human macrophages with Viromer Green (Lipocalyx), human MDMs were transfected with siGLO Green Transfection Indicator (Dharmacon) for 24 hours. The resulting images represent MDMs transfected by Viromer Green (Lipocalyx) without siGLO Green Transfection Indicator (Dharmacon) as a negative control, and MDMs transfected with siGLO Green Transfection Indicator (Dharmacon). All images were captured by wide-field microscope 20x lens and the images were adjusted with ImageJ.

Appendix 2. Optimization of TRIB1 fluorescence staining

Initially, we were stained tumour sections by fixing the tissues in 95% and 70% of ethanol for 5 minutes each and rehydrate in the running water for 1-3 minutes. TRIB1 antibody sample was provided by Primerdesign (anti-TRIB1 rabbit polyclonal antibody) for us to check the application on fluorescence staining before they are on sale and we have tested with different conditions (without any detergent, Treated with either 0.1% Triton X-100 or H_2O_2, and treated with both Triton X-100 and H_2O_2 and none of the conditions was able to show TRIB1 signals in the tumour sections (Supplementary figure 2). Therefore, we decided to use TRIB1 antibody from Millipore we were using previously in the lab and tested the TRIB1 antibody either with and without detergent. Though TRIB1 staining with Millipore antibody detected some signals, the signals looked similar to the non-specific, and it was difficult to find (Supplementary figure 3). Finally, we have changed the fixation method from ethanol to acetone for 10 minutes and was able to observe TRIB1 signals on mouse breast tumour tissues (Supplementary figure 4).

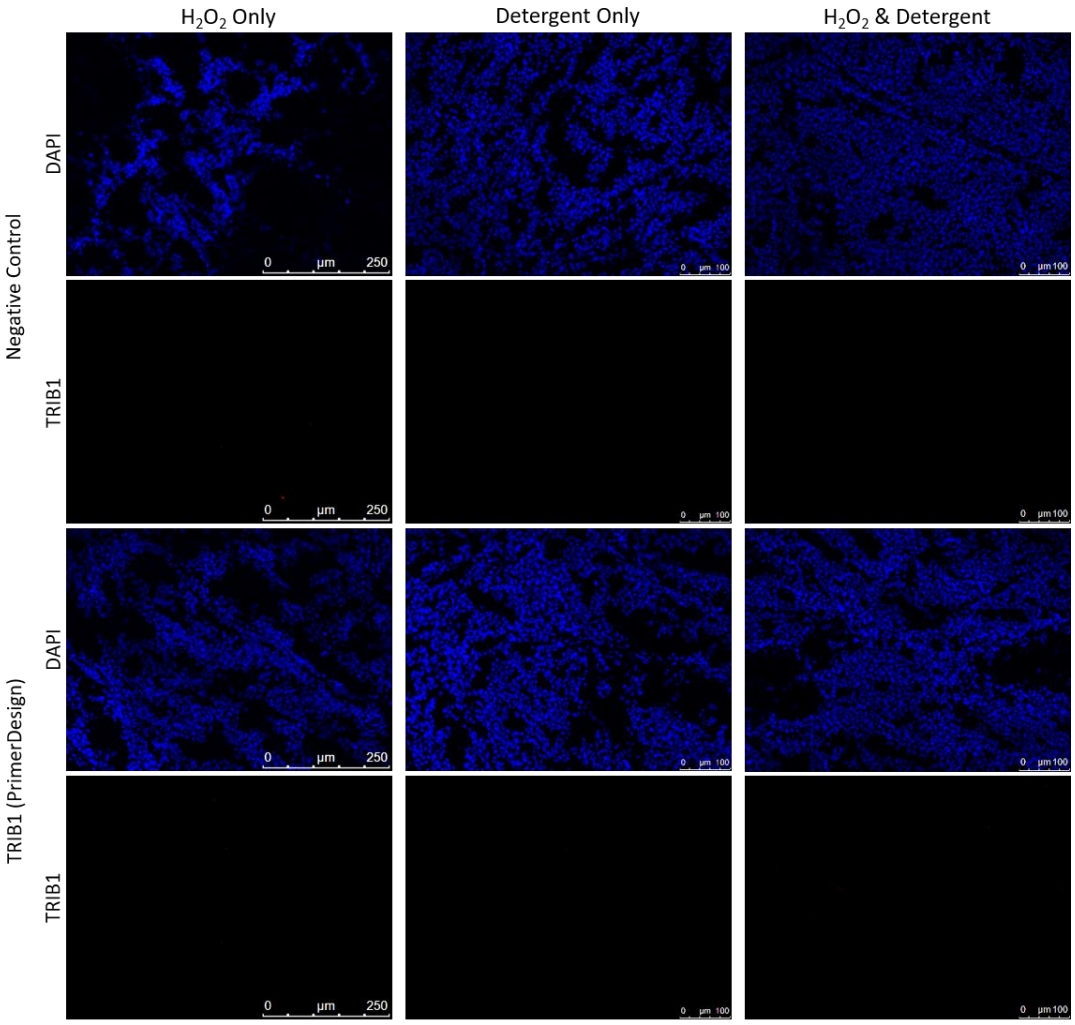

Supplementary figure 2. Immunofluorescence staining of Primerdesign TRIB1 antibody on a mouse breast tumour. In order to test the antibody and optimise the TRIB1 fluorescence staining, TRIB1 was stained on mouse breast tissues with different conditions. Staining without any detergent, with mild detergent (0.1% Triton X-100), with H_2O_2, and with both mild detergent and H_2O_2 were tested, but no signals were detected in all the conditions. All images were captured by a wide-field microscope 20x lens, and the images were adjusted with ImageJ.

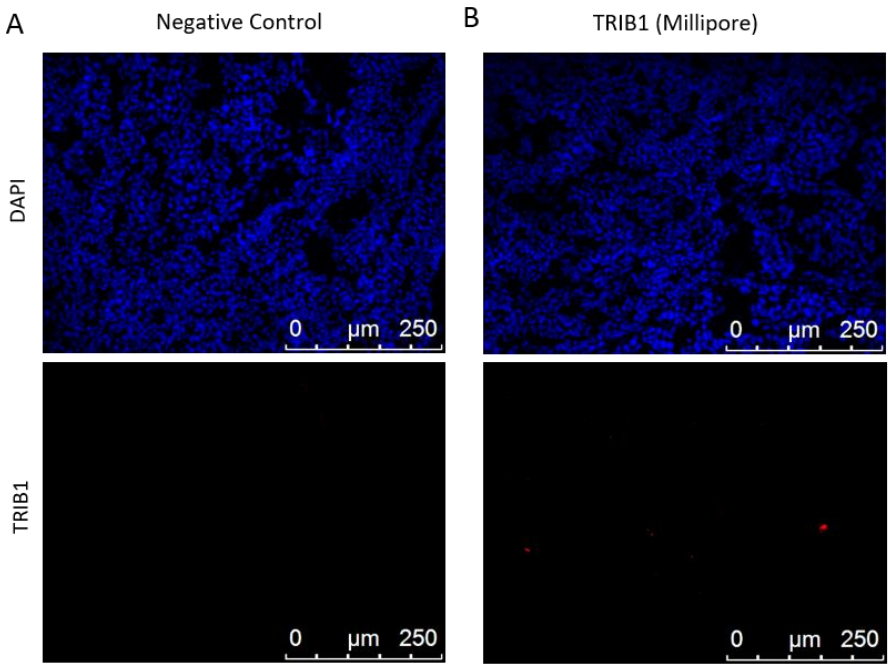

Supplementary figure 3. Testing fluorescence staining with TRIB1 antibody from Millipore. In order to test and optimise the TRIB1 fluorescence staining on breast tumour tissues, TRIB1 antibody from Millipore was used to staining tumour sections either with or without detergent treatment. Compared to (A) negative control with IgG isotypes, (B) staining with Millipore TRIB1 antibody showed spots of signals which are inspected as non-specific signals from debris or dust. All images were captured by a wide-field microscope 20x lens, and the images were adjusted with ImageJ.

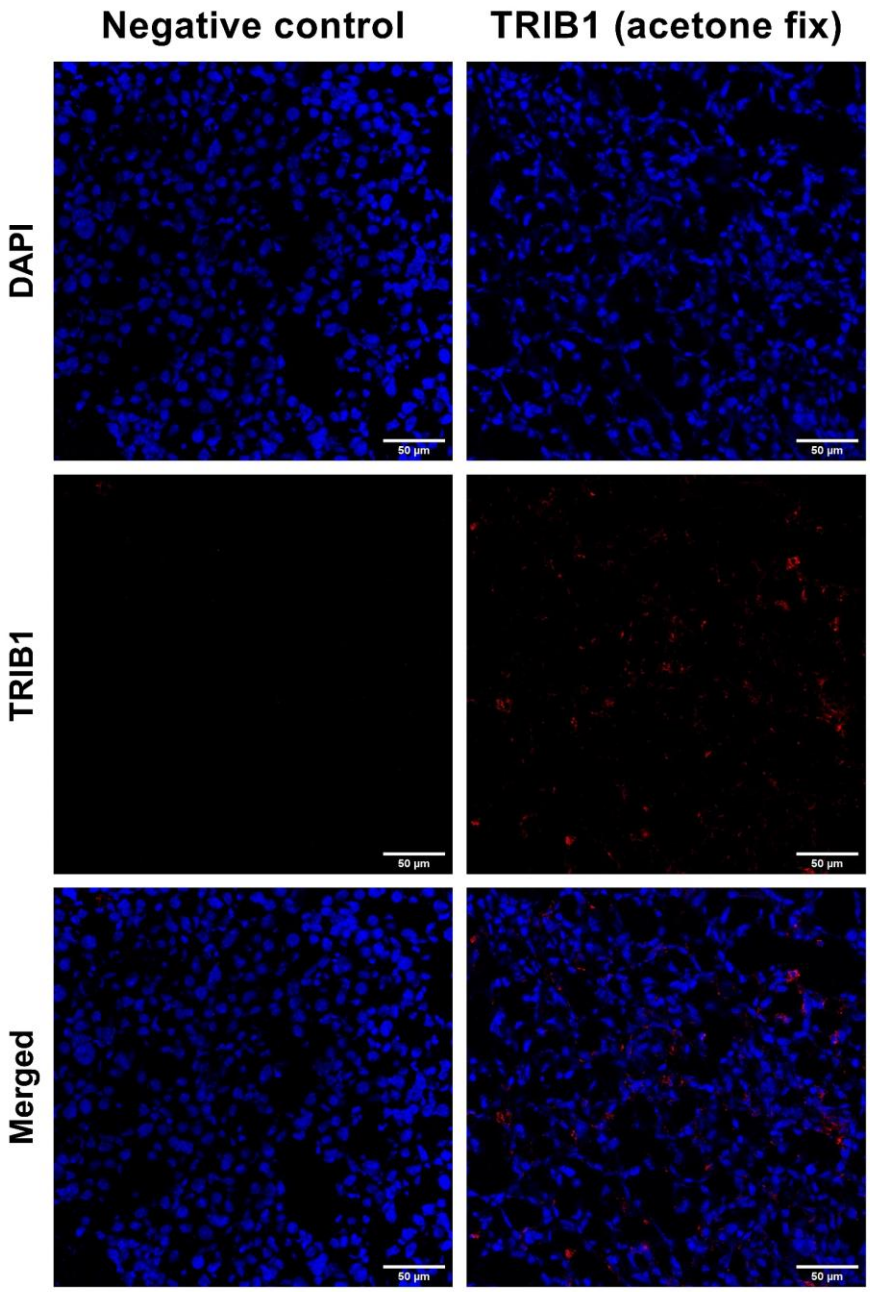

Supplementary figure 4. Confirmation of Millipore TRIB1 staining on breast tumour tissues with acetone fixation. In order to optimise the fluorescence staining of TRIB1 from Millipore on breast tumour tissues, tissues were fixed with ice-cold acetone for 10 minutes at room temperature and stained. All images were captured by a Nikon A1 confocal microscope 40x lens, and the images were adjusted with ImageJ.

Appendix 3. Additional qPCR of TRIB1 KD macrophages and TAMs

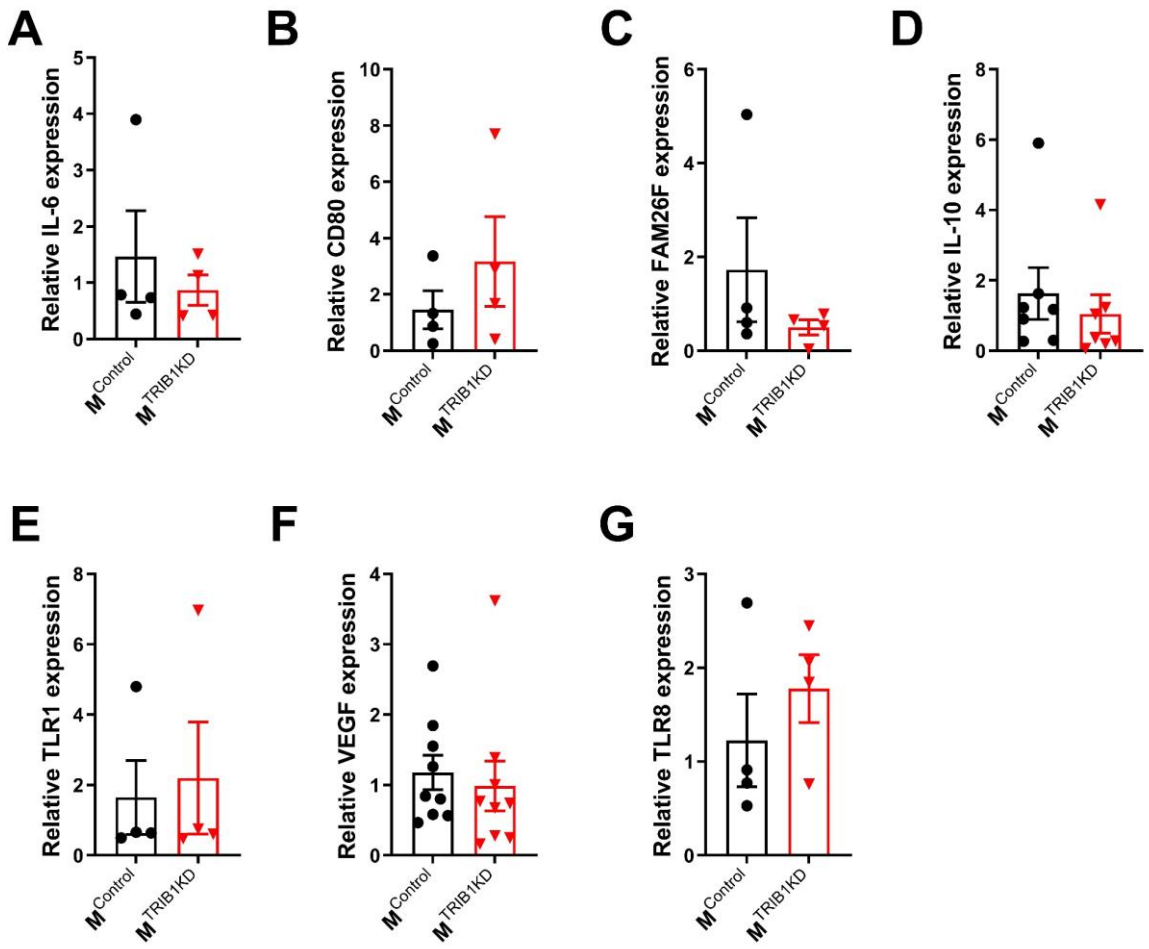

Supplementary figure 5. qPCR analysis of TRIB1 siRNA transfected macrophages. Human MDMs were generated from monocytes isolated from human blood. The isolated monocytes were differentiated to macrophages for 7 days and transfected with *TRIB1* siRNA to knockdown *TRIB1* expression. Cells were then analysed with RT-qPCR. RNA levels of *IL-6* (A) *CD80* (B) *FAM26F* (C) *IL-10* (D) *TLR1* (E) VEGF (F) and *TLR8* (G) 48 hours after control or *TRIB1* siRNA transfection. Results represent mean±SEM of n= 4-9donor/group.

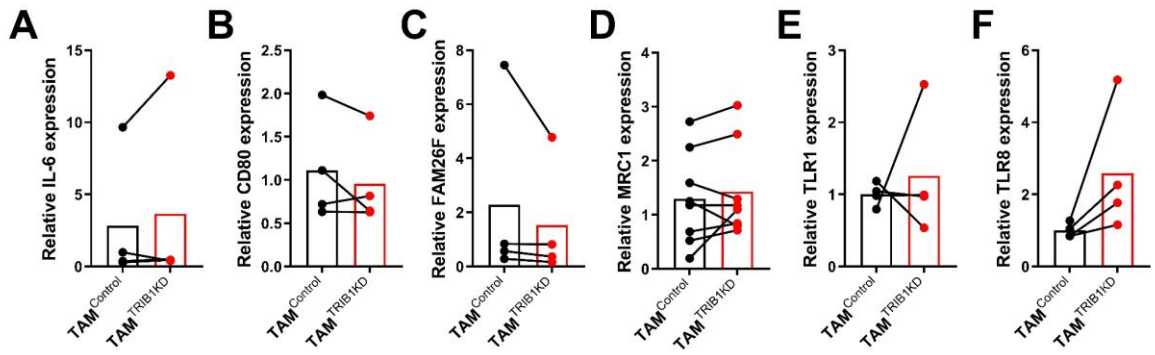

Supplementary figure 6. qPCR analysis of TRIB1 siRNA transfected macrophages. Human MDMs isolated and differentiated from blood were transfected with either control or *TRIB1* siRNA for 48 hours and polarised to TAMs using the tumour-conditioned medium for 24 hours. Cells were then analysed using RT-qPCR. RNA levels of *IL-6* (A), *CD80* (B), *FAM26F* (C), *MRC1* (D), *TLR1* (E) and *TLR8* (G) 72 hours after control or *TRIB1* siRNA transfection and polarisation. Results represent the mean of n= 4-8donor/group.

Appendix 4. Immunofluorescence staining of human breast tissue

Human breast tissues that were left after experiment performed previously in the lab were stained with CD68 (macrophage marker) and TRIB1 to optimise the immunofluorescence staining protocol before analysing TRIB1 in macrophages and correlation TRIB1 expressing TAMs and T cell infiltrations in TRIB1 high and low human breast cancer tissues in Madrid, Spain. The human tissues were acquired with NHS National Research Ethics Service Sheffield Research Ethics Committee REC reference number 09/H1308/138. The PEFF human breast tissues were dewaxed, blocked endogenous peroxide activity with H_2O_2, and antigens were retrieved with 0.01M trisodium citrate (TSC) pH6. The diluted antibodies were stained and imaged the fluorescence with Nikon A1 confocal microscope (detailed protocol in page 56, 2.2.18 Immunofluorescence staining of PEFF tissues). Staining of TRIB1 (1:50 dilution) worked fine but we were not able to detect CD68 signals. We were not able to further develop this experiment due to COVID19 lockdown and were not able to go to Spain.

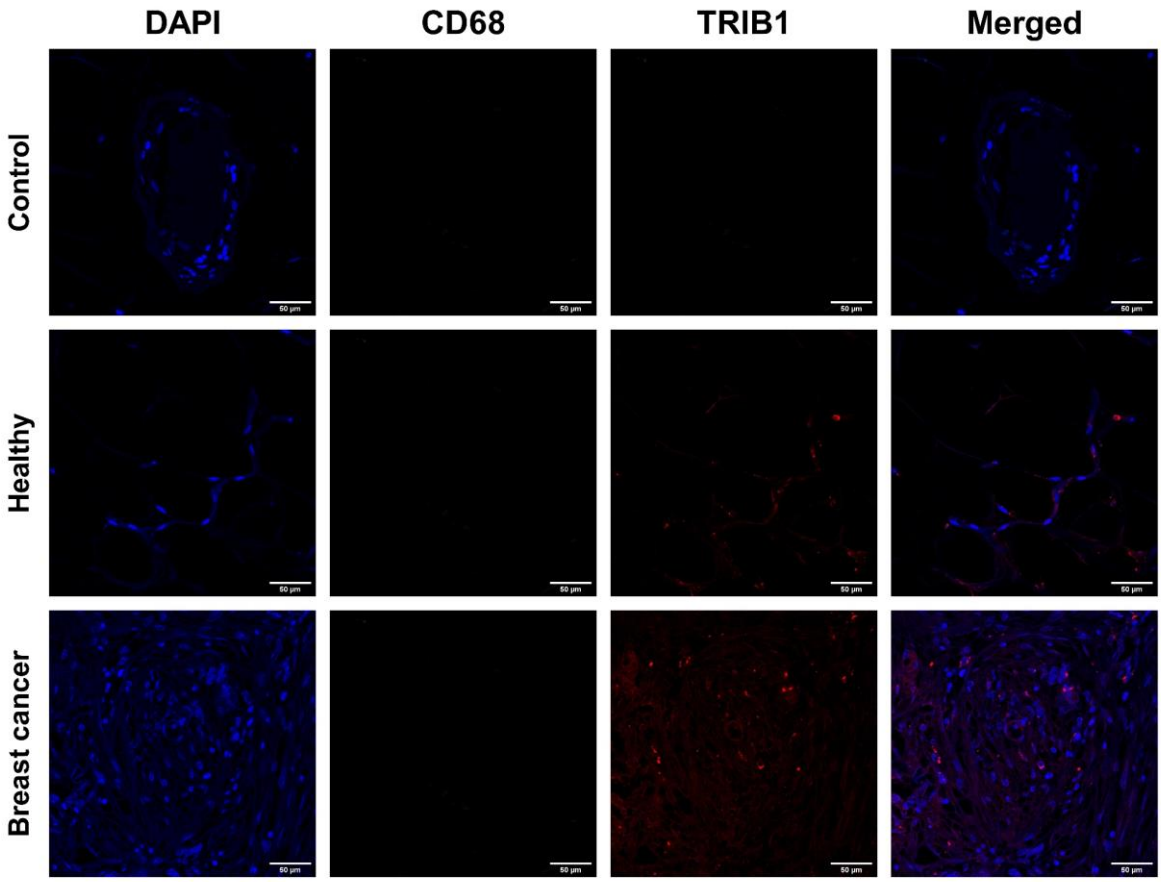

Supplementary figure 7. Fluorescence staining of PEFF human breast tissues. The human breast tissues were stained with CD68 and TRIB1 to test the immunofluorescence staining on PEFF human tissues. Cells were stained with DAPI (blue), TRIB1 (Red) and CD68 (green). All images were captured by a Nikon A1 confocal microscope 40x lens, and the images were adjusted with ImageJ.